STUDIES ON SOME COMPLEXES OF 3d AND 4f METAL IONS WITH A BI- AND A TETRADENTATE LIGAND

A Thesis
Submitted for the Degree of
Doctor of Philosophy

By
TULIKA GHOSH

School of Chemistry
University of Hyderabad
Hyderabad 500 046
India

June 2012

Where the mind is without fear and the head is held high
Where knowledge is free
Where the world has not been broken up into fragments
By narrow domestic walls
Where words come out from the depth of truth
Where tireless striving stretches its arms towards perfection
Where the clear stream of reason has not lost its way
Into the dreary desert sand of dead habit
Where the mind is led forward by thee
Into ever-widening thought and action
Into that heaven of freedom, my Father, let my country awake

Rabindranath Tagore
(Gitanjali)

To My

Parents and Brothers

CONTENTS

STATEMENT	**i**
CERTIFICATE	**iii**
ACKNOWLEDGEMENT	**v**
CHAPTER ▪ 1 ► Introduction	
1.1. Abstract	**1**
1.2. Prelude	**2**
1.3. Motivation behind the present work	**3**
1.3.1. Supramolecular structures of coordination complexes	**3**
1.3.2. Some copper(II) and nickel(II) complexes reported from our group	**5**
1.3.2.1. Copper(II) complexes	**5**
1.3.2.2. Nickel(II) complexes	**9**
1.3.3. Lanthanide complexes and their versatile applications	**12**
1.4. About the present investigation	**16**
1.5. References	**18**
CHAPTER ▪ 2 ► Nickel(II) and copper(II) complexes with biacetyl bis(benzoylhydrazone): Self-assembly via π–π interaction and hydrogen bonding	
2.1. Abstract	**25**
2.2. Introduction	**26**
2.3. Experimental	**26**
2.3.1. Materials	**26**
2.3.2. Physical measurements	**27**
2.3.3. Synthesis of [Ni(babh)]	**27**
2.3.4. Synthesis of [Cu(babh)]	**27**
2.3.5. X-ray crystallography	**28**
2.4. Result and discussion	**30**
2.4.1. Synthesis and some properties	**30**
2.4.2. Spectral features	**31**

2.4.3. Molecular structures **33**
2.4.4. Intermolecular interactions and self- assembly **36**
2.5. Conclutions **38**
2.6. References **40**
CHAPTER ▪ 3 ► A double helical dinuclear copper(II) complex with biacetyl bis(benzoylhydrazone)
3.1. Abstract **42**
3.2. Introduction **43**
3.3. Experimental **45**
3.3.1. Materials **45**
3.3.2. Physical measurements **45**
3.3.3. Synthesis of $[Cu_2(\mu\text{-babh})_2]$ **45**
3.3.4. X-ray crystallography **46**
3.4. Results and discussion **48**
3.4.1. Synthesis and some properties **48**
3.4.2. Spectral features **48**
3.4.3. Molecular Structure **51**
3.5. Conclusions **53**
3.6. References **55**
CHAPTER ▪ 4 ► Effects of counteranions on molecular and supramolecular structures of bis(2-(1H-imidazol-2-yl)-pyridine)copper(II)
4.1. Abstract **58**
4.2. Introduction **59**
4.3. Experimental **59**
4.3.1. Materials **59**
4.3.2. Physical measurements **60**
4.3.3. Synthesis of $[Cu(impy)_2Cl_2]\cdot 3H_2O$ (1) **60**
4.3.4. Synthesis of $[Cu(impy)_2(NO_3)](NO_3)\cdot H_2O$ (2) **60**
4.3.5. Synthesis of $[Cu(impy)_2(ClO_4)](ClO_4)\cdot H_2O$ (3) **61**

4.3.6. X-ray Crystallography **61**
4.4. Result and discussion **64**
4.4.1. Synthesis and some properties **64**
4.4.2. Spectral features **65**
4.4.3. Molecular structures **68**
4.4.4. Supramolecular structures **73**
4.5. Conclusions **77**
4.6. References **78**
CHAPTER ▪ 5 ► Syntheses and structures of cerium(IV) and gadolinium(III) complexes with biacetyl bis(benzoylhydrazone)
5.1. Abstract **81**
5.2. Introduction **82**
5.3. Experimental **82**
5.3.1. Materials **82**
5.3.2. Physical measurements **83**
5.3.3. Synthesis of [Ce(babh)$_2$] **83**
5.3.4. Synthesis of [Gd(babh)(Hbabh)] **84**
5.3.5. X-ray Crystallography **84**
5.4. Results and discussion **87**
5.4.1. Synthesis and some properties **87**
5.4.2. Spectroscopic characterization **88**
5.4.3. Cryomagnetic behavior of [Gd(babh)(Hbabh)] **92**
5.4.4. Molecular structures **93**
5.4.5. Supramolecular structures **98**
5.5. Conclusions **100**
5.6. References **102**
List of publications **104**
Posters and presentations **104**

STATEMENT

I hereby declare that the matter embodied in the thesis entitled ***"Studies on Some Complexes of 3d and 4f Metal Ions with a Bi- and a Tetradentate Ligand"*** is the result of investigations carried out by me in the School of Chemistry, University of Hyderabad, Hyderabad, India under the supervision of **Prof. Samudranil Pal**.

In keeping with the general practice of reporting scientific investigations, due acknowledgements have been made wherever the work described is based on the findings of other investigators. Any omission or error that might have crept in is regretted.

June 2012 **Tulika Ghosh**

PROF. SAMUDRANIL PAL
SCHOOL OF CHEMISTRY
UNIVERSITY OF HYDERABAD
HYDERABAD–500 046, INDIA

Phone:+91-40-23134756 (Office)
Fax: +91-40-2301 2460
Email: spsc@uohyd.ernet.in

28th June, 2012

CERTIFICATE

Certified that the work embodied in the thesis entitled ***"Studies on Some Complexes of 3d and 4f Metal Ions with a Bi- and a Tetradentate Ligand"*** has been carried out by **Ms. Tulika Ghosh** under my supervision and that the same has not been submitted elsewhere for any degree.

Prof. Samudranil Pal
(Thesis Supervisor)

Dean
School of Chemistry
University of Hyderabad

ACKNWOLEDGEMENT

It gives me immense pleasure to express my profound gratitude and deep respect to my research supervisor Prof. Samudranil Pal, for his constant cooperation, encouragement and invaluable guidance throughout my research work. He has been always approachable, helpful and extremely patient during my research period. I will always treasure the care and concern of him towards me.

I would like to thank the former and present Deans, School of Chemistry for providing all essential facilities to carry out my research works without any interruption. I am extremely thankful individually to all the faculty members of our school for their help and cooperation at various stages of my stay in the school.

I thank all non-teaching staff of the School and CIL for their help and cooperation to execute my research work. I am thankful to IGM library for providing excellent collection of books and journals.

Financial assistance from University Grants Commission (UGC), New Delhi and Department of Science and Technology (DST), New Delhi are sincerely acknowledged.

I am extremely thankful to my all teachers for their admirable teaching and priceless suggestions in different stages of my life. I specially thank Roma pishi, my first teacher; Head Mistress, Sati Bhattacharya of my first high school, Hakimpara Balika Bidyalaya; Joy Kishan sir; Raj Kishor sir; Manotosh sir; Shukla di and Partha da. I would like to extend my thanks to all Professors of North Bengal University, especially Prof. Pinaki Bandhopadhyay for their excellent guidance and teaching.

Each of the members of our group has helped me to enrich my experience in their own way. I thank my seniors in the lab: Dr. Raji and Dr. Anindita, with whom I was associated at earlier stages of my research work in the lab. I thank my juniors Nagaraju, Swamy, Balabardhan and Sathish for help in my work and for creating cheerful atmosphere in lab.

I am very thankful to my entire School, B.Sc. and M.Sc. friends, especially Debjani, Sucharita and Rumki for their love, care and being there with me through all difficulties.

It is my pleasure to thank all my seniors Manab da, Abhijit da, Moloy da, Ani da, Saikat da, Subhash da, Prashant da, Ghona da, Utpal da, Shatabdi di, Bhaswati di, Joya di,Vasudhara di, Rumpa, Gitoshree di, Suparna di, Pradeep da, Arindam da, Tapta da,

Tanmoy da, Subrata da, Sandip da, Ghanta da, Pati da, Bipul da, Ranjit da, Naba da, Sanjib da, Arunbabu, Sajna, Manshi di, Bhargavi for giving me constant moral support. I am glad to thank batchmates and juniors like Susruta, Rishi, Dinesh, Palash, Nabomita, Chandrani (Acharya), Monima, Mousumi, Chhoto Tanmoy, Sanghamitra, Pramiti, Raja, Nayan, Supratim, Sudhangshu, Anup, Sandip (maiti), Meheboob, Satyajit, Sugata, Rudra, Debparna, Suman (Ghosh), Shubhra, Sutanuka, Poulomi, Olivia, Suman (Sen), Krishnendu, Raju, Kaijar, Archana, Tungadri, Chandrani (Bose), Paromita, Mona, Deboshree, Oindrila, Shyamashree, Sharmistha, Anindita, Moumita, Arghya, Indraneel, Shreetama, Somya, Shakti, Kalpana and many more for their help in my work and maintaining a cheerful atmosphere. My special thanks to my friends Bhaswatidi, Joya di, Vasudhara di, Rumpa, Tapta da, Tanmoy da, Subrata da, Sanghamitra, Pramiti, Chhoto Tanmoy, Suman Sen, Raju, Kaijar, Rudra, Sugata, Debparna, Mona for their love and care. They made my stay at the University of Hyderabad, a memorable one. A special thank to Soumya, one of my good friends for her help in my research work. I always remember the wonderful memories of Saraswati Puja, Freshers, and campus fire as we celebrate those occasions with high passion and lots of enthusiasm.

I am also thankful to my grandparents and all Jethu-Jethima, Kaku-Kakima, Pishi-Pishamoshai, Mama-Mami, Mashi-Mesho, cousin brothers, sisters, sister-in-laws, brother-in-laws, nephews and nieces with whom I am always spending wonderful times.

I would like to express my gratitude and admiration to Alok. He is always there to understand me and encourage me with his great friendly support.

My special thanks to my beloved brothers Shuva and Dip with whom I grew up, for their love, care and affection.

Without my Parents' relentless support, love, care and blessing I cannot be whatever I am today. My parents' has been a great source of inspiration for my life. My mother has been extremely patient with me and always supported me in any situations of my life as my best friend. My father is also very much friendly with me. His liveliness and passion towards his works always motivates me to be active throughout my life. I am greatly indebted from bottom of my heart to my father for his encouragement and moral support.

June, 2012 ***Tulika Ghosh***

Chapter 1

Introduction:

1.1. Abstract:

In this chapter, a general idea on supramolecular structures of coordination complexes assembled by non-covalent interactions has been briefly discussed. Some selective results on copper(II) and nickel(II) complexes reported from our group have been summarized. A few important applications of lanthanide complexes in a variety of research areas have been highlighted. In light of the above, the objectives of the present investigation have been stated.

1.2. Prelude:

The coordination chemistry is considered to be initiated by Tassaert with the synthesis of an orange colour compound, $CoCl_3 \cdot 6NH_3$ in 1798. At that time people assigned this type of compounds as “complex compounds” because they challenge usual rules of valency. However, Warner [1] and Jørgensen, two great scientists of late nineteenth century, with their noble efforts were successful to attract people’s attention to coordination chemistry. After a long controversy, Warner’s coordination theory satisfactorily succeeded to explain almost all doubts about unusual valency, bonding and molecular geometries of coordination complexes. For that he was awarded Nobel Prize in chemistry in 1913. Afterwards this part of chemistry developed very quickly and today coordination complexes embrace a wide range of research areas. From the beginning, coordination chemists have been fascinated towards the ability of pure organic ligands to bind the metal ions and provide complex molecules with interesting structural features and various amazing physical properties such as photochemical, magnetic, electrochemical, catalytic etc. Not only molecular structures, but also the supramolecular structures assembled by various non-covalent intra- and intermolecular interactions and their effects on several chemical and physical properties have attracted immense attention of inorganic as well as materials chemists. Studies on transition metal (d-block) complexes have now been expanded to lanthanide (4f) complexes due to their unique physicochemical properties which are extremely useful in some important chemical and biological fields. In this way coordination chemistry bridges more or less all branches of chemistry that include inorganic, physical, organic, biological, material, analytical and theoretical.

1.3. Motivation behind the present work:

1.3.1. Supramolecular structures of coordination complexes:

Growing interest in supramolecular structures is because of tremendous applications of such architectures in a vast range of research fields such as catalysis, separation science, gas storage, drug delivery, molecule based optical and magnetic materials and enantiospecific processes [2−14].

Supramolecular structure can be defined as aggregation of identical molecular structures in any of one, two or three dimensions with the help of intermolecular non-covalent interactions [15,16].

The important factors that control the supramolecular packing of coordination complexes have developed gradually [4]. Metal centre of the complex plays a vital role in the packing process. Coordinating capability of the ligand, nature and strength of bonding between metal and ligand, coordination number and coordination geometry around the metal centre and finally charge on the metal decide the molecular structure of the complex [17].The metal ion is at the core of the complex molecule and surrounded by the ligands which are pure organic in nature [16]. These organic ligands mainly govern the overall shape of the molecule as well as the supramolecular structure by participating in intermolecular non-covalent interactions. A few suitable polar functional groups at periphery of the ligand generate important directional interactions and these directional interactions are the actual administers of dimensions and architectures of packing arrangements.

Most important directional interaction is hydrogen bonding. Hydrogen bond is defined as an electrostatic, directional and mostly three-centred four electron interaction [16]. The type and strength of the hydrogen bonds depend on the donors and the acceptors present in the system. The O−H···O, N−H···O, O−H···N and N−H···N interactions involving $–NH_2$, –OH, $–CO_2H$, $–CONH_2$, –CONHR type of functional groups are considered as strong hydrogen bonds [15−18]. M−X···H−N (X = halide) is also quite strong interaction and its directionality increases with the increase of positive charge on the H atom [19]. The C−H···O, C−H···N, O−H···π, N−H···π, C−H···π type of hydrogen bonds are comparably weaker interactions [15−17,20] but very frequently they participate in packing of coordination complexes.

Some other hydrogen bond type interactions are: (1) X−H···M interaction [21−23] where metal atom is in low oxidation state and it acts as acceptor and N−H, O−H, C−H etc are donors; (2) M−H···X interaction [24−26] where metal bound H-atoms (in polynuclear cluster) are involved in μ or μ_3 bonding; (3) agostic interaction [27−29], a three centred two electron interaction, involves an electron deficient metal atom (Ti, Ta, Zr, Ni, Fe, Ru, Rh etc) as acceptor and an electron rich σ bond of C−H group as donor making the M···(C−H) interaction T shaped; (4) dihydrogen bonds (M−H···H−X) [30−33] where M−H hydrides with $M^{\delta+}$–$H^{\delta-}$ polarisation are the acceptors (M = group III elements including B and transition metals) and X−H (N−H, O−H, C−H) with $X^{\delta-}$–$H^{\delta+}$ polarisation are donors and (5) last but not the least inverse hydrogen bonds, where $D^{\delta+}$–$H^{\delta-}$···$A^{\delta+}$ type of interaction occurs [34−36].

Another important type of non-covalent interactions to build supramolecule involves π-electrons in coordination complexes [37]. Such interactions are divided in two categories face to face or stacked arrangement due to π–π interactions and face to edge or T-shaped arrangement due to C−H···π interactions [38−46]. Some electrostatic forces and van der Waals interactions such as dipole-dipole interaction; dipole-induced dipole interaction; induced dipole-induced dipole interaction; Pauli repulsion and charge transfer are the basic reasons behind the formation of π-stacked arrangements [47−54]. Two parallel interacting aromatic moieties separated by interplanar distance of 3.3–3.8 Å help to stack the molecules. In π–π interactions, aromatic rings are always in slipped or offset alignment to minimize repulsion between π electron clouds and hence exactly face to face arrangement of rings is very rare.

Cationic or anionic parts coordinated or non-coordinated to the metal centre and solvent molecules bonded to the metal ion or trapped in the crystal can participate in various intermolecular non-covalent interactions between themselves and with metal bound ligands to provide interesting packing arrangements [55−69]. Types of solvent, their number and position in trapped condition also afford versatility in supramolecular architectures.

1.3.2. Some copper(II) and nickel(II) complexes reported from our group:

1.3.2.1. Copper(II) complexes:

π-Stacking and metal ion spin exchange: The mixed ligand copper(II) complex, [Cu(bhac)(Hdmpz)] with acetylacetone benzoylhydrazone (H_2bhac) and 3,5-dimethylpyrazole (Hdmpz) has an N_2O_2 square plane around the metal centre. The $bhac^{2-}$ is enolate-O, imine-N and deprotonated amide-O donor and Hdmpz is imine-N donor [58]. With respect to CuN_2O_2 containing mean plane, twisting of phenyl ring is negligible (3.0˚) as well as twisting of Hdmpz ring is also small (11.5˚). Hence the molecule is essentially planar and very much suitable for π–π interactions. Intermolecular Hdmpz ring–chelate ring and Hdmpz ring–Hdmpz ring π–π interactions lead to one-dimensional π-stacked staircase structure of [Cu(bhac)(Hdmpz)] molecules with alternating long (5.596 Å) and short (3.595 Å) Cu···Cu distances. Temperature variable magnetic susceptibility measurements show the antiferromagnetic behavior of the complex. Least-squares fitting of the data using Bleany–Bowers expression provide coupling constant $J = -6.0(1)$ cm^{-1}. EPR measurements also support weakly antiferromagnetically coupled dicopper(II) system. Perhaps π–π interaction between plate like molecules causes direct Cu···Cu spin exchange interaction.

Solvent-dependent zipper and columnar structures: Two ternary copper(II) complexes of general formula [Cu(pyp)X] with 2-N-(picolinylidene)phenol (Hpyp) and halides (X^-= Cl^-, Br^-) have square planar ON_2X coordination geometry around metal centres [65]. Both complexes crystallize as $[Cu(pyp)X]\cdot 2H_2O$ and $[Cu(pyp)X]\cdot CH_3OH$ from their aqua-methanol solutions and dry methanol solutions, respectively. X-ray studies reveal that each complex molecule is perfectly planar and hence can produce π-stacked structure. But the presence of suitable functionalities in the complex molecule that can participate in several intermolecular hydrogen bonding interactions with themselves or with trapped solvent molecules provides the possibilities for different type of packing arrangements other than the π-stacked columnar structure. In $[Cu(pyp)X]\cdot 2H_2O$ complexes, the zipper like structure is formed by (water)O–H···O(water) hydrogen bonded water chain and π-stacked complex molecules connected to the water chain through (water)O–H···O(phenolate)

hydrogen bonds. Two adjacent zippers are again connected via a second (water)O–H···O(water) hydrogen bond and a two-dimensional sheet structure is formed. In [Cu(pyp)X]·CH_3OH complexes, unlike water molecule methanol has only one hydrogen bond donor site and it participates in (methanol)O–H···O(phenolate) and (azomethine)C–H···O(methanol) hydrogen bonds. As a result, a dimer of [Cu(pyp)X]·CH_3OH is formed where two methanol molecules act as bridging units between two molecules of [Cu(pyp)X]. The dimers of [Cu(pyp)X]·CH_3OH form a one-dimensional column-like structure via π–π interactions.

One-, two- and three-dimensional structures: [Cu(bhac)(Hpyrz)]·C_2H_5OH (**1**) [Cu(bhac)(py)] (**2**) and [Cu(bhac)(Himdz)] (**3**) are crystallized forms of three ternary copper(II) complexes with tridentate acetylacetone benzoylhydrazone(H_2bhac) and monodentate N-heterocycles such as pyrazole (Hpyrz), pyridine (py) and imidazole (Himdz) [62]. Each complex has square planar N_2O_2 coordination sphere provided by N,O,O-donor $bhac^{2-}$ and imine-N donor heterocycle. These complexes are not planar due to significant twisting of $bhac^{2-}$ phenyl ring with respect to the CuN_2O_2 containing mean plane. Both **1** and **2** give dimers due to weak apical interactions between copper(II) centre and enolate-O atom of $bhac^{2-}$ in a reciprocal manner, whereas **3** remains as monomer. Molecules of **1** form one-dimensional assembly via intermolecular (ethanol)O–H···O(amide) and (pyrazole)N–H···O(ethanol) hydrogen bonds and intermolecular π–π interactions between pyrazole rings with alternating short (3.602 Å) and long (5.454 Å) Cu···Cu distances. The monomers of **3** form two-dimensional crimped sheet structure with the help of (imidazole)N–H···O(amide) hydrogen bond and weak C–H···π(double bond of methine) interactions. In dimers of **2**, *meta* and *para* C–H of pyridine rings and phenyl π-cloud of $bhac^{2-}$ are involved in intermolecular C–H···π interactions to form a three-dimensional network. Temperature variable magnetic susceptibility measurements suggest that monomeric [Cu(bhac)(Himdz)] is Curie paramagnetic, while dimers of [Cu(bhac)(Hpyrz)]·C_2H_5OH and [Cu(bhac)(py)] show antiferromagnetic spin exchange between metal ions.

Helical self-assembly: Crystal structures of a series of copper(II) complexes of general formula [Cu(L^n)$_2$] (n = 1−4) with bidentate N-(2-hydroxy-5-X-benzyl)-(*R*)-α-methylbenzylamine (HL^n) (HL^1 (X = Cl) and HL^2 (X = Br)) and N-(2-hydroxy-5-X-benzyl)-(*S*)-α-methylbenzylamine (HL^n) (HL^3 (X = Cl) and HL^4 (X = Br)) have been

determined [67]. The enantiomeric pair $[Cu(L^1)_2]$ and $[Cu(L^3)_2]$ crystallize in $P2_12_12_1$ space group, while the other enantiomeric pair $[Cu(L^2)_2]$ and $[Cu(L^4)_2]$ crystallize in $P2_1$ space group. Each of the two space groups is noncentrosymmetric. The metal centre is in N_2O_2 square-plane with a small tetrahedral distortion in each complex. The chiral C centers have *R*-configuration in $[Cu(L^1)_2]$ and $[Cu(L^2)_2]$ and *S*-configuration in $[Cu(L^3)_2]$ and $[Cu(L^4)_2]$. The N-atom of the ligand becomes chiral centre after it is coordinated to the metal centre. The coordinated N-atom has *R*-configuration in $[Cu(L^1)_2]$ and $[Cu(L^2)_2]$, while it has *S*-configuration in $[Cu(L^3)_2]$ and$[Cu(L^4)_2]$. The self assembly of these complexes through C–H···O(phenolate) hydrogen bonds leads to helical structures. In chloro substituted complexes, C–H group of C–H···O interaction is *ortho* to both chloro and methylene while it is *ortho* to bromo and *para* to methylene in bromo substituted complexes. $[Cu(L^1)_2]$ (*R*,*R*) and $[Cu(L^4)_2]$ (*S*,*S*) produce right-handed helices whereas $[Cu(L^2)_2]$ (*R*,*R*) and $[Cu(L^3)_2]$ (*S*,*S*) give left-handed helices.

Enantiospecific inclusion and perfectly polar alignment: Copper(II) complexes of enantiomeric bidentate Schiff base pairs N-(2-hydroxy-5-nitro-benzyl)-(*R*)-α-methylbenzylamine (HL^5) and N-(2-hydroxy-5-nitrobenzyl)-(*S*)-α-methylbenzylamine (HL^6) are synthesized as enantiomers, $[CuL^5{}_2(H_2O)]$ and $[CuL^6{}_2(H_2O)]$ respectively [60,66]. Each of these complexes has square pyramidal coordination geometry where N_2O_2 basal plane has been made by two ligands and the apical site is occupied by water O-atom. The presence of electron withdrawing nitro group facilitates coordination of one water molecule at the apical site of each copper(II). Both complexes crystallize from 1,2-dichloroethane, 1,2-dibromoethane and acetonitrile as six host-guest species $[CuL^5{}_2(H_2O)]\cdot C_2H_4Cl_2$ (**4**) and $[CuL^6{}_2(H_2O)]\cdot C_2H_4Cl_2$ (**5**); $[CuL^5{}_2(H_2O)]\cdot C_2H_4Br_2$ (**6**) and $[CuL^6{}_2(H_2O)]\cdot C_2H_4Br_2$ (**7**); and $[CuL^5{}_2(H_2O)]\cdot CH_3CN$ (**8**) and $[CuL^6{}_2(H_2O)]\cdot CH_3CN$ (**9**), respectively. All these six host-guest species have noncentrosymmetric C_2 space group. Both chiral C centre and metal coordinated N-atom have *R*-configuration in **4**, **6** and **8** and *S*-configuration in **5**, **7** and **9**. In **4**, **5**, **6** and **7**, the guest 1,2-dihaloethane molecules have *gauche* form. These *gauche* 1,2-dihaloethane molecules are in right-handed or P-form in **4** and **6** and in left-handed or M-form in **5** and **7**. All six host-guest species form perfectly polar assembly which is very rare. The host complex molecules create two-dimensional polar layered structure via intermolecular (water)O–H···O(nitro) and (methylene)C–

H···O(water) hydrogen bonds. Guest solvent molecules are trapped and aligned in polar order between two parallel layers of host molecules. The guest molecules are connected with the host molecules via (solvent)C–H···O(nitro) interactions. As a result a polar three-dimensional structure of host-guest molecules is assembled in each case.

Copper(II) complexes with 2-pyridine–carboxaldehyde aroylhydrazones: The Schiff bases 2-pyridine-carboxaldehyde benzoylhydrazone (Hpabh), 2-pyridine-carboxaldehyde 4-methoxybenzoylhydrazone (Hpamh) and 2-pyridine-carboxaldehyde 4-dimethylaminobenzoylhydrazone (Hpadh) have been derived by condensation of 2-pyridinecarboxaldehyde with benzhydrazide, 4-methoxybenzhydrazide and 4-dimethylaminobenzhydrazide, respectively.

Hexacoordinated copper(II) complexes with general formula $[CuL_2]$ (HL = Hpabh, Hpamh and Hpadh) have been prepared by reacting $Cu(OAc)_2 \cdot H_2O$ and HL in 1:2 ratio in methanol [70]. X-ray structure of $[Cu(pabh)_2]$ reveals that the metal centre is in distorted octahedral N_4O_2 environment provided by two N,N,O-donor $pabh^{2-}$. EPR spectra of $[Cu(pabh)_2]$ and $[Cu(pamh)_2]$ at room temperature show rhombic distortion of CuN_4O_2 octahedron where the former display more rhombicity than the latter. The spectrum of $[Cu(padh)_2]$ suggests tetragonal elongation of CuN_4O_2 octahedron.

Reaction of $[Cu(OAc)_2] \cdot H_2O$ with Hpabh and Hpamh (in 1:1 ratio) afford $[Cu_2(\mu\text{-}OAc)_2(pabh)_2]$ (**10**) and $[Cu_2(\mu\text{-}OAc)_2(pamh)_2]$ (**11**), respectively while reaction of $CuCl_2 \cdot 2H_2O$ in presence of KOH with same ligands produce $[Cu_2(\mu\text{-}Cl)_2(pabh)_2]$ (**12**) and polymeric $[Cu(pamh)Cl]_n$ (**13**), respectively [71]. In these complexes, metal ions are in distorted square pyramidal N_2O_3 (**10** and **11**) or N_2OCl_2 (**12** and **13**) environment. In case of dimers, acetate-O atoms act as bridging units in **10** and **11** while two chlorides (Cl^-) act as bridging units for **12**. In **13**, polymeric chain is generated via Cl^- bridges. The bridging units are in equatorial-apical fashion. All four complexes show copper(II)/copper(I) reduction in cyclic voltammetry. In **10** and **11,** each dimer is connected to two neighbouring dimers on both sides via two pairs of intermolecular and reciprocal (azomethine)C–H···O(acetate) interactions. Due to these interactions a one-dimensional chain structure is formed in each case.

Reaction of $[Cu(OAc)_2] \cdot H_2O$ with Hpadh (HL) in 1:1 ratio in methanol affords dimeric $[Cu_2(\mu\text{-}OAc)_2L'_2] \cdot 2H_2O$ where azomethine functionality (–CH=N–) of HL is

transformed to imidate (–C(OMe)=N–) in the coordinated ligand L^{-} [72]. Each copper(II) centre in this dimeric species is in distorted square pyramidal N_2O_3 environment where acetate-O atoms act as the bridging units. This is a rare example of metal ion activated azomethine to imidate transformation.

Reaction of $CuCl_2 \cdot 2H_2O$ with Hpadh produces monomeric $[Cu(Hpadh)Cl_2]$ which has square pyramidal N_2OCl_2 coordination sphere around the metal centre. One Cl atom completes the basal N_2OCl square plane and another Cl-atom occupies the apical site [55]. Two adjacent complex molecules form a dimer through two intermolecular and reciprocal (amide)N–H···Cl(apical) hydrogen bonds. Further π–π interactions between aroyl rings of adjacent dimers lead to one-dimensional assembly with alternating long and short Cu···Cu distances.

1.3.2.2. Nickel(II) complexes:

Nickel(III) species: Two nickel(II) complexes, $[Ni(pamh)_2]$ and $[Ni(pabh)_2]$, with Schiff bases 2-pyridine-carboxaldehyde benzoylhydrazone (Hpabh) and 2-pyridine-carboxaldehyde 4-methoxybenzoylhydrazone (Hpamh), respectively have been prepared. In each complex, the metal centre is in distorted octahedral N_4O_2 coordination sphere assembled by two N,N,O-donor ligands ($pamh^{2-}$ or $pabh^{2-}$) [73]. Both complexes display nickel(II)/nickel(III) oxidation in cyclic voltammetry. The oxidation potentials are 0.97 and 0.91 V vs. Ag/AgCl for $[Ni(pabh)_2]$ and $[Ni(pamh)_2]$, respectively. Lower potential value of $[Ni(pamh)_2]$ than that of $[Ni(pabh)_2]$ is due to the presence of the electron releasing methoxy group in phenyl ring of the ligands in $[Ni(pamh)_2]$. The observed oxidation potential values of these complexes suggest that the nickel(III) species can act as reasonably strong one-electron oxidising agents.

Nickel complexes by ring opening: The condensation of acetylacetone with benzoylhydrazine in a 1:2 mole ratio in methanol provides the cyclized product 1-benzoyl-3,5-dimethyl-5-(1'-benzoylhydrazido)-pyrazoline (bzpyzn). The reaction of bzpyzn with $Ni(O_2CCH_3) \cdot 4H_2O$ in 1:1 ratio under aerobic condition causes the pyrazoline ring opening and produces a green complex thought to be [Ni(bbhac)] where $bbhac^{3-}$ is deprotonated acetylacetone bis(benzoylhydrazone) [74]. However, it turned out to be a dinuclear species [Ni(L–L)Ni] where $(L–L)^{6-}$ represents the product

formed due to oxidative C–C coupling involving the central −CH= fragments of two $bbhac^{3-}$ ligands [75].Room temperature magnetic moment of this complex (1.71 μ_B per nickel) exhibits *S*= ½ spin state. EPR spectra reveal that metal centers in [Ni(L–L)Ni] are in between nickel(III) and nickel(II) stabilised ligand radical systems. In an attempt to grow single crystals of [Ni(L–L)Ni] in wet solvent, crystals of a new complex [Ni(bbhacO)] have been isolated. The central C−C of [Ni(L–L)Ni] is oxidised and converted into keto (−C=O) groups in [Ni(bbhacO)] with the help of moisture. Each [Ni(bbhacO)] molecule is connected to the neighbouring two molecules on both sides through two pair of intermolecular and reciprocal (methyl)C–H···π(phenyl) hydrogen bonds. Due to these interactions [Ni(bbhacO)] molecules form a one-dimensional array in the crystal lattice.

Dimeric and one-dimensional structures: [Ni(bhac)(Hdmpz)] (**14**) and [Ni(bhac)(Himdz)] (**15**) complexes with tridentate acetylacetone benzoylhydrazone (H_2bhac) and monodentate N-heterocycles 3,5-dimethylpyrazole (Hdmpz) and imidazole (Himdz) have been synthesized. In each complex, the metal centre is in square planar N_2O_2 coordination sphere assembled by the N,N,O-donor $bhac^{2-}$ and N-donor heterocycle [57]. Twisting of phenyl rings of $bhac^{2-}$ and the heterocyclic rings (Hdmpz and Himdz) with respect to NiN_2O_2 containing mean plane create non-planarity in both complexes. Hdmpz ring twists by a larger angle in **14** than Himdz ring in **15**. As a result self-assembly pattern of the two complexes are very different due to dissimilar orientations of heterocyclic acidic N−H group involved in intermolecular hydrogen bond formation. Hence **15** forms one-dimensional array via intermolecular (Himdz)N−H···N(amide) hydrogen bond whereas **14** gives dimeric structure through a pair of intermolecular and reciprocal (Hdmpz)N−H···O(amide) hydrogen bonds.

Two dimensional structures: $[Ni(paap)_2]\cdot CH_3COOH\cdot H_2O$ (**16**) and $[Ni(paab)_2]\cdot 2H_2O$ (**17**) with tridentate Schiff bases Hpaap and Hpaab (derived from 2-pyridinecarbaldehyde and *ortho*-aminophenol and *ortho*-aminobenzoic acid, respectively) have distorted octahedral N_4O_2 environment around metal centre provided by two N,N,O-donor ligands ($paap^-$ or $paab^-$) [76]. In **16**, both of the metal bound phenolate-O atoms are hydrogen bonded with CH_3COOH and H_2O. A two-dimensional network of **16** is formed through intermolecular (azomethine)C−H···O(water) interaction. In **17**, the uncoordinated carboxylate-O

atoms act as acceptor in hydrogen bonds with the water molecules. One of the two water molecules is hydrogen bonded with the corresponding symmetry related water molecule to generate a water dimer. The $[Ni(paap)_2]$ molecules form a chain structure via intermolecular (azomethine)C−H···O(carboxylate) hydrogen bonds. The parallel chains of $[Ni(paab)_2]$ are connected by the water dimers to yield a two-dimensional network structure of **17**.

Helices and chiral and achiral networks: Reactions of $Ni(NO_3)_2·6H_2O$, $Na_2(suc)·6H_2O$ (suc = succinate) and 4,4'-bipyridine (bipy) in 1:1:1 molar ratio under different conditions yield coordination polymers $[Ni(suc)(bipy)(H_2O)_2]_n·2nH_2O$ (**18**) and $[Ni(suc)(bipy)(H_2O)_2]_n·nH_2O$ (**19**) [77]. In both complexes, metal centers are in distorted octahedral N_2O_4 coordination sphere provided by mutually *trans* pairs of 4,4'-bipyridine, succinate and water molecules. In **18**, succinate ligands are in right-handed chiral *gauche* conformation that leads to a right-handed six-fold nickel-succinate helix with hydrogen bonded water molecules inside the helix. In **19**, succinate ligands have both right- and left-handed *gauche* conformations and as a result nickel-succinate chains forms both right- and left-handed four-fold helices with hydrogen bonded water molecules outside the helical chain. Bipyridine connected homo-chiral nickel–succinate helices in **18** form a three dimensional dense chiral twisting $7^5.9$ network, whereas bipyridine connected racemic nickel–succinate helices in **19** form a three dimensional achiral distorted $6^5.8$ network.

Intramolecular apical C−H···Ni interaction: Nickel(II) complexes [Ni(bhac)(phim)] (**20**) and [Ni(ahac)(phim)] (**21**) (H_2bhac = acetylacetone benzoylhydrazone, H_2ahac = acetylacetone acetylhydrazone and phim = 2-phenylimidazole) have been synthesized. In each complex, the metal centre is in square planar N_2O_2 coordination sphere assembled by tridentate N,O,O-donor ligand ($bhac^{2-}$ or $ahac^{2-}$) and monodentate N-donor phim [78]. X-ray studies confirm the existence of intramolecular apical C–H···Ni interaction involving the *ortho* C–H group of phenyl ring of monodentate ligand phim in each complex. Both complexes form one-dimensional arrays via intermolecular (imidazole)N–H···O(amide) hydrogen bonds. Variable temperature NMR experiments show a down-field shift of the signal due to the phim phenyl *ortho* C–H indicating the hydrogen bond character of the C–H···Ni interaction in **20** and **21**.

1.3.3. Lanthanide complexes and their versatile applications:

Coordination number: Most stable oxidation state of lanthanides is +3. Hence the chemistry of lanthanide complexes is essentially restricted to this oxidation state. A very interesting topic in lanthanide chemistry is its coordination number (CN) which can vary from 7–12. Large ionic radii of lanthanide metal ions help them to have high coordination numbers. Unlike transition metal complexes, the coordination number of lanthanide complexes is not decided by crystal field effect of ligands. One of the most important factors which determines the coordination number of lanthanides is steric hindrance by coordinating ligands around the metal ion. Steric hindrance by crowding of the donor atoms bound directly with metal centre is called first-order steric effect, whereas second-order steric effect is generated by the other groups attached to the donor atoms [79]. The second order steric effect mainly decides the number of ligands that can bind the metal centre. Normally lanthanide complexes exhibit CN > 6 and that can be upto 12 in case of ligands such as nitrate, 1,8-naphthyridine etc [80]. For complex formation, lanthanide ions always prefer anionic ligands with high electronegative donor atoms like O, F etc. In lanthanide complexes, ligand field effect on deeply seated f-electrons is negligible and as a result spectroscopic and magnetic properties of these complexes are insensitive to coordination number as well as coordination geometry. Therefore X-ray diffraction technique is the only tool to determine the structures and coordination numbers of lanthanide complexes till now. In such a situation, investigation on coordination number of lanthanide complexes is still an interesting research topic to inorganic chemists [80]. Flexible coordination capabilities enable lanthanide tris(β-diketonates) and lanthanide porphyrinates to be used for chiral recognition and chirality sensing agents for biological substrates [81].

MRI agents: Gadolinium(III) chelate complexes are used as contrast agents (CA) for magnetic resonance imaging (MRI) in medical sciences [82]. CA causes drastic variation in water proton relaxation rates and provides important physiological information that could not be provided by uncontrasted images. The drastic variation in water proton relaxation rates significantly affects intensity of MRI signals [83,84]. An efficient CA should be highly paramagnetic metal complex to obtain intense MRI signals in short time and better signal to noise ratio with the attainment of large

number of measurements. Paramagnetism of gadolinium(III) complexes are very high due to the presence of seven unpaired electrons in f orbitals and they have convenient electron relaxation property. Since Gd(III) as free ion even in less amount has tremendous toxicity, the thermodynamically and kinetically stable chelate complexes of gadolinium(III) are preferred as contrast agents where chelating ligands wrap around the metal centre. Gadolinium(III) ion yields highly stable complexes with few cyclic or linear polyaminocarboxilic acids. The first clinically approved contrast agent is Gd-DTPA (Magnevist®, Schering AG, Germany) [82]. Gd-DOTA (Dotarem®, Guerbert SA, France), Gd-DTPA-BMA (Omniscan®, GE Health, USA), Gd-HPDO3A (Prohance®, Bracco Imaging, Italy) are some other examples of CA similar to Gd-DTPA [85].

Single molecule magnets: Now a days, research on single molecule magnets (SMMs) containing lanthanide (4f) ions has attracted considerable attention [86]. The molecules with slow relaxation of magnetisation are considered as single molecule magnet. Large magnetic moments and magnetic anisotropy of 4f ions have made them useful for designing SMMs. Weak exchange interaction due to deeply seated f-electrons in lanthanides further motivates to combine them with organic radicals (2p), transition metals (3d) to design next generation SMMs. Mononuclear double-decker complexes of few 4f ions such as Tb, Dy and Ho with phthalocyanine are examples of some SMMs with 4f ions exclusively [87−89]. Another example of polynuclear pure 4f slow relaxation system is triangular Dy(III) cluster with *ortho*-vanillin ligand, of formula $[Dy_3(OH)_2(o\text{-van})_3(H_2O)_5Cl]^{3+}$ [90]. SMMs having combination 4f−2p involve paramagnetic organic molecules such as nitronyl-nitroxide radicals and rare earth metals. An example of 4f−2p SMM is $[Dy(hfac)_3\{NITpPy\}]_2$ (hfac = hexafluoroacetylacetonate and NITpPy = 2-(4-pyridyl)-4,4,5,5-tetramethyl-4,5-dihydro-1H-imidazolyl-3-oxide) [91]. Most appealing slow relaxation magnetisation is shown by 3d−4f systems. This is because electronic structures as well as magnetic properties of 3d metal ions are immensely influenced by ligand field while ligand field effect on f-electrons is almost negligible and spin-orbit coupling is strong for 4f metal ions. Hence 3d−4f systems provide complicated but promising magnetic property by influencing magnetic behaviours of each other resulting slow relaxation of magnetisation. gadolinium(III) ion containing SMMs have isotropic gadolinium(III) ion to increase only the spin of ground state and the necessary magnetic anisotropy is

provided by the 3d transition metal. In contrast, anisotopic lanthanide(III) ions can also be united with almost isotropic transition metals to enhance exchange interaction. Recent investigations afford number of SMMs with 3d−4f metal ions [92−106]. $[Gd_2Cu_5(OH)_4(Br)_2(H_2L)_2(H_3L)_2(NO_3)_2(OH_2)_4]^{2+}$ [107] (where, H_4L = 2-{[(2-hydroxy-3-methoxyphenyl)methylene]amino}-2-(hydroxymethyl)-1,3-propan-ediol) and $[Fe^{III}_{LS}(bpca)(\mu\text{-}bpca)Dy^{III}(NO_3)_4]$ [108] (where, Hbpca = bis(2-pyridylcarbonylamine)) are excellent examples of SMMs based on 3d−4f combination.

Luminescent complexes of lanthanides: Use of lanthanide (4f) ions such as europium(III), terbium(III), samarium(III), ytterbium(III), neodymium(III) etc in luminescent supramolecular systems has turned into an interesting area of research [109−115]. In lanthanides, f-electrons are deeply seated and hence they have very less interaction with ligand fields. As a result, f−f transitions provide narrow bands in visible region and life time of excited states of lanthanides are in the range of microseconds (e.g. Yb, Nd) and milliseconds (e.g. Eu, Tb) [116]. Such comparatively long-lived emission is an attractive feature in analytical viewpoint, as it is easily distinguished from other short-lived systems. Lanthanides always emit at longer wavelength regions (e.g. 500−750 nm for europium(III)) which help to differentiate them from regular systems emitting at shorter wavelengths. The lanthanide luminescence containing systems have significant advantages over analogous fluorescent systems as it overcomes the general drawbacks such as light scattering and auto fluorescence associated with short wavelengths. The f−f transition is Laporte forbidden and consequently very weak with quite low extinction coefficients (~ 5-10 M^{-1} cm^{-1}). Hence the lanthanide ions need to be excited directly by laser or indirectly by populating suitable sensitising antennae (chromophore) in the ligand [117,118]. Sensitising antenna absorbs a photon and gets excited to singlet excited state (S_1) which passes energy to triplet excited state (T_1) of antenna by intersystem crossing (ISC). The energy transfer from excited S_1 to T_1 (spin forbidden process) in antenna by ISC becomes efficient in presence of heavy metal like lanthanides. Sufficient amount of spin-orbit coupling by lanthanides provides a mechanism for intersystem crossing from S_1 to T_1. The excited state of lanthanide is populated from triplet excited state of antenna by intermolecular energy transfer and in such cases, triplet state of antenna is higher in energy than lanthanide's excited state and must be

positioned in close proximity to the lanthanide ions [119]. Now the lanthanide ions lose its excitation energy by emitting light resulting in long wavelength emission. Lanthanide excited state can lose its energy via non-radiative decay e.g. by vibrational interaction with other molecules such as water molecules. To acquire better emission spectra, vibrational quenching by O−H and N−H oscillators provided by metal bound water molecules and amide of ligand respectively should be minimised. Lanthanide ions tightly bound with chelating ligands are designed with minimum number of metal bound water molecules and with high stability and solubility to reduce non-radiative quenching. Since emission of the luminescent lanthanide complex depends strongly on the nature of the antenna, a small perturbation in the antenna structure caused by the change in the environment (like pH or presence of metal ions) can result in a huge difference in the emission behaviour (wavelength, lifetime and quantum yields) of the complex. By utilising this property, these complexes can be efficiently used as chemical sensors to sense cations such as H^+ and group I and II metal ions as well as transition metal ions [120]. Moreover, these complexes can also be used to study the physical properties and formation of supramolecular structures and self-assemblies [121]. Furthermore, emission at longer wavelength and line-like emission band (~ 10 nm bandwidth) of lanthanides can give better signal to noise ratio compared to wide fluorescent bands (several 100 nm) and hence they are particularly fascinating for diagnostic applications [122−125].

Catalytic property: Lanthanide complexes are also used as catalysts in many organic syntheses. Borohydride complexes of lanthanides catalyse polymerisation reaction [126]. Lanthanide chalcogenolate complexes effectively catalyse several reactions such as conjugate addition, epoxide opening reaction, insertion reaction, polymerization of olefin etc [127]. Utility of lanthanide complexes in asymmetric catalysis is a novel area of research these days to produce enantioselective compounds [128].

1.4. About the present investigation:

In the present investigation,we have explored the chemistry of copper(II), nickel(II), cerium(IV) and gadolinium(III) with a tetradentate Schiff base biacetyl bis(benzoylhydrazone) (H_2babh) and copper(II) chemistry with bidentate 2-(1H-imidazol-2-yl)-pyridine (impy).

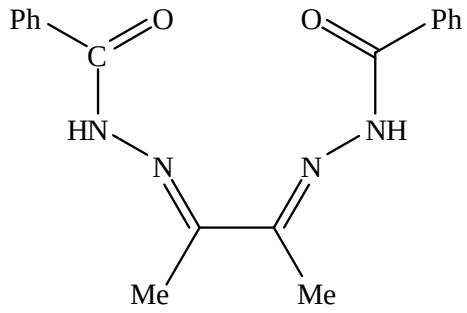

H_2babh

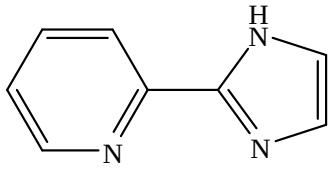

impy

Copper(II) and nickel(II) complexes with biacetyl bis(benzoylhydrazone) (H_2babh) are described in chapter 2. Synthesis, physical properties and X-ray structures are the contents of this chapter [129]. The square-planar [Ni(babh)] complex crystallizes from 1:1 dichrolomethane-*n*-hexane mixture and generates π-stacked columnar structure with uniform Ni···Ni (3.695 Å) distance. Copper(II) complex crystallizes as [Cu(babh)(CH_3OH)] from methanol. Presence of one coordinated methanol at apical site facilitates [Cu(babh)(CH_3OH)] complex to form a methanol bridged dimer through hydrogen bonding. These dimers give a π-stacked columnar assembly with alternating long (5.998 Å) and short (3.934 Å) Cu···Cu distances.

To obtain a π-stacked assembly of [Cu(babh)] with uniform Cu···Cu distance similar to that observed for [Ni(babh)] we have tried to grow single crystals of the copper(II) complex from various non-coordinating solvents. Single crystals without solvent molecule were obtained only from dichloromethane-*n*-hexane (1:1) solution of the complex. However, instead of solvent free mononuclear [Cu(babh)], a double helical dinuclear species [Cu_2(μ-babh)$_2$] has been isolated [130]. Synthetic procedure, characterization, physical properties and structural aspects of this novel dicopper(II) complex are described in chapter 3.

The chapter 4 deals with the copper(II) complexes of 2-(1H-imidazol-2-yl)-pyridine (impy) containing three different counteranions (Cl^-, NO_3^- and ClO_4^-). The complexes were isolated as $[Cu(impy)_2Cl_2]\cdot 3H_2O$, $[Cu(impy)_2(NO_3)]NO_3\cdot H_2O$ and $[Cu(impy)_2(ClO_4)]ClO_4\cdot H_2O$ [131]. The molecular as well as supramolecular structures depend on the nature of the counteranion and the number of water molecules. A three-dimensional honeycomb like structure for $[Cu(impy)_2Cl_2]\cdot 3H_2O$, a ladder like structure for $[Cu(impy)_2(NO_3)]NO_3\cdot H_2O$ and a ribbon like structure for $[Cu(impy)_2(ClO_4)]ClO_4\cdot H_2O$ have been observed as their self-assembly patterns via intra- and intermolecular hydrogen bonding.

Synthesis, characterization, molecular as well as supramolecular structures and properties of cerium(IV) and gadolinium(III) complexes with biacetyl bis(benzoylhydrazone) (H_2babh) are described in the last chapter. Both $[Ce(babh)_2]$ and [Gd(babh)(Hbabh)] complexes have been synthesised by reacting H_2babh with the hydrated salts of the corresponding metal ions in presence of KOH in alcoholic media. The complexes crystallize as $[Ce(babh)_2]\cdot CH_2Cl_2$ and [Gd(babh)(Hbabh)]$\cdot H_2O$. The X-ray structures of two solvated complexes reveal a dodecahedral N_4O_4 coordination environment assembled by the two N_2O_2-donor ligands in each complex. Self-assembly via intermolecular hydrogen bonds and π–π interaction leads to one-dimensional ladder like arrangement of $[Ce(babh)_2]\cdot CH_2Cl_2$. On the other hand, [Gd(babh)(Hbabh)$\cdot H_2O$ forms a two-dimensional sheet structure through hydrogen bonds only.

1.5. References:

[1] A. Werner; *Z. Anorg. Chem.* 3 (1893) 267.

[2] C. Piguet, G. Bernardinelli, G. Hopfgartner; *Chem. Rev.* 97 (1997) 2005.

[3] M. Munakata, L. P. Wu, T. Kuroda-Sowa; *Adv. Inorg. Chem.* 46 (1999) 173.

[4] Proceedings of the Inorganic Crystal Engineering (Dalton Discussion No. 3); *J. Chem. Soc. Dalton Trans.* (2000) 3705.

[5] M, Eddaoudi, D. B. Moler, H. Li, B. Chen, T. M. Reineke, M. O'Keeffe, O. M. Yaghi; *Acc. Chem. Res.* 34 (2001) 319.

[6] M. J. Zaworotko, B. Moulton; *Chem. Rev.* 101 (2001) 1629.

[7] M. Albrecht; *Chem. Rev.* 101 (2001) 3457.

[8] L. Pérez-García, D. B. Amabilino; *Chem. Soc. Rev.* 31 (2002) 342.

[9] O. R. Evans, W. Lin; *Acc. Chem. Res.* 35 (2002) 511.

[10] B. Kesanli, W. Lin; *Coord. Chem. Rev.* 246 (2003) 305.

[11] L. Brammer; *Chem. Soc. Rev.* 33 (2004) 476.

[12] W. Lin; *J. Solid State Chem.* 178 (2005) 2486.

[13] N. Gimeno, R. Vilar; *Coord. Chem. Rev.* 250 (2006) 3161.

[14] S. Kitagawa, R. Matsuda; *Coord. Chem. Rev.* 251 (2007) 2490.

[15] G. R. Desiraju; *Chem. Commun.* (1997) 1475.

[16] G. R. Desiraju; *J. Chem. Soc. Dalton Trans.* (2000) 3745.

[17] D. Braga, F. Grepioni, G. R. Desiraju; *Chem. Rev.* 98 (1998) 1375.

[18] D. Braga, F. Grepioni, P. Sabatino, G. R Desiraju; *Organometallics* 13 (1994) 3532.

[19] A. L. Gillon, G. R. Lewis, A. G. Orpen, S. Rotter, J. Starbuck, X.-M. Wang, Y. Rodriguez-Martin, C. Ruiz-Pérez; *J. Chem. Soc. Dalton Trans.* (2000) 3897.

[20] L. Brammer, J. C. M. Rivas, R. Atencio, S. Fang, F. C. Pigge; *J. Chem. Soc. Dalton Trans.* (2000) 3855.

[21] L. Brammer; in: *Implications of Molecular and Materials Structure for New Technologies, eds*. J. A. K. Howard and F. H. Allen, Kluwer, Dordrecht, (1999) pp. 197.

[22] D. Braga, F. Grepioni, E. Tedesco, K. Biradha, G. R. Desiraju; *Organometallics* 16 (1997) 1846.

[23] F. Calderazzo, G. Fachinetti, F. Marchetti, P. F. Zanazzi; *J. Chem. Soc. Chem. Commun.* (1981) 181.

[24] R. G. Pearson; *Chem. Rev.* 85 (1985) 41.

[25] R. G. Teller, R. Ba; *Struct. Bonding (Berlin)* 44 (1981) 1.

[26] D. Braga, F. Grepioni, E. Tedesco, K. Biradha, G. R. Desiraju; *Organometallics* 15 (1996) 2692.

[27] R. H. Crabtree; *Angew. Chem. Int. Ed. Engl.* 32 (1993) 789.

[28] D. Braga, F. Grepioni, K. Biradha, G. R. Desiraju; *J. Chem. Soc. Dalton Trans.* (1996) 3925.

[29] W. J. Youngs, J. D. Kinder, J. D. Bradshaw, C. A. Tessier; *Organometallics* 12 (1993) 2406.

[30] R. H. Crabtree, P. E. M. Siegbahn, O. Eisenstein, A. L. Rheingold, T. F. Koetzle; *Acc. Chem. Res.* 29 (1996) 348.

[31] P. Kelly, M. Loza; *Chem. Br.* 26 (November issue) (1999).

[32] T. B. Richardson, S. de Gala, R. H. Crabtree; *J. Am. Chem. Soc.* 117 (1995) 12875.

[33] J. P. Campbell, J.-W. Hwang, V. G. Young, Jr., R. B. Von Dreele,C. J. Cramer, W. L. Gladfelter; *J. Am. Chem. Soc.* 120 (1998) 521.

[34] I. Rozas, I. Alkorta, J. Elguero; *J. Phys. Chem. A* 101 (1997) 4236.

[35] J. D. Dill, P. v. R. Schleyer, J. S. Binkley, J. A. Pople; *J. Am. Chem. Soc.* 99 (1977) 6159.

[36] D. J. DeFrees, K. Raghavachari, H. B. Schlegel, J. A. Pople, P. v. R. Schleyer; *J. Phys. Chem.* 91 (1987) 1857.

[37] C. Janiak; *J. Chem. Soc. Dalton Trans.* (2000) 3885.

[38] Review and overviews on C–H···π interactions: M. Nishio, M. Hirota, Y. Umezawa; *The CH/π Interaction (Evidence, Nature and Consequences)*, Wiley-VCH, New York, (1998).

[39] Y. Umezawa, S. Tsuboyama, K. Honda, J. Uzawa, M. Nishio; *Bull. Chem. Soc. Jpn.*71 (1998) 1207.

[40] M. J. Calhorda; *Chem. Commun.* (2000) 801.

[41] G. R. Desiraju, T. Steiner; *The Weak Hydrogen Bond (IUCr Monograph on Crystallography 9)*, Oxford Science Publ, (1999).

[42] Recent examples of C–H···π interactions: M. J. Hannon, C. L. Painting, N. W. Alcock; *Chem. Commun.*, (1999) 2023.

[43] B. J. McNelis, L. C. Nathan, C. J. Clark; *J. Chem. Soc. Dalton Trans.* (1999) 1831.

[44] K. Biradha, C. Seward, M. J. Zaworotko; *Angew. Chem. Int. Ed.* 38 (1999) 492.

[45] N. N. L. Madhavi, A. K. Katz, H. L. Carrell, A. Nangia, G. R. Desiraju; *Chem. Commun.* (1997) 1953.

[46] H.-C. Weiss, D. Bläser, R. Boese, B. M. Doughan, M. M. Haley; *Chem. Commun.* (1997) 1703.

[47] C. A. Hunter; *Chem. Soc. Rev.* (1994) 101.

[48] C. A. Hunter; *Angew. Chem. Int. Ed. Engl.* 32 (1993) 1653.

[49] P. W. Atkins; *Physical Chemistry*, Oxford University Press, (1978) p. 760ff.

[50] J. E. Huheey, E. A. Keiter, R. L. Keiter; *Inorganic Chemistry*, 4th edn., Harper Collins, New York, (1993) p. 296ff.

[51] F. Cozzi, J. S. Siegel; *Pure Appl. Chem.* 67 (1995) 683.

[52] S. B. Ferguson, E. M. Sanford, E. M. Seward, F. Diederich; *J. Am. Chem. Soc.* 113 (1991) 5410.

[53] C. A. Hunter, J. K. M. Sanders; *J. Am. Chem. Soc.* 112 (1990) 5525.

[54] F. Cozzi, M. Cinquini, R. Annuziata, J. S. Siegel; *J. Am. Chem. Soc.* 115 (1993) 5330.

[55] N. R. Sangeetha, S. N. Pal, C. E. Anson, A. K. Powell, S. Pal; *Inorg. Chem. Commun.* 3 (2000) 415.

[56] S. N. Pal, K. R. Radhika, S. Pal; *Z. Anorg. Allg. Chem.* 627 (2001) 1631.

[57] A. Mukhopadhyay, G. Padmaja, S. N. Pal, S. Pal; *Inorg. Chem. Commun.* 6 (2003) 381.

[58] S. Das, G. P. Muthukumaragopal, S. N. Pal, S. Pal; *New J. Chem.* 27 (2003) 1102.

[59] V. K. Muppidi, T. Htwe, P. S. Zacharias, S. Pal; *Inorg. Chem. Commun.* 7 (2004) 1045.

[60] V. K. Muppidi, P. S. Zacharias, S. Pal; *Chem. Commun.* (2005) 2515.

[61] V. K. Muppidi, P. S. Zacharias, S. Pal; *Inorg. Chem. Commun.* 8 (2005) 543.

[62] S. Das, S. Pal; *J. Mol. Struct.* 741 (2005) 183.

[63] S. Das, S. Pal; *J. Mol. Struct.* 753 (2005) 68.

[64] V. K. Muppidi, S. Pal; *Eur. J. Inorg. Chem.* (2006) 2871.

[65] S. Das, S. A. Maloor, S. N. Pal, S. Pal; *Cryst. Growth Des.*, 6 (2006) 2103.

[66] V. K. Muppidi, P. S. Zacharias, S. Pal; *J. Solid. State. Chem.* 180 (2007) 132.

[67] V. K. Muppidi, S. Das, P. Raghavaiah, S. Pal; *Inorg. Chem. Commun.* 10 (2007) 234.

[68] S. Pal; *Rev. Inorg. Chem.* 29 (2009) 111.

[69] S. Das, S. Pal; *Inorg. Chim. Acta.* 363 (2010) 3028.

[70] S. Pal, J. Pushparaju, N. R. Sangeetha, S. Pal; *Trans. Metal. Chem.* 25 (2000) 529.

[71] N. R. Sangeetha, S. Pal; *Polyhedron* 19 (2000) 1593.

[72] N. R. Sangeetha, S. Pal, S. Pal; *Polyhedron* 19 (2000) 2713.

[73] G. V. Karunakar, N. R. Sangeetha, V. Susila, S. Pal; *J. Coord. Chem.* 50 (2000) 51.

[74] A. Mukhopadhyay, S. Pal; *Polyhedron* 23 (2004) 1997.

[75] A. Mukhopadhyay, S. Pal; *Eur. J. Inorg. Chem.* (2009) 4141.

[76] A. Mukhopadhyay, S. Pal; *J. Chem. Cryst.* 35 (2005) 737.

[77] S. Das, S. Maloth, S. Pal; *Eur. J. Inorg. Chem.* (2011) 4270.

[78] A. Mukhopadhyay, S. Pal; *Eur. J. Inorg. Chem.* (2006) 4879.

[79] K. W. Bagnall, X.-F. Li; *J. Chem. Soc. Dalton Trans.* (1982) 1365.

[80] S. A. Cotton; *C. R. Chimie* 8 (2005) 129.

[81] H. Tsukube, S. Shinoda, H. Tamiaki; *Coord. Chem. Rev.* 226 (2002) 227.

[82] S. Aime, S. G. Crich, E. Gianolio, G. B. Giovenzana, L. Tei, E. Terreno; *Coord. Chem. Rev.* 250 (2006) 1562.

[83] M. F. Tweedle; in: J.-C. G. Bünzli, G. R. Choppin (Eds.), *Lanthanide Probes in Life, Chemical and Earth Sciences: Theory and Practice*, Elsevier, Amsterdam, (1989) p. 127.

[84] E. Brücher, A. D. Sherry; in: A. E. Merbach, E. Tóth (Eds.), *The Chemistry of Contrast Agents in Medical Magnetic Resonance Imaging*, Wiley, Chichester, (2001) p. 243.

[85] H. J. Weinmann, A. Mühler, B. Radüchel; in: I. R. Young (Ed.), *Biomedical Magnetic Resonance Imaging and Spectroscopy*, John Wiley & Sons Ltd., Chichester, (2000) p. 705.

[86] R. Sessoli, A. K. Powell; *Coord. Chem. Rev.* 253 (2009) 2328.

[87] N. Ishikawa, M. Sugita, T. Ishikawa, S. Koshihara, Y. Kaizu; *J. Am. Chem. Soc.* 125 (2003) 8694.

[88] N. Ishikawa, M. Sugita, T. Okubo, N. Tanaka, T. Lino, Y. Kaizu; *Inorg. Chem.* 42 (2003) 2440.

[89] N. Ishikawa, M. Sugita, N. Tanaka, T. Ishikawa, S. Y. Koshihara, Y. Kaizu; *Inorg. Chem.* 43 (2004) 5498.

[90] J. K. Tang, I. Hewitt, N. T. Madhu, G. Chastanet, W. Wernsdorfer, C. E. Anson, C. Benelli, R. Sessoli, A. K. Powell; *Angew. Chem. Int. Ed.* 45 (2006) 1729.

[91] G. Poneti, K. Bernot, L. Bogani, A. Caneschi, R. Sessoli, W. Wernsdorfer, D. Gatteschi; *Chem. Commun.* (2007) 1807.

[92] S. Osa, T. Kido, N. Matsumoto, N. Re, A. Pochaba, J. Mrozinski; *J. Am. Chem. Soc.* 126 (2004) 420.

[93] A. Mishra, W. Wernsdorfer, K. A. Abboud, G. Christou; *J. Am. Chem. Soc.* 126 (2004) 15648.

[94] C. M. Zaleski, E. C. Depperman, J. W. Kampf, M. L. Kirk, V. L. Pecoraro; *Angew. Chem. Int. Ed.* 43 (2004) 3912.

[95] F. Mori, T. Ishida, T. Nogami; *Polyhedron* 24 (2005) 2588.

[96] J. P. Costes, F. Dahan, W. Wernsdorfer; *Inorg. Chem.* 45 (2006) 5.

[97] S. Ueki, T. Nogami, T. Ishida, M. Tamura; *Mol. Cryst. Liquid Cryst.* 455 (2006) 129.

[98] C. Aronica, G. Pilet, G. Chastanet, W. Wernsdorfer, J. F. Jacquot, D. Luneau; *Angew. Chem. Int. Ed.* 45 (2006) 4659.

[99] T. Hamamatsu, K. Yabe, M. Towatari, S. Osa, N. Matsumoto, N. Re, A. Pochaba, J. Mrozinski, J. L. Gallani, A. Barla, P. Imperia, C. Paulsen, J. P. Kappler; *Inorg. Chem.* 46 (2007) 4458.

[100] S. Ueki, A. Okazawa, T. Ishida, T. Nogami, H. Nojiri; *Polyhedron* 26 (2007) 1970.

[101] S. Ueki, T. Ishida, T. Nogami, K. Y. Choi, H. Nojiri; *Chem. Phys. Lett.* 440 (2007) 263.

[102] C. M. Zaleski, J. W. Kampf, T. Mallah, M. L. Kirk, V. L. Pecoraro; *Inorg. Chem*. 46 (2007) 1954.

[103] V. Mereacre, D. Prodius, A. M. Ako, N. Kaur, J. Lipkowski, C. Simmons, N. Dalal, I. Geru, C. E. Anson, A. K. Powell, C. Turta; *Polyhedron* 27 (2008) 2459.

[104] T. Yamaguchi, Y. Sunatsuki, H. Ishida, M. Kojima, H. Akashi, N. Re, N. Matsumoto, A. Pochaba, J. Mrozinski, *Inorg. Chem.* 47 (2008) 5736.

[105] V. Mereacre, A. M. Ako, R. Clerac, W. Wernsdorfer, I. J. Hewitt, C. E. Anson, A. K. Powell; *Chem. Eur. J.* 14 (2008) 3577.

[106] G. Novitchi, J. P. Costes, J. P. Tuchagues, L. Vendier, W. Wernsdorfer; *New J. Chem.* 32 (2008) 197.

[107] G. Wu, I. J. Hewitt, S. Mameri, Y. Lan, R. Clerac, C. E. Anson, S. Qiu, A. K. Powell; *Inorg. Chem.* 46 (2007) 7229.

[108] M. Ferbinteanu, T. Kajiwara, K. Y. Choi, H. Nojiri, A. Nakamoto, N. Kojima, F. Cim-poesu, Y. Fujimura, S. Takaishi, M. Yamashita; *J. Am. Chem. Soc.* 128 (2006) 9008.

[109] T. Gunnlaugsson, J. P. Leonard; *Chem. Commun.* (2005) 3114.

[110] J.-C. G. Bünzli; *Acc. Chem. Res.* 39 (2006) 53.

[111] M. Cantuel, F. Gumy, J-C. G. Bünzli, C. Piguet; *Dalton Trans.* (2006) 2647.

[112] J.-C. G. Bünzli, C. Piguet; *Chem. Soc. Rev.* 34 (2005) 1048.

[113] D. Imbert, M. Cantuel, J.-C. G. Bünzli, G. Bernardinelli, C. Piguet; *J. Am. Chem. Soc.* 1251 (2003) 5698.

[114] D. Imbert, M. Cantuel, J. C. G. Bünzli, G. Bernardinelli, C. Piguet; *J. Am. Chem. Soc.* 125 (2003) 15698.

[115] T. Gunnlaugsson, F. Stomeo; *Org. Biomol. Chem.* 5 (2007) 1999.

[116] J. P. Leonard, C. B. Nolan, F. Stomeo, T. Gunnlaugsson, *Top Curr. Chem.* 281 (2007) 1.

[117] R.S. Dickins, C.S. Love, H. Puschmann; *Chem. Commun.* (2001) 2308.

[118] J. I. Bruce, R. S. Dickens, L. J. Govenlock, T. Gunnlaugsson, S. Lopinski, M. P. Lowe, D. Parker, R. D. Peacock, J. J. B. Perry, S. Aime, M. Botta; *J. Am. Chem. Soc.* 122 (2000) 9674.

[119] B. Alpha, J. M. Lehn, R. Ballardini, V. Balzani, S. Perathoner, N. Sabbatini; *Pho-tochem. Photobiol.* 52 (1990) 299.

[120] C. M. G. dos Santos, A. J. Harte, S. J. Quinn, T. Gunnlaugsson; *Coord. Chem. Rev.* 252 (2008) 2512.

[121] D. L. Caulder, K.N. Raymond; *Acc. Chem. Res.* 32 (1999) 975.

[122] I. Hemmilä, V. M. Mukkala; *Crit. Rev. Clin. Lab. Sci*. 38 (2001) 441.

[123] P. G. Sammes, G. Yahioglu; *Nat. Prod. Rep.* (1996) 1.

[124] E. F. Gudgin Dickson, A. Pollak, E. P. Diamandis; *J. Photochem. Photobiol. B: Biol.* 27 (1995) 3.

[125] J. Coates, P. G. Sammes, R. M. West; *J. Chem. Soc. Perkin Trans.* 2 (1996) 1275.

[126] M. Visseaux, F. Bonnet; *Coord. Chem. Rev*. 255 (2011) 374.

[127] H.-X. Li, Y.-J. Zhu, M.-L. Cheng, Z.-G. Ren, J.-P. Lang, Q. Shen; *Coord. Chem. Rev.* 250 (2006) 2059.

[128] M. Shibasaki, N. Yoshikawa; *Chem. Rev.* 102 (2002) 2187.

[129] T. Ghosh, A. Mukhopadhyay, K. S. C. Dargaiah, S. Pal; *Struct. Chem.* 21 (2010) 147.

[130] T. Ghosh, S. Pal; *Inorg. Chim. Acta.* 363 (2010) 3632.

[131] T. Ghosh, S. Das, S. Pal; *Polyhedron* 29 (2010) 3074.

Chapter 2

Nickel(II) and copper(II) complexes with biacetyl bis(benzoylhydrazone): Self-assembly via π–π interaction and hydrogen bonding[§]

2.1. Abstract:

Reactions of $Ni(O_2CCH_3)_2 \cdot 4H_2O$ and $Cu(O_2CCH_3)_2 \cdot H_2O$ with biacetyl bis(benzoylhydrazone) (H_2babh) in alcoholic media afford mononuclear nickel(II) and copper(II) complexes of general formula [M(babh)]. The complexes have been characterized by microanalysis (C, H, N), magnetic susceptibility and various spectroscopic (IR, UV-Vis, NMR and EPR) measurements. X-ray structures of both complexes have been determined. The metal centre in [Ni(babh)] is in square-planar N_2O_2 environment provided by the tetradentate babh^{2-}. On the other hand, [Cu(babh)] crystallizes as distorted square-pyramidal [Cu(babh)(CH_3OH)] from methanol. Here the tetradentate babh^{2-} constitutes the N_2O_2 square-base and the O-coordinating methanol occupies the apical site. In the crystal lattice, the molecules of [Ni(babh)] form a one-dimensional π-stacked structure. The [Cu(babh)(CH_3OH)] molecules also form a one-dimensional structure with alternating long and short Cu···Cu distances via intermolecular O–H···N hydrogen bonding and π–π interaction.

[§]This work has been published in *Struct. Chem.* 21 (2010) 147.

2.2. Introduction:

Over the past few years our group has been working on square-planar/square-pyramidal complexes of nickel(II) and copper(II) with acid hydrazide based tridentate Schiff bases and various monodentate ancillary ligands [1–11]. Structural investigations on these complexes revealed formation of a variety of self-assembled one-, two- and three-dimensional networks via different types of intermolecular non-covalent interactions. In the present chapter, we have described the synthesis and characterization of mononuclear nickel(II) and copper(II) complexes with the tetradentate Schiff base biacetyl bis(benzoylhydrazone) (H_2babh, 2H represent the dissociable amide protons). The crystal structures of both complexes have been determined and the self-assembled motifs formed by them are reported.

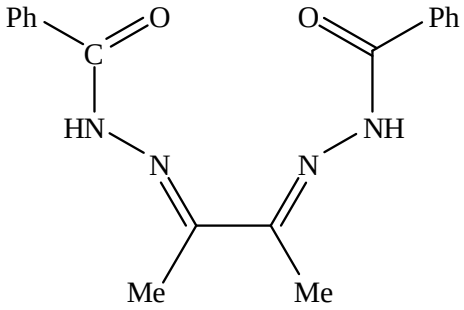

H_2babh

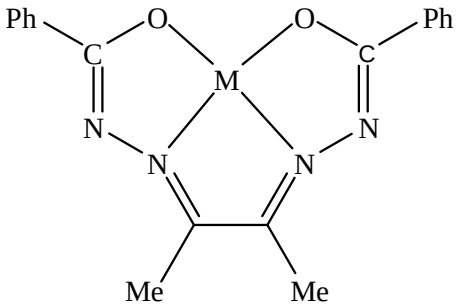

[M(babh)]

2.3. Experimental:

2.3.1. Materials:

The tetradentate Schiff base biacetyl bis(benzoylhydrazone) (H_2babh) was synthesized in ~70% yield by condensation of one mole equivalent of biacetyl with two mole equivalents of benzoylhydrazine in dry ethanol. All other chemicals and solvents were of analytical grade available commercially and were used as received.

2.3.2. Physical measurements:

A Thermo Finnigon Flash EA1112 series elemental analyzer was used for the microanalysis (C, H, N) data. Infrared spectra were recorded by using KBr pellets on a Jasco-5300 FT-IR spectrophotometer. A Cary 100 Bio UV/vis spectrophotometer was used to record the electronic spectra. The ^{1}H NMR spectrum of the nickel(II) complex in $CDCl_3$ solution was recorded with the help of a Bruker 400 MHz NMR spectrometer. X-band EPR measurements with the copper(II) complex were performed on a Jeol JES-FA200 spectrometer. Room temperature (300 K) magnetic susceptibilities were measured using a Sherwood Scientific balance. Diamagnetic corrections calculated from Pascal's constants [12] were used to obtain the molar paramagnetic susceptibilities. A Digisun DI-909 conductivity meter was used to measure the solution electrical conductivities.

2.3.3. Synthesis of [Ni(babh)]:

An ethanol solution (10 ml) of $Ni(O_2CCH_3)_2{\cdot}4H_2O$ (155 mg, 0.62 mmol) was added to an ethanol solution (15 ml) of H_2babh (200 mg, 0.62 mmol) and the mixture was refluxed for 4 h. The dark crystalline solid formed after cooling to room temperature was collected by filtration, washed with ice-cold ethanol and finally dried in air. The yield was 115 mg (49%). Anal. calcd. for $NiC_{18}H_{16}N_4O_2$ (379.06): C, 57.04; H, 4.25; N, 14.78%. Found: C, 57.12; H, 4.11; N, 14.63%. UV-Vis (in CH_3OH) (λ_{max}/nm (10^{-3} x ε/M^{-1} cm^{-1})): 395 (12), 298 (17.8), 220^{sh} (21.7).

2.3.4. Synthesis of [Cu(babh)]:

A methanol solution (15 ml) of $Cu(O_2CCH_3)_2{\cdot}H_2O$ (124 mg, 0.62 mmol) was added to a methanol solution (15 ml) of H_2babh (200 mg, 0.62 mmol) and the mixture was stirred in air at room temperature for 5 h. The brown microcrystalline solid separated was collected by filtration, washed with ice-cold methanol and finally dried in air. The yield was 174 mg (73%). Anal. calcd. for $CuC_{18}H_{16}N_4O_2$ (383.89): C,

56.32; H, 4.20; N, 14.59%. Found: C, 56.11; H, 4.02; N, 14.36%. UV-Vis (in CH_3OH) (λ_{max}/nm (10^{-3} x ε/M^{-1} cm^{-1})): 450 (15.6), 280 (38.4), 220^{sh} (25.5).

2.3.5. X-ray crystallography:

Single crystals of the nickel(II) complex were grown by slow evaporation of its solution in dichloromethane–*n*-hexane (1:1) mixture. On the other hand, single crystals of the copper(II) complex were obtained by slow evaporation of the filtrate obtained from the synthetic reaction mixture. The crystals of the copper(II) complex lose solvent rapidly and become amorphous when they are taken out of the mother liquor. The crystal used for data collection was coated with a thin layer of epoxy to prevent the solvent loss. In each case, unit cell parameters and the intensity data were obtained on a Bruker-Nonius SMART APEX CCD single crystal diffractometer, equipped with a graphite monochromator and a Mo Kα fine-focus sealed tube (λ = 0.71073 Å) operated at 2.0 kW. The detector was placed at a distance of 6.0 cm from the crystal. Data were collected at 298 K with a scan width of 0.3º in ω and an exposure time of 15 s/frame. The SMART software was used for data acquisition and the SAINT-Plus software was used for data extraction [13]. The absorption corrections were performed with the help of SADABS program [14]. The nickel(II) complex [Ni(babh)] crystallizes in the orthorhombic space group *P*bca, while the copper(II) complex crystallizes as [Cu(babh)(CH_3OH)] in the triclinic space group $P\bar{1}$. The structures were solved by direct methods and refined on F^2 by full-matrix least-squares procedures. In each case, the asymmetric unit contains a whole complex molecule. The non-hydrogen atoms in both structures were refined using anisotropic thermal parameters. The positional parameters of the methanol OH group hydrogen atom in [Cu(babh)(CH_3OH)] located in a difference Fourier map were refined with U_{iso}(H) = 1.5U_{eq}(O). The remaining hydrogen atoms in [Cu(babh)(CH_3OH)] and all the hydrogen atoms in [Ni(babh)] were included in the structure factor calculations at idealized positions by using a riding model. The SHELX-97 programs [15] available in the WinGX package [16] were used for structure solution and refinement. The ORTEX6a [17] and Platon [18] packages were used for molecular graphics. Selected crystallographic data are listed in Table 2.1.

Table 2.1: Crystallographic data for [Ni(babh)] and [Cu(babh)(CH$_3$OH)]

Complex	[Ni(babh)]	[Cu(babh)(CH$_3$OH)]
Empirical formula	$NiC_{18}H_{16}N_4O_2$	$CuC_{19}H_{20}N_4O_3$
Formula weight	379.06	415.93
Temperature (K)	298(2)	298(2)
Crystal size (mm)	0.48 x 0.36 x 0.15	0.48 x 0.48 x 0.25
Crystal system	Orthorhombic	Triclinic
Space group	*P*bca	$P\bar{1}$
a(Å)	18.1487(15)	8.3576(7)
b(Å)	6.6434(6)	10.1357(8)
c(Å)	28.386(2)	12.032(1)
α(°)	90	111.661(1)
β(°)	90	96.755(1)
γ(°)	90	94.502(1)
V(Å^3)	3422.5(5)	932.44(13)
Z	8	2
Calculated density (g cm^{-3})	1.471	1.481
Absorption coefficient (mm^{-1})	1.152	1.198
Reflections collected	36884	9712
Reflections unique	4160	3644
Reflections ($I \geq 2\sigma(I)$)	3481	3149
Data/restraints/parameters	4160/0/228	3644/0/250
*R*1, *wR*2 ($I \geq 2\sigma(I)$)	0.0555, 0.1171	0.0687, 0.1821
*R*1, *wR*2 (all data)	0.0687, 0.1229	0.0774, 0.1895
Goodness-of-fit on F^2	1.206	1.052
Largest diff. peak and hole (e Å^{-3})	0.514, –0.320	0.910, –0.808

2.4. Result and discussion:

2.4.1. Synthesis and some properties:

Mononuclear nickel(II) and copper(II) complexes of general empirical formula [M(babh)] were prepared in good yields by reacting the tetradentate Schiff base (H_2babh) with the corresponding hydrated bivalent metal acetate in alcoholic media. The microanalytical data for both complexes support the empirical formula. Room temperature (298 K) magnetic susceptibility measurements with powdered samples of the complexes revealed the diamagnetic character of [Ni(babh)] and paramagnetic nature of [Cu(babh)]. Thus, the coordination geometry around the metal centre in [Ni(babh)] is square-planar. The effective magnetic moment (1.89 μ_B) of [Cu(babh)] is consistent with the S = 1/2 spin state. Both complexes are soluble in common organic solvents such as methanol, ethanol, acetonitrile, dichloromethane etc. [Ni(babh)] provides a green solution, whereas [Cu(babh)] gives a brown solution. Both complexes behave as non-electrolyte in solution phase.

2.4.2. Spectral features:

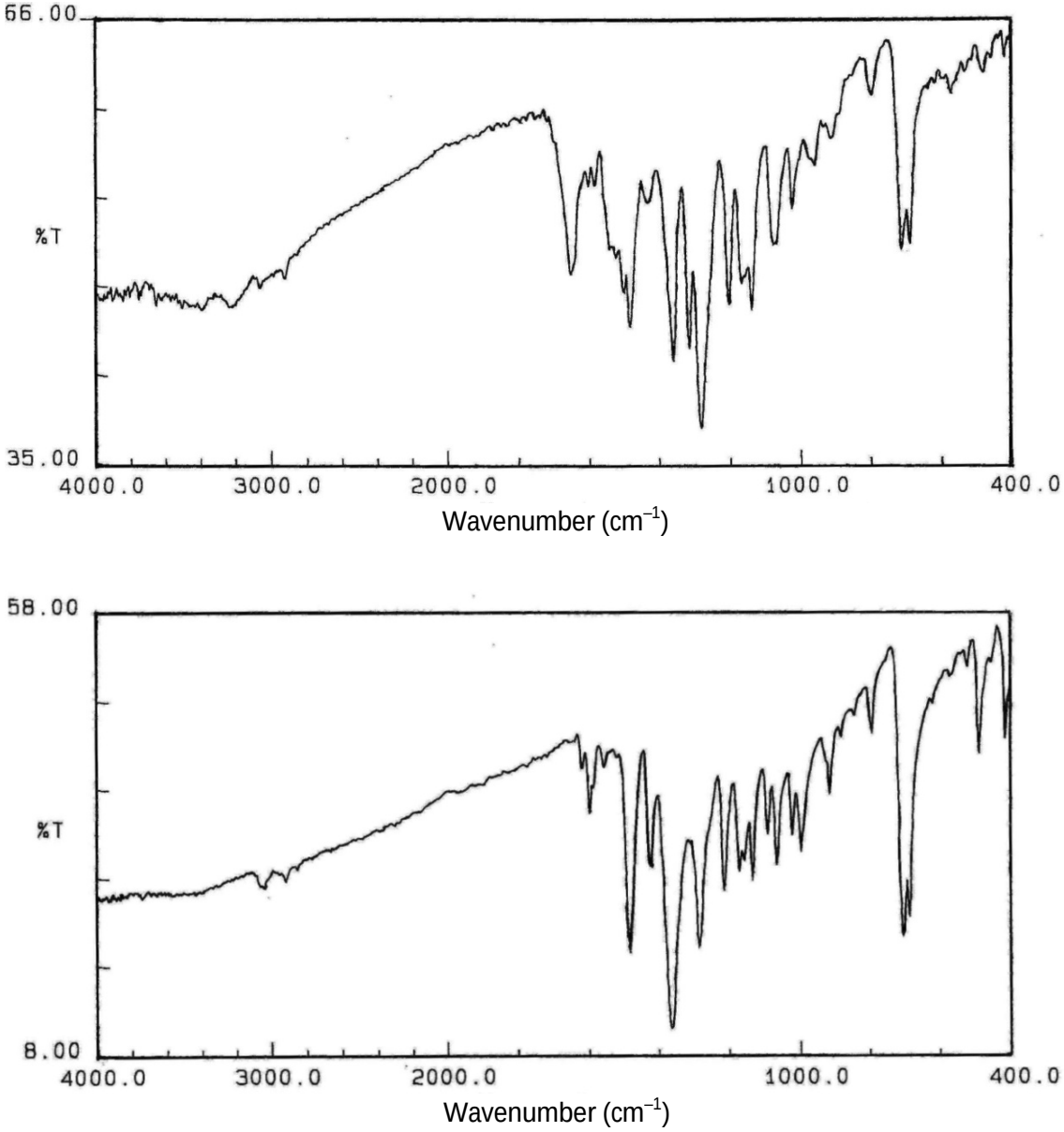

Fig. 2.1: Infrared spectra of [Ni(babh)] (top) and [Cu(babh)] (bottom).

Infrared spectrum of the free Schiff base H_2babh displays the N–H and the C=O stretches of the amide functionalities as a medium intensity band at ~3200 cm^{-1} and a very strong broad band at ~1655 cm^{-1}, respectively [19]. These two bands are not observed in the spectra of the complexes (Fig. 2.1). Absence of these bands is consistent with the iminolate form [1–11,20] of both amide fragments of the ligand (babh^{2-}). [Ni(babh)] displays a strong sharp band at ~1640 cm^{-1}, while [Cu(babh)]

shows a medium intensity band at 1618 cm^{-1}. These bands are presumably associated with the –C=N–N=C– moieties of the ligand.

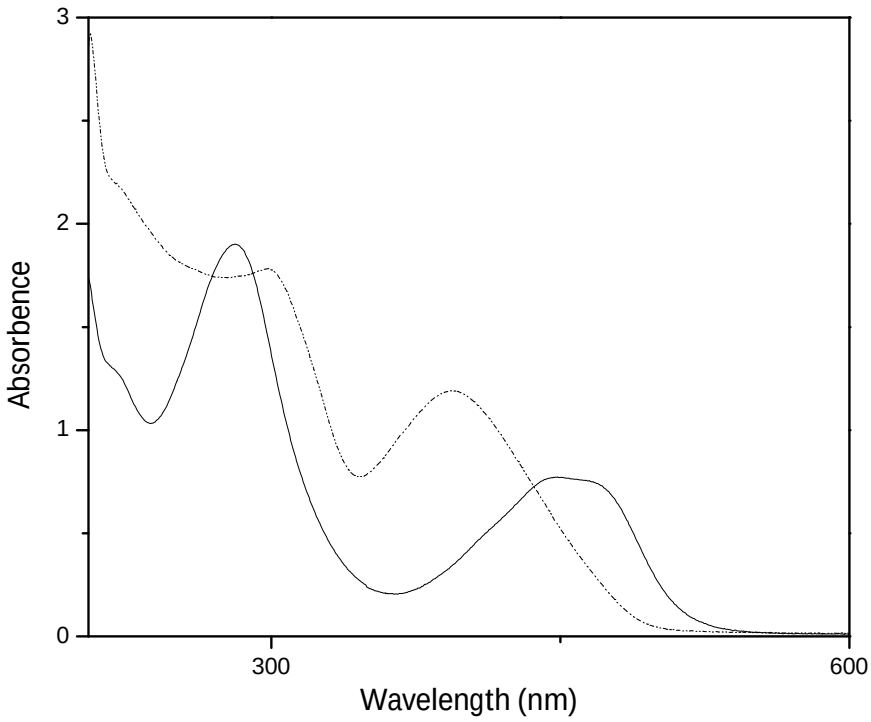

Fig. 2.2: Electronic spectra of [Ni(babh)] (····) and [Cu(babh)] (—) in methanol.

Electronic spectra of the complexes were recorded in methanol solution (Fig. 2.2). Both complexes display a strong band in the visible region. Below 300 nm they display a very intense band and a shoulder. The visible region absorption is attributed to the ligand-to-metal charge transfer transition. Due to this strong band no ligand field band is observed for either of the two complexes. The absorptions in the UV range are in all likelihood due to intra-ligand transitions.

A $CDCl_3$ solution of the diamagnetic nickel(II) complex was used to record the proton NMR spectrum. The protons of the two methyl groups resonate as a singlet at δ 1.97 ppm. The *ortho* protons of the two phenyl rings appear as a doublet at δ 7.95 ppm (J = 8 Hz). The *para* and *meta* protons are observed as triplets at δ 7.45 ppm (J = 7 Hz) and δ 7.34 ppm (J = 8 Hz), respectively.

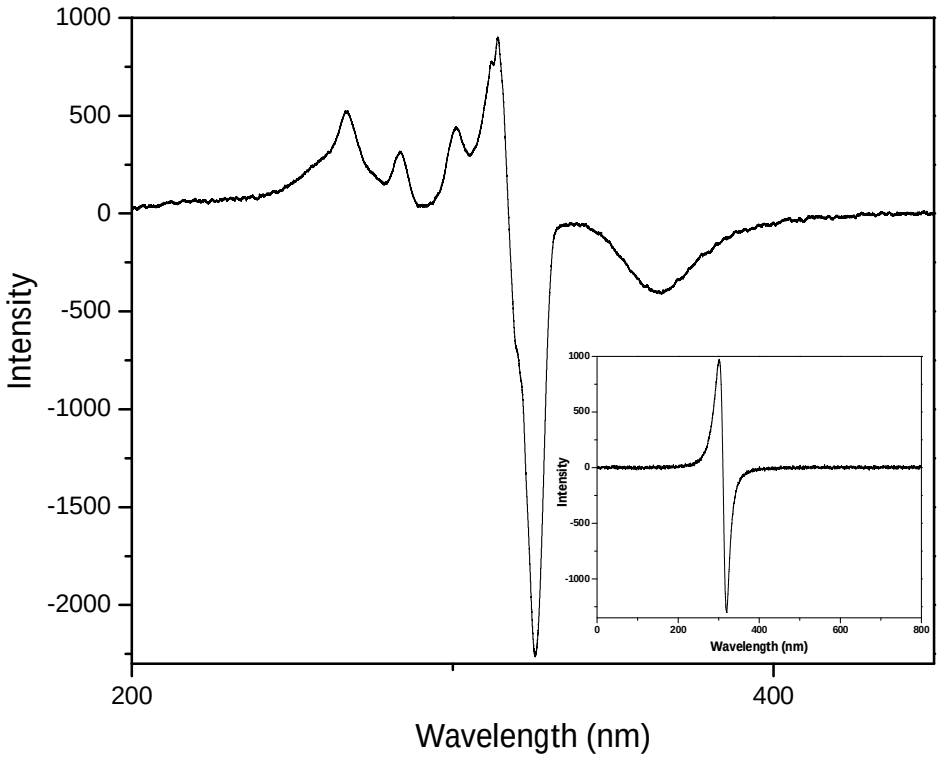

Fig. 2.3: EPR spectra of [Cu(babh)] in frozen methanol and ethanol solution and in powder (inset).

The EPR spectra of the one electron paramagnetic copper(II) complex were recorded in powder as well as in frozen (115 K) methanol-ethanol (1:1) solution (Fig. 2.3). The room temperature (298 K) powder spectrum displays an asymmetric signal at g = 2.07. An axial spectrum typical of mononuclear square-planar or square-pyramidal copper(II) species was obtained with the frozen solution of the complex [8–10]. The $g_{\|}$, $A_{\|}$ and $g_{\perp}$ values are 2.23, 170 G and 2.03, respectively.

2.4.3. Molecular structures:

The molecular structures of the nickel(II) and the copper(II) complex determined by X-ray crystallography have been depicted in Figs. 2.4 and 2.5, respectively. The nickel(II) complex is square-planar and contains only the tetradentate ligand, while the copper(II) complex is distorted square-pyramidal due to

coordination of an additional methanol molecule at the apical site. The bond parameters associated with the metal ions are listed in Table 2.2. In both complexes, $babh^{2-}$ binds the metal centre through the two imine-N and the two deprotonated amide-O atoms forming three five-membered chelate rings and an N_2O_2 square-plane around the metal centre. The C–O (1.282(6)–1.303(3) Å) and the C=N (1.323(3)–1.337(6) Å) bond lengths in the amide functionalities of $babh^{2-}$ are within the ranges observed for its O-coordinating iminolate form (–N=C(O^-)–) in various complexes [1–11,20]. The remaining intraligand bond parameters are unexceptional. The metal to O(amide) and metal to N(imine) bond lengths in [Ni(babh)] and [Cu(babh)(CH_3OH)] (Table 2.2) are similar to the bond lengths observed in the corresponding bivalent metal ion complex having the same coordinating atoms [1–11]. In the latter complex, the apical Cu–O(methanol) bond length is relatively longer than the equatorial bond lengths. Such long copper(II) to apical solvent bond lengths in square-pyramidal copper(II) species are not unusual [4,21,22].

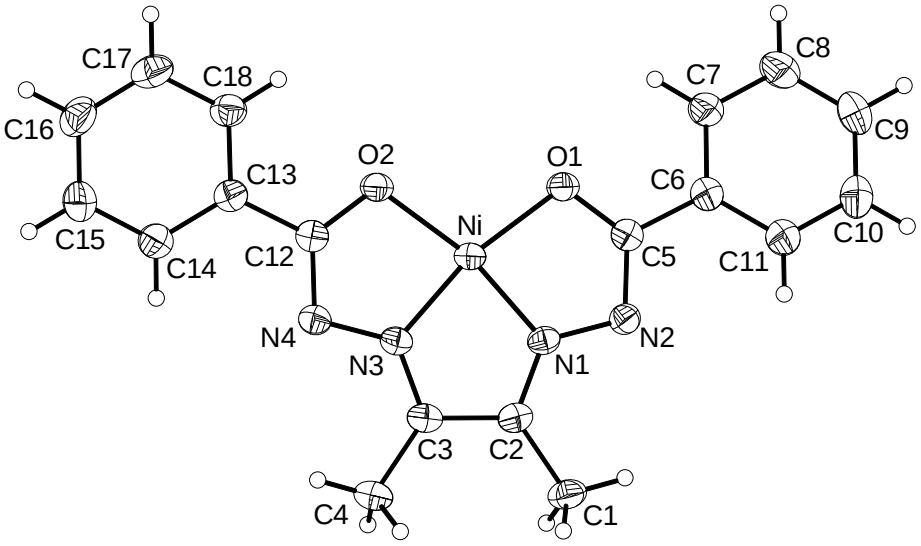

Fig. 2.4: Molecular structure of [Ni(babh)] with the atom labeling scheme. The non-hydrogen atoms are represented by their 30% probability thermal ellipsoids.

In the square-planar [Ni(babh)], there is no displacement of the metal centre from the N_2O_2 square plane. In fact except for the two phenyl rings the remaining part of [Ni(babh)] is perfectly planar (Fig. 2.4). The maximum and minimum deviations from the mean plane constituted by Ni, O(1), O(2), N(1)–N(4), C(1)–C(5) and C(12)

are 0.034(2) and 0.002(2) Å, respectively. However, the whole molecule is not completely planar due to small but noticeable twisting of the phenyl rings along the C–C bonds that connect them with the chelate rings. The dihedral angles formed by the mean planes constituted by C(6)–C(11) (mean deviation 0.004 Å) and C(13)–C(18) (mean deviation 0.003 Å) with the mean plane constituted by the remaining atoms of the molecule are 17.4(1) and 16.6(1)^o, respectively. However, the two rings are twisted in opposite direction.

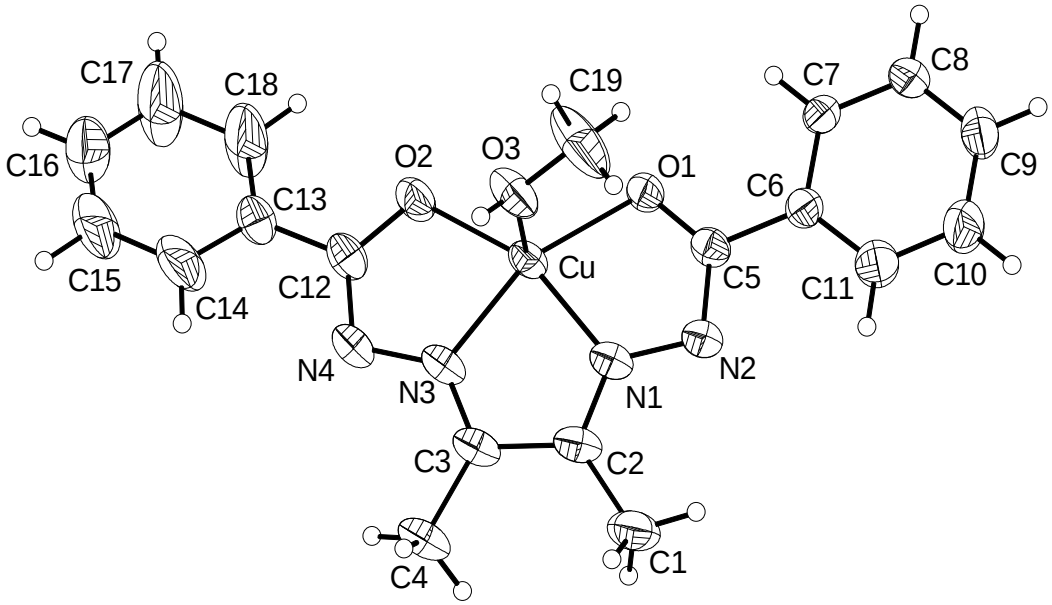

Fig. 2.5: Molecular structure of [Cu(babh)(CH$_3$OH)] with the atom labeling scheme. The non-hydrogen atoms are represented by their 30% probability thermal ellipsoids.

As commonly observed in square-pyramidal copper(II) species, the metal centre is displaced by 0.201(2) Å from the N_2O_2 square-base (mean deviation 0.02 Å) towards the apical methanol oxygen atom O(3) in [Cu(babh)(CH$_3$OH)] (Fig. 2.5). Due to this displacement of the copper centre from the square-base, the chelate bite angles (79.03(17)–80.52(18)^o) are smaller than the chelate bite angles (83.38(8)–84.25(10)^o) in [Ni(babh)]. As in [Ni(babh)], here also excluding the two phenyl rings the other atoms of babh^{2-} namely O(1), O(2), N(1)–N(4), C(1)–C(5) and C(12) are satisfactorily planar. The maximum and minimum deviations from the mean plane are 0.102(4) and 0.005(4) Å, respectively. However, here only the second phenyl ring

(C(13)–C(18), mean deviation 0.02 Å) is twisted along the C(12)–C(13) bond. The dihedral angle between the mean plane containing C(13)–C(18) and the previously described mean plane is 11.0(9)^{o}. The corresponding dihedral angle formed by the first phenyl ring (C(6)–C(11), mean deviation 0.009 Å) is only 3.9(3)^{o}.

Table 2.2: Selected bond lengths (Å) and bond angles (^{o}) for [Ni(babh)] and [Cu(babh)(CH_3OH)]

[Ni(babh)]			
Ni–N(1)	1.7969(19)	Ni–N(3)	1.796(2)
Ni–O(1)	1.8834(17)	Ni–O(2)	1.8845(17)
N(1)–Ni–N(3)	84.25(10)	N(1)–Ni–O(1)	83.38(8)
N(1)–Ni–O(2)	167.67(8)	N(3)–Ni–O(1)	167.55(8)
N(3)–Ni–O(2)	83.45(8)	O(1)–Ni–O(2)	108.93(8)
[Cu(babh)(CH_3OH)]			
Cu–N(1)	1.907(4)	Cu–N(3)	1.929(4)
Cu–O(1)	1.981(3)	Cu–O(2)	1.975(4)
Cu–O(3)	2.216(4)		
N(1)–Cu–N(3)	80.52(18)	N(1)–Cu–O(1)	79.64(15)
N(1)–Cu–O(2)	156.77(17)	N(1)–Cu–O(3)	101.47(19)
N(3)–Cu–O(1)	158.31(17)	N(3)–Cu–O(2)	79.03(17)
N(3)–Cu–O(3)	101.81(15)	O(1)–Cu–O(2)	118.27(13)
O(1)–Cu–O(3)	90.67(14)	O(2)–Cu–O(3)	93.42(19)

2.4.4. Intermolecular interactions and self- assembly:

Square-planar or square-pyramidal complexes can participate in intermolecular π–π interaction and form one-dimensional infinite chain structure or discrete dimeric species [3,6,8–10,21,22]. We have scrutinized in detail the crystal structures of both [Ni(babh)] and [Cu(babh)(CH_3OH)] to find out their self-assembly patterns via different possible intermolecular non-covalent interactions.

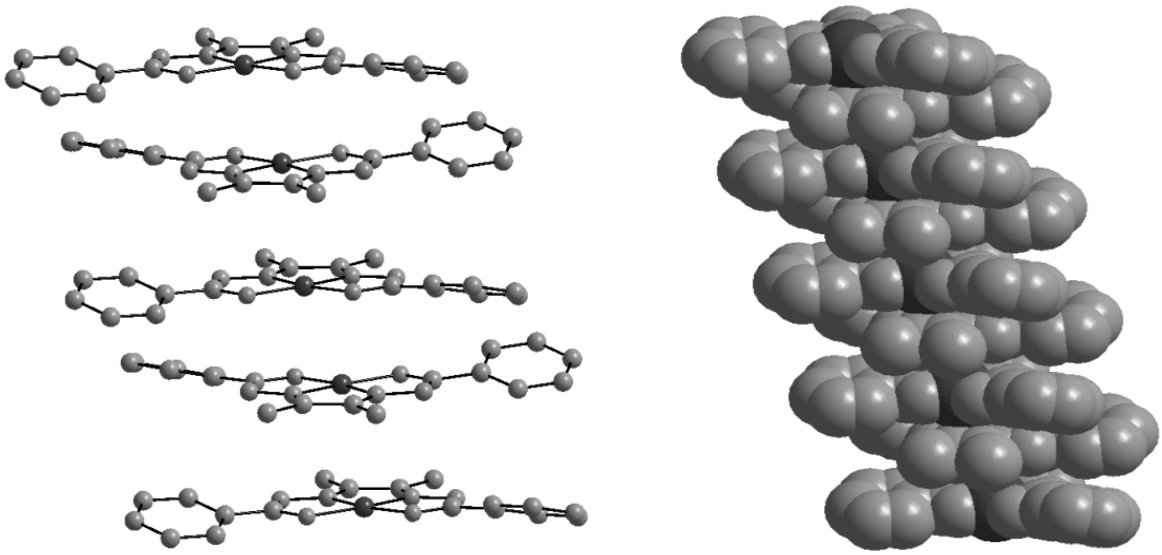

(a) (b)

Fig. 2.6: One-dimensional π-stacked assembly of [Ni(babh)]. (a) Ball and stick and (b) space filling models. Hydrogen atoms are omitted for clarity.

The planar [Ni(babh)] molecules are indeed involved in π–π interaction and form one-dimensional π-stacked structure (Fig. 2.6). In this infinite chain, the chelate rings of each molecule participate in the π–π interactions with the chelate rings of the adjacent molecules. Among the overlapping chelate rings, the distance (3.322(1) Å) between the centroids (cg) of NiN(1)C(2)C(3)N(3) and NiN(3)N(4)C(12)O(2) rings is the shortest (Fig. 2.4). The Ni···Ni distance in this chain is 3.6954(4) Å. There is no other noteworthy intra- and interchain non-covalent interaction.

The square-pyramidal [Cu(babh)(CH$_3$OH)] molecules form dimeric units via a pair of reciprocal O–H···N hydrogen bonds (Fig. 2.7). In this hydrogen bonding, the methanol OH group acts as the donor and the uncoordinated deprotonated amide N-atom acts the acceptor. The O···N distance and the O–H···N angle are 2.807(5) Å and 173(9)^o, respectively. In this hydrogen bonded dimeric unit, the Cu···Cu distance is 5.998(1) Å. As observed in the case of [Ni(babh)] the chelate rings of [Cu(babh)(CH$_3$OH)] are involved in intermolecular π–π interaction. Here the shortest cg···cg distance (3.471(3) Å) involves the CuN(1)N(2)C(5)O(1) and CuN(3)N(4)C(12)O(2) chelate rings (Fig. 2.5)

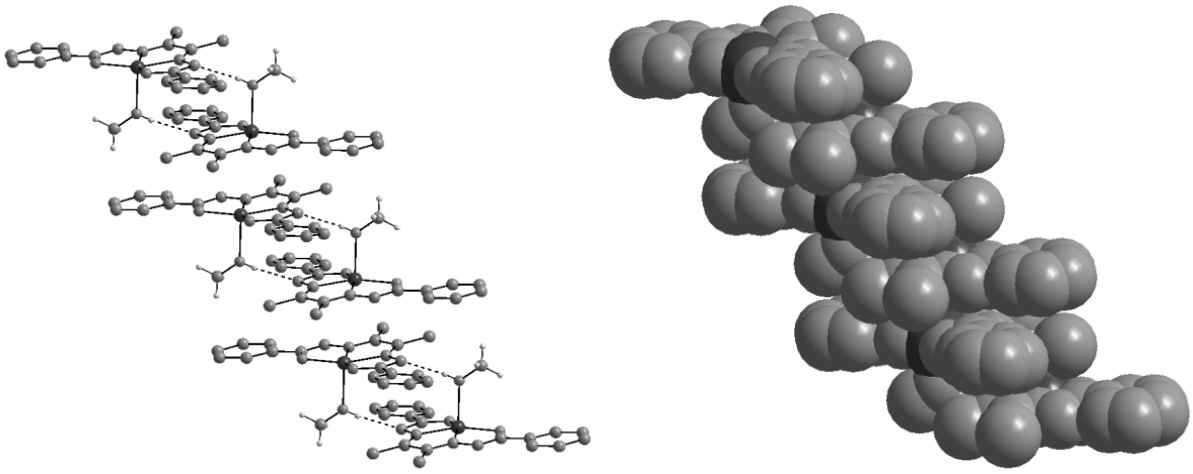

(a) (b)

Fig. 2.7: One-dimensional ordering of [Cu(babh)(CH_3OH)] via O–H···N hydrogen bonding and π–π interaction. (a) Ball and stick model with only the methanol hydrogen atoms and (b) space filling model without hydrogen atoms.

Each hydrogen bonded dimer of [Cu(babh)(CH_3OH)] participates in such π–π interaction with its adjoining dimers (Fig. 2.7). As a result these dimeric units are ordered in a one-dimensional array. The Cu···Cu distance (3.934(1) Å) in the π-stacked fragments is significantly less than that in the hydrogen bonded fragments of this array. Thus the self-assembly of [Cu(babh)(CH_3OH)] via the O–H···N hydrogen bonding and the π–π interaction leads to an infinite chain structure (Fig. 2.7) with atypical alternating long and short Cu···Cu distances [3,8,9,23]. There is no significant short contact or non-covalent interaction between the adjacent chains.

2.5. Conclutions:

Nickel(II) and copper(II) complexes with the Schiff base biacetyl bis(benzoylhydrazone) (H_2babh) are described. Elemental analysis and physical properties of the complexes suggest a general formula [M(babh)]. X-ray structural investigation reveals that the square-planar [Ni(babh)] crystallizes as it is from dichloromethane–*n*-hexane (1:1), whereas the copper(II) complex crystallizes as

distorted square-pyramidal [Cu(babh)(CH_3OH)] from methanol. In each of the two complexes, the tetradentate ligand $babh^{2-}$ forms an N_2O_2 square-plane around the metal centre via the two imine-N and the two deproptonated amide-O atoms. The methanol O-atom occupies the apical site in the copper(II) complex. But for slight twisting of the two phenyl ring planes of $babh^{2-}$ along the connecting C–C bonds, the remaining part of [Ni(babh)] is perfectly planar. In the crystal lattice, the essentially planar molecules of this complex form a π-stacked one-dimensional assembly where the Ni···Ni distance is constant. The square-pyramidal [Cu(babh)(CH_3OH)] molecules also form a one-dimensional assembly via intermolecular alternating O–H···N hydrogen bonding and π–π interaction. Consequently this chain structure has alternating long and short Cu···Cu distances.

2.6. References:

[1] N. R. Sangeetha, K. Baradi, R. Gupta, C. K. Pal, V. Manivannan, S. Pal; *Polyhedron* 18 (1999) 1425.

[2] N. R. Sangeetha, S. Pal; *J. Chem. Crystallogr.* 29 (1999) 287.

[3] N. R. Sangeetha, S. N. Pal, C. E. Anson, A. K. Powell, S. Pal; *Inorg. Chem. Commun.* 3 (2000) 415.

[4] N. R. Sangeetha, S. Pal; *Polyhedron* 19 (2000) 1593.

[5] N. R. Sangeetha, S. N. Pal, S. Pal; *Polyhedron* 19 (2000) 2713.

[6] S. Pal; *Proc. Indian Acad. Sci. (Chem Sci)* 114 (2002) 417.

[7] A. Mukhopadhyay, G. Padmaja, S. N. Pal, S. Pal; *Inorg. Chem. Commun.* 6 (2003) 381.

[8] S. Das, G. P. Muthukumaragopal, S. N. Pal, S. Pal; *New J. Chem.* 27 (2003) 1102.

[9] S. Das, S. Pal; *J. Mol. Struct.* 741 (2005) 183.

[10] S. Das, S. Pal; *J. Mol. Struct.* 753 (2005) 68.

[11] A. Mukhopadhyay, S. Pal; *Eur. J. Inorg. Chem.* (2006) 4879.

[12] W. E. Hatfield; In: E. A. Boudreaux, L. N. Mulay (eds), *Theory and applications of molecular paramagnetis,* Wiley, New York, (1976) p 491.

[13] SMART version 5.630, SAINT-plus version 6.45: *Pro-grams for data collection and extraction,* Bruker-Nonius Analytical X-ray Systems Inc., Madison, WI, USA, (2003).

[14] G. M. Sheldrick; SADABS: *Program for empirical absorption correction,* University of Göttingen, Göttingen, Germany, (1997).

[15] G. M. Sheldrick; SHELX-97: *Programs for structure solution and refinement,* University of Göttingen, Göttingen, Germany, (1997).

[16] L. J. Farrugia; *J. Appl. Crystallogr.* 32 (1999) 837.

[17] P. McArdle; *J. Appl. Crystallogr.* 28 (1995) 65.

[18] A. L. Spek; PLATON: *A multipurpose crystallographic tool.* Utrecht University, Utrecht, The Netherlands, (2002).

[19] W. Kemp; *Organic spectroscopy,* Macmillan, Hampshire, (1987) p62.

[20] R. Raveendran, S. Pal; *Eur. J. Inorg. Chem.* (2008) 5540.

[21] C. B. Castellani, O. Carugo, A. Coda; *Acta. Crystallogr. C* 44 (1988) 267.

[22] B. Chiari, O. Piovesana, T. Tarantelli, P. F. Zanazzi; *Inorg. Chem.* 27 (1988) 3246.

[23] S. Das, S. A. Maloor, S. N. Pal, S. Pal; *Cryst. Growth. Des.* 6 (2006) 2103.

Chapter 3

A double helical dinuclear copper(II) complex with biacetyl bis(benzoylhydrazone)[§]

3.1. Abstract:

A dinuclear double helicate of copper(II) with the Schiff base biacetyl bis(benzoylhydrazone) (H_2babh) is reported. The solid state physical properties of the dicopper(II) species are compared with that of its mononuclear precursor. The O,N,N,O-donor babh^{2-} shows an unusual bridging coordination mode in [Cu_2(μ-babh)$_2$]. Each metal centre in the complex is in very similar tetrahedrally distorted square-planar N_2O_2 coordination sphere assembled by the two halves of the two babh^{2-}. Two halves of each ligand are twisted along the =(CH_3)C–C(CH_3)= bond to accommodate the two metal centres.

[§]This work has been published in *Inorg. Chim. Acta*. 363 (2010) 3632

3.2. Introduction:

Helical coordination complexes or metallohelicates are of contemporary interest because of their potential applications in a variety of fields such as enantioselective processes, optical and magnetic materials, probing of DNA structures and helical self-organization processes found in nature [1–15]. Ligands having more than one chelating sites connected by a flexible spacer are well known to provide multinuclear double helical and triple helical complexes with metal ions that prefer tetrahedral and octahedral geometry, respectively [4,12,16–19]. The diazenes where the two chelating sites are connected by a single bond are the simplest in this class of ligands. These diazenes can form dinuclear helical complexes due to the twisting of the two chelating sites along the N–N single bond. The crystal structures of a number of dinuclear metallohelicates with the neutral N_4-donor Schiff base N,N′-bis(picolinylidene)hydrazine or its derivatives are known [20–29]. Some dinuclear triple helicates with the similar N_2O_2-donor Schiff base N,N′-bis(salicylidene)hydrazine and analogous species have been also reported by our group [30–32].

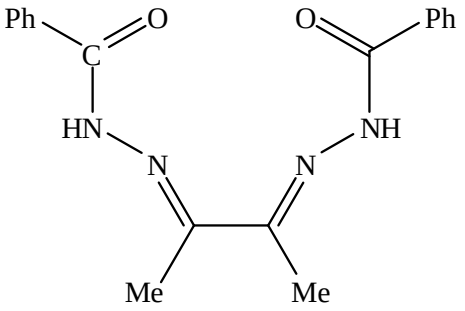

H_2babh

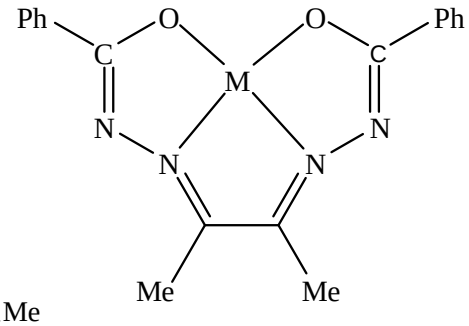

[M(babh)]

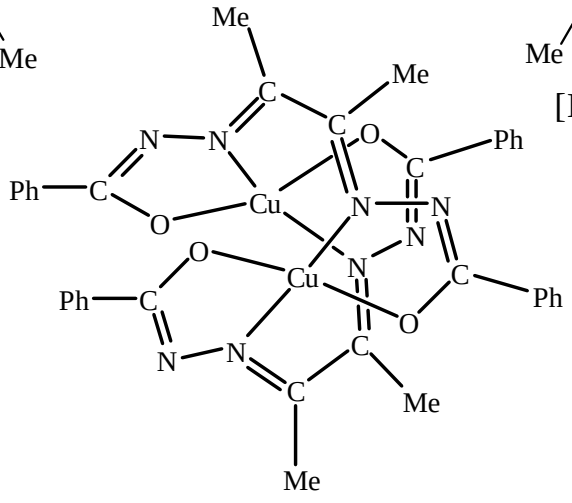

$[Cu_2(\mu\text{-babh})_2]$

The tetradentate Schiff base biacetyl bis(benzoylhydrazone) (H_2babh) described in the preceding chapter is very unlikely to provide dinuclear species as the two chelating sites are connected by the rigid =C(Me)–C(Me)= fragment. The deprotonated Schiff base ($babh^{2-}$) is expected to provide an N_2O_2 square-plane with the formation of three five-membered chelate rings around a single metal centre that prefers square-based coordination geometry. We have described such mononuclear square-planar nickel(II) and copper(II) complexes with H_2babh having the general molecular formula [M(babh)] in chapter 2 [33]. X-ray quality single crystal of the nickel(II) complex was obtained from dichloromethane, while that of the copper(II) complex was obtained from methanol. The structure determination revealed that the nickel(II) complex crystallizes as square-planar [Ni(babh)], while the copper(II) complex crystallizes as [Cu(babh)(CH_3OH)] where the copper centre is square-pyramidal. The dark crystals of [Cu(babh)(CH_3OH)] are very unstable due to solvent loss and eventually they become brown amorphous unsolvated [Cu(babh)]. In both complexes, the ligand provides the anticipated N_2O_2 square-plane around the metal centre. Plate-like diamagnetic [Ni(babh)] molecules form a π-stacked columnar structure with a constant Ni···Ni distance, whereas the self-assembly of the square-pyramidal [Cu(babh)(CH_3OH)] molecules via intermolecular alternating hydrogen bonding and π–π interaction leads to a chain structure with alternating long and short Cu···Cu distances [33]. We sought after a π-stacked columnar ordering of [Cu(babh)] with a constant metal···metal distance as observed in the case of [Ni(babh)]. Such an assembly is very interesting due to the possibility of metal ion spin coupling via π-π interaction [34,35]. After several attempts we were able to grow single crystals from the solution of [Cu(babh)] in the non-coordinating solvent mixture of dichloromethane and *n*-hexane. However, the complex crystallized as [$Cu_2(\mu\text{-babh})_2$], a double helical dinuclear species instead of a plate-like mononuclear species due to the unusual dinucleating coordination mode of $babh^{2-}$. In the present chapter, the comparison of the solid state physical properties of the unsolvated mononuclear [Cu(babh)] and [$Cu_2(\mu\text{-babh})_2$] with the X-ray structure of the latter have been described.

3.3. Experimental:

3.3.1. Materials:

The Schiff base H_2babh and the mononuclear complex [Cu(babh)] was prepared by following same methods as reported in chapter 2 [33]. All other chemicals and solvents used in this work were of analytical grade available commercially and were used without further purification.

3.3.2. Physical measurements:

Microanalytical (C, H, N) data were obtained with a Thermo Finnigan Flash EA1112 elemental analyzer. The magnetic susceptibility was measured using a Sherwood Scientific balance. A diamagnetic corrections calculated from Pascal's constants [36], were used to obtain the molar paramagnetic susceptibilities. A Jasco-5300 FT-IR spectrophotometer was used to collect the infrared spectra using KBr pellets. The electronic spectra in solid state were recorded on a Shimadzu UV-3600 UV-VIS-NIR spectrophotometer by diffuse reflectance technique using $BaSO_4$ pellets. X-ray powder diffraction patterns were collected on a Philips PW1830 X-ray diffractometer.

3.3.3. Synthesis of [Cu_2(μ-babh)$_2$]:

The brown mononuclear [Cu(babh)] (100 mg, 0.26 mmol) was taken in a 50 ml beaker and dissolved in dichloromethane (25 ml) followed by addition of *n*-hexane (20 ml). The clear solution in the beaker was covered with a paper and kept in a refrigerator at ~0^o C. After about 3-4 days the solvent was evaporated and the dinuclear [Cu_2(μ-babh)$_2$] was deposited as dark needle shaped crystals on the wall of the beaker and green microcrystalline material at the bottom of the beaker. One of the needle-like crystals was used for X-ray data collection. *Anal.* Calc. for $Cu_2C_{36}H_{32}N_8O_4$ (767.80): C, 56.32; H, 4.20; N, 14.59%. Found: C, 56.23; H, 3.98; N, 14.45%.

3.3.4. X-ray crystallography:

Unit cell parameters and the intensity data for [Cu_2(μ-babh)$_2$] were obtained on a Bruker-Nonius SMART APEX CCD single crystal diffractometer, equipped with a graphite monochromator and a Mo Kα fine-focus sealed tube (λ = 0.71073 Å) operated at 2.0 kW. The detector was placed at a distance of 6.0 cm from the crystal. Data were collected at 298 K with a scan width of 0.3º in ω and an exposure time of 10 s/frame. The SMART software was used for data acquisition and the SAINT-Plus software was used for data extraction [37]. An absorption correction was performed with the help of SADABS program [38]. The structure was solved by direct method and refined on F^2 by full-matrix least-squares procedures. All non-hydrogen atoms were refined anisotropically. The hydrogen atoms were included in the structure factor calculation at idealized positions by using a riding model. The SHELX-97 [39] programs available in the WinGx [40] package were used for structure solution and refinement. The ORTEX6a [41] and Platon [42] packages were used for molecular graphics. Significant crystallographic data are summarized in Table 3.1.

Table 3.1: Selected crystallographic data for $[Cu_2(\mu\text{-babh})_2]$

Complex	$[Cu_2(\mu\text{-babh})_2]$
Empirical formula	$Cu_2C_{36}H_{32}N_8O_4$
Formula weight	767.80
Temperature (K)	298(2)
Crystal size (mm)	0.38 x 0.10 x 0.06
Crystal system	Monoclinic
Space group	$P2_1/c$
a (Å)	13.264(4)
b (Å)	21.810(6)
c (Å)	12.235(3)
α(°)	90
β (°)	103.303(5)
γ(°)	90
V (Å^3)	3444.4(16)
Z	4
Calculated density (g cm^{-3})	1.481
Absorption coefficient (mm^{-1})	1.287
Reflections collected	29435
Reflections unique	5507
Reflections ($I \geq 2\sigma(I)$)	3160
Data/restraints/Parameters	5507/0/455
$R1$, $wR2$ ($I \geq 2\sigma(I)$)	0.0751, 0.1695
$R1$, $wR2$ (all data)	0.1309, 0.2056
Goodness-of-fit on F^2	1.00
Largest diff. peak and hole (e Å^{-3})	1.356, –0.778

3.4. Results and discussion:

3.4.1. Synthesis and some properties:

The dicopper(II) complex is obtained by crystallization of the mononuclear complex from a mixture of dichloromethane and *n*-hexane. The microanalysis data of the green [Cu_2(μ-babh)$_2$] are consistent with 1:1 metal to ligand ratio as observed for the brown [Cu(babh)] [33]. The room temperature magnetic moment (3.04 μ_B) of [Cu_2(μ-babh)$_2$] is slightly higher than the spin only moment expected for a dinuclear copper(II) species where each of the two metal centers has one uncoupled or weakly coupled unpaired spin.

3.4.2. Spectral features:

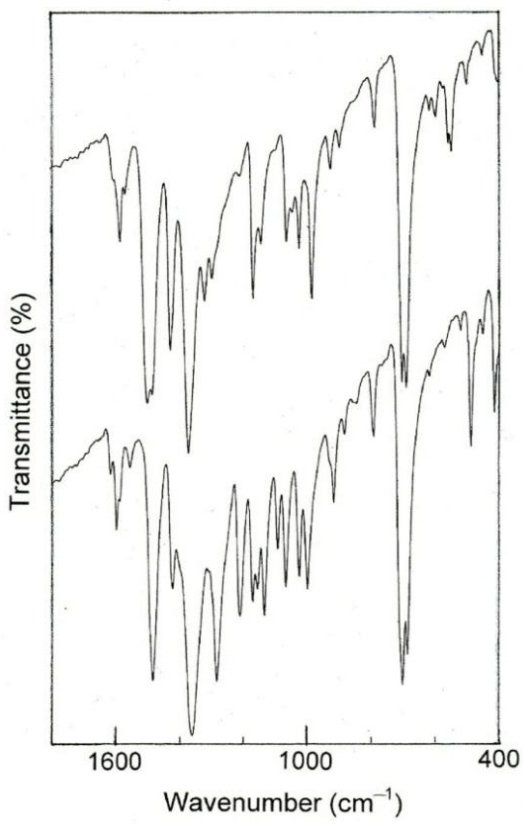

Fig. 3.1: The infrared spectra of [Cu_2(μ-babh)$_2$] (top) and [Cu(babh)] (bottom) in KBr pellets.

The infrared spectra of [Cu(babh)] and [Cu_2(μ-babh)$_2$] in KBr pellets are shown in Fig. 3.1. The spectra are quite different in the region above 900 cm^{-1}.

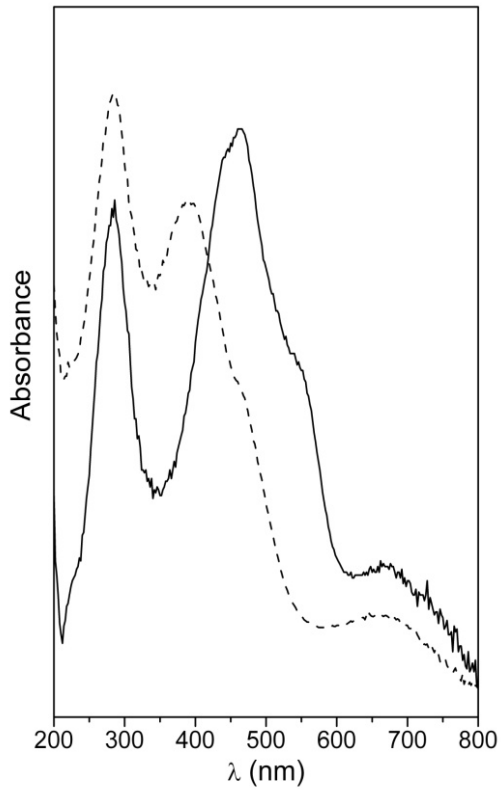

Fig. 3.2: The electronic spectra of [Cu_2(μ-babh)$_2$] (-----) and [Cu(babh)] (——) in solid state.

The electronic spectral profiles of [Cu(babh)] and [Cu_2(μ-babh)$_2$] in dichloromethane as well as in methanol are essentially identical. However, their solid state electronic spectra are very different (Fig. 3.2). Both complexes display two absorptions at 665 nm and 285 nm. The low energy band is perhaps associated with ligand-field transition, while the high energy band is assigned to a ligand centered transition. The positions of the other two absorptions observed within 600 to 350 nm are different for the mononuclear and the dinuclear species. These are red-shifted by ~80 nm in the case of [Cu(babh)] compared to their positions (470 nm and 385 nm) in the case of [Cu_2(μ-babh)$_2$]. These two absorptions are attributed to ligand-to-metal charge transfer transitions.

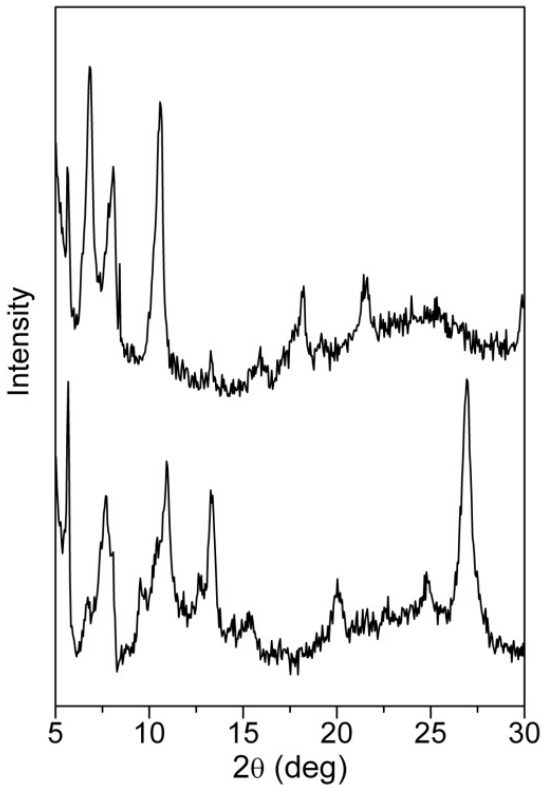

Fig. 3.3: The X-ray powder diffraction patterns of [Cu$_2$(μ-babh)$_2$] (top) and [Cu(babh)] (bottom).

The different molecular structures of [Cu(babh)] and [Cu$_2$(μ-babh)$_2$] are further corroborated by their very different powder X-ray diffraction patterns (Fig. 3.3).

3.4.3. Molecular Structure:

The unusual dinucleating coordinating mode of $babh^{2-}$ in $[Cu_2(\mu\text{-}babh)_2]$ is confirmed by single crystal X-ray structure determination.

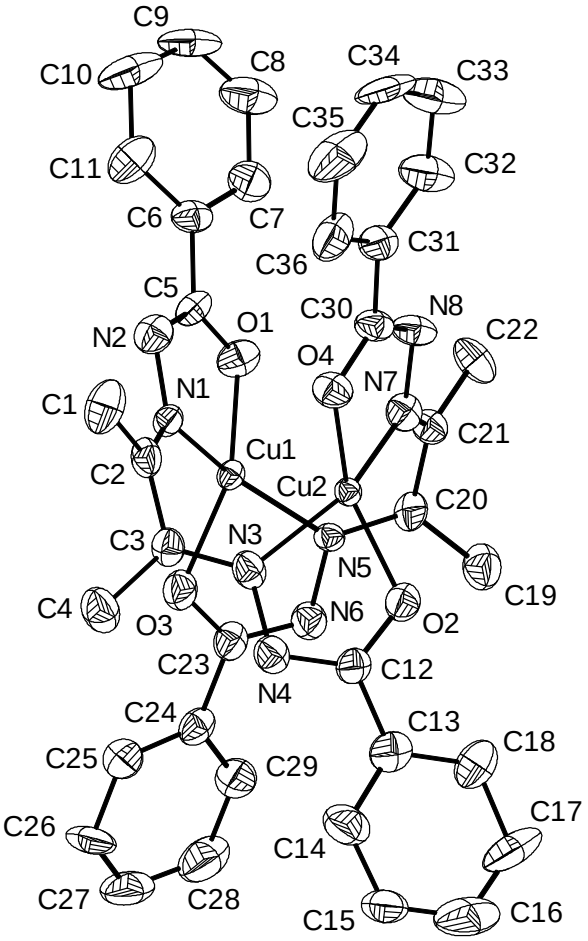

Fig. 3.4: The molecular structure of $[Cu_2(\mu\text{-}babh)_2]$ with the atom labeling scheme. Hydrogen atoms are omitted for clarity.

The molecular structure is depicted in Fig. 3.4 and the bond parameters associated with both metal ions are listed in Table 3.2. Each of the two $babh^{2-}$ binds the two metal centres through the two imine-N and the two deprotonated amide-O atoms forming two five-membered chelate rings. The bond parameters for both metal centres are comparable (Table 3.2).

Table 3.2: Selected bond lengths (Å) and angles (°) for [Cu_2(μ-babh)$_2$]

[Cu_2(μ-babh)$_2$]			
Cu(1)–O(1)	1.861(5)	Cu(2)–O(2)	1.908(5)
Cu(1)–O(3)	1.940(5)	Cu(2)–O(4)	1.879(5)
Cu(1)–N(1)	1.970(5)	Cu(2)–N(3)	2.002(6)
Cu(1)–N(5)	1.972(5)	Cu(2)–N(7)	1.946(6)
O(1)–Cu(1)–O(3)	151.7(2)	O(2)–Cu(2)–O(4)	150.3(2)
O(1)–Cu(1)–N(1)	79.8(2)	O(2)–Cu(2)–N(3)	80.5(2)
O(1)–Cu(1)–N(5)	108.1(2)	O(2)–Cu(2)–N(7)	106.4(2)
O(3)–Cu(1)–N(1)	105.0(2)	O(4)–Cu(2)–N(3)	105.8(2)
O(3)–Cu(1)–N(5)	80.1(2)	O(4)–Cu(2)–N(7)	82.6(2)
N(1)–Cu(1)–N(5)	153.8(2)	N(3)–Cu(2)–N(7)	150.6(2)

The C–O (1.278(8)–1.296(8) Å) and the C=N (1.305(8)–1.343(9) Å) bond lengths in the amide functionalities of the two $babh^{2-}$ are within the ranges observed for its O-coordinating iminolate form (–N=C(O^-)–) in various complexes [33,43–46]. The other intraligand bond parameters are unexceptional. All the five-membered chelate rings are satisfactorily planar. The mean deviations are within 0.04 and 0.05 Å. However, the N_2O_2 environment around each copper(II) centre are significantly distorted from the square-planar geometry. The dihedral angles between the two chelate rings are 44.1(1)° and 46.5(2)° for the first (Cu(1)) and the second (Cu(2)) copper(II) centres, respectively. The bond parameters associated with both metal ions and these two dihedral angles indicate that the coordination spheres around the two metal centres are very similar and essentially in the middle of square-planar and tetrahedral geometry. The average of Cu–O(amide) bond lengths is shorter by 0.08 Å and the average of Cu–N(imine) bond lengths is longer by 0.06 Å compared to the corresponding average bond lengths observed in the copper(II) complex where $babh^{2-}$ coordinates a single metal centre and provides a N_2O_2 square-plane around it with the formation of three five-membered chelate rings [33].

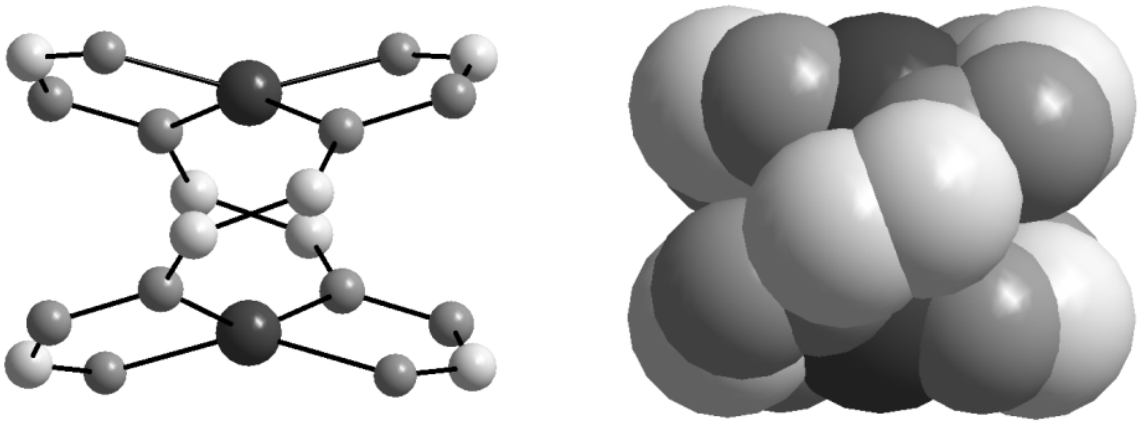

Fig. 3.5: The double helical structure of $[Cu_2(\mu\text{-babh})_2]$. (a) Ball and stick and (b) space filling models. For clarity the phenyl and the methyl groups are not shown

These differences are perhaps due to the difference in the coordination geometries and the twisting of each $babh^{2-}$ along the $=(CH_3)C–C(CH_3)=$ single bond to accommodate two copper(II) centres in $[Cu_2(\mu\text{-babh})_2]$. The twisting is reflected by the dihedral angle between the planes containing the methyl carbon, the imine carbon and nitrogen atoms of the two halves of $babh^{2-}$. Both ligands are twisted by essentially the same amount as the dihedral angles are $54.2(6)^o$ and $54.3(6)^o$ for the first and the second ligand, respectively. Thus $[Cu_2(\mu\text{-babh})_2]$ has a very close to ideal D_2-symmetric double helical structure due to the very similar distortion of the two N_2O_2 coordination spheres around Cu(1) and Cu(2) and essentially identical twisting of the two ligands (Fig. 3.5).

3.5. Conclusions:

In search of crystals of mononuclear unsolvated [Cu(babh)] from the non-coordinating solvent mixture of dichloromethane and *n*-hexane, we have isolated a double helical dinuclear copper(II) complex $[Cu_2(\mu\text{-babh})_2]$. The comparisons of

infrared and electronic spectroscopic features in the solid state clearly indicate that the brown [Cu(babh)] crystallizes out from the said solvent mixture not as mononuclear but as a green material with a different structure. Molecular structure determined by X-ray crystallography shows the near D_2-symmetric double helical structure of the green [Cu_2(μ-babh)$_2$], where each of the two O,N,N,O-donor ligands are twisted along the =(CH_3)C–C(CH_3)= single bond to accommodate the two copper(II) centers.

3.6. References:

[1] C.-T. Chen, K. S. Suslick; *Coord. Chem. Rev.* 128 (1993) 293.

[2] J.-M. Lehn; *Supramolecular Chemistry*, VCH, Weinheim, (1995).

[3] B. Schoentjes, J.-M. Lehn; *Helv. Chim. Acta* 78 (1995) 1.

[4] C. Piguet, G. Bernardinelli, G. Hopfgartner; *Chem. Rev.* 97 (1997) 2005.

[5] A. Williams; *Chem.–Eur. J.* 3 (1997) 15.

[6] M. Albrecht; *Chem. Rev.* 101 (2001) 3457.

[7] M. Eddaoudi, D. B. Moler, H. Li, B. Chen, T. M. Reineke, M. O'Keeffe, O. M. Yaghi; *Acc. Chem. Res.* 34 (2001) 319.

[8] I. Meistermann, V. Moreno, M. J. Prieto, E. Molderheim, E. Sletten, S. Khalid, M. Rodger, J. Perberdy, C. J. Isaac, A. Rodger, M. J. Hannon; *Proc. Natl. Acad. Sci. U.S.A.* 99 (2002) 5069.

[9] J. L. Serrano, T. Sierra; *Coord. Chem. Rev.* 242 (2003) 73.

[10] B. Kesanli, W. Lin; *Coord. Chem. Rev.* 246 (2003) 305.

[11] M. J. Hannon, L. J. Childs; *Supramol. Chem.* 16 (2004) 7.

[12] C. Piguet, M. Borkovec, J. Hamacek, K. Zeckert; *Coord. Chem. Rev.* 249 (2005) 705.

[13] V. Amendola, L. Fabbrizzi, F. Foti, M. Licchelli, C. Mangano, P. Pallavicini, A. Poggi, D. Sacchi, A. Taglietti; *Coord. Chem. Rev.* 250 (2006) 273.

[14] G. Aromí, P. Gamez, J. Reedijk; *Coord. Chem. Rev.* 252 (2008) 964.

[15] F. R. Keenea, J. A. Smitha, J. G. Collins; *Coord. Chem. Rev.* 253 (2009) 2021.

[16] J.-M. Lehn, J. Siegel, J. Harrowfield, B. Chevrier, D. Moras; *Proc. Natl. Acad. Sci. U.S.A.* 84 (1987) 2565.

[17] E. C. Constable; *Tetrahedron* 48 (1992) 10013.

[18] R. Krämer, J. -M. Lehn, A. Marquis-Rigault; *Proc. Natl. Acad. Sci. U.S.A.* 90 (1993) 5394.

[19] M. A. Houghton, A. Bilyk, M. M. Harding, P. Turner, T. W. Hambley; *J. Chem. Soc. Dalton Trans.* (1997) 2725.

[20] P. D. W. Boyd, M. Gerloch, G. M. Sheldrick; *J. Chem. Soc. Dalton Trans.* (1974) 1097.

[21] C. J. O'Connor, R. J. Romananch, D. M. Robertson, E. E. Eduok, F. R. Fronezek; *Inorg. Chem.* 22 (1983) 449.

[22] Z. Xu, L. K. Thompson, D. O. Miller; *Inorg. Chem.* 36 (1997) 3985.

[23] L. K. Thompson, Z. Xu, A. E. Goeta, J. A. K. Howard, H. J. Clase, D. O. Miller; *Inorg. Chem.* 37 (1998) 3217.

[24] Z. Xu, L. K. Thompson, D. O. Miller, H. J. Clase, J. A. K. Howard, A. E. Goeta; *Inorg. Chem.* 37 (1998) 3620.

[25] Z. Xu, L. K. Thompson, C. J. Matthews, D. O. Miller, A. E. Goeta, C. Wilson, J. A. K. Howard, M. Ohba, H. Okawa; *J. Chem. Soc. Dalton Trans.* (2000) 69.

[26] G. Dong, D. Chun-ying, F. Chen-jie, M. Qing-jin; *J. Chem. Soc. Dalton Trans.* (2002) 834.

[27] J. Hamblin, A. Jackson, N. W. Alcock, M. J. Hannon; *J. Chem. Soc. Dalton Trans.* (2002) 1635.

[28] G. Dong, P. Ke-liang, D. Chin-ying, H. Cheng, M. Qing-jin; *Inorg. Chem.* 41 (2002) 5978.

[29] P. V. Bernhardt, P. Chin, D. R. Richardson; J. *Chem. Soc. Dalton Trans.* (2004) 3342.

[30] J. Saroja, V. Manivannan, P. Chakraborty, S. Pal; *Inorg. Chem.* 34 (1995) 3099.

[31] S. G. Sreerama, S. Pal; *Inorg. Chem.*44 (2005) 6299.

[32] S. G. Sreerama, A. Mukhopadhyay, S. Pal; *Polyhedron* 26 (2007) 4101.

[33] T. Ghosh, A. Mukhopadhyay, K. S. C. Dargaiah, S. Pal; *Struct. Chem*. 21 (2010) 147.

[34] S. Das, G. P. Muthukumaragopal, S. N. Pal, S. Pal; *New J. Chem.* 27 (2003) 1102.

[35] S. Das, S. Pal; *J. Mol. Struct.* 753 (2005) 68.

[36] W. E. Hatfield; in: E. A. Boudreaux, L. N. Mulay (Eds.), *Theory and Applications of Molecular Paramagnetis*, Wiley, New York, (1976) p. 491.

[37] SMART version 5.630, SAINT-plus version 6.4: *Pro-grams for data collection and extraction,* Bruker-Nonius Analytical X-ray Systems Inc., Madison, WI, USA, (2003).

[38] G. M. Sheldrick; SADABS: *Program for Area Detector Absorption Correction,* University of Göttingen, Göttingen, Germany, (1997).

[39] G. M. Sheldrick; XHELX-97: *Structure Determination Software,* University of Göttingen, Göttingen, Germany, (1997).

[40] L. J. Farrugia; *J. Appl. Crystallogr.* 32 (1999) 837.
[41] P. McArdle; *J. Appl. Crystallogr.* 28 (1995) 65.
[42] A. L. Spek; Platon: *A Multipurpose Crystallographic Tool,* Utrecht University, Utrecht, The Netherlands, (2002).
[43] A. Mukhopadhyay, S. Pal; *Eur. J. Inorg. Chem.* (2006) 4879.
[44] R. Raveendran, S. Pal; *J. Organomet. Chem.* 692 (2007) 824.
[45] R. Raveendran, S. Pal; *Eur. J. Inorg. Chem.* (2008) 5540.
[46] A. Sarkar, S. Pal; *Eur. J. Inorg. Chem.* (2009) 5391.

Chapter 4

Effects of counteranions on molecular and supramolecular structures of bis(2-(1H-imidazol-2-yl)-pyridine)copper(II)[§]

4.1. Abstract:

Synthesis and physical properties of bis(2-(1H-imidazol-2-yl)-pyridine)copper(II) with chloride, nitrate and perchlorate as counteranions have been described. Microanalysis, magnetic susceptibility, conductivity and various spectroscopic (IR, UV-Vis and EPR) measurements have been used for the characterization of the complexes. Crystal structures of all the three complexes have been determined. The intermolecular hydrogen bonding interactions and the resulting self-assembly patterns for each of the species have been scrutinized. The chloride containing complex crystallizes as trihydrate where the metal ion is in tetragonally elongated *cis*-N_4Cl_2 coordination sphere. This complex provides a three-dimensional honeycomb-like structure through N–H···Cl, O–H···Cl and O–H···O hydrogen bonds. In the nitrate containing species, one of the two counteranions coordinates the metal centre to provide an irregular N_4O_2 coordination sphere, while the other counteranion with the help of a lattice water molecule assembles a ladder-like structure via N–H···O and bifurcated O–H···O,O hydrogen bonds. A one-dimensional polymeric species has been formed when perchlorate is the counteranion. Here one of the two perchlorates acts as bridge between the metal centres that are in tetragonally elongated *trans*-N_4O_2 coordination sphere. This polymeric chain together with the second perchlorate and a water molecule form a ribbon-like structure due to N–H···O and O–H···O hydrogen bonds.

[§]This work has been published in *Polyhedron* 29 (2010) 3074.

4.2. Introduction:

Self-assembly of small and simple complex molecules via various intermolecular non-covalent interactions involving suitable functionalities on the metal coordinated organic ligands and solvent molecules trapped in the crystal lattice is one of the powerful strategies for the design and preparation of such materials. Our group has been working on such species over the past several years [1–16]. Herein this chapter, we have reported three hydrated copper(II) complexes with the N,N-donor 2-(1H-imidazol-2-yl)-pyridine (impy) and different counteranions. The counteranions used are chloride, nitrate and perchlorate. The reason for the choice of this ligand is the N–H functionality on the imidazolyl fragment which can participate as a donor in strong hydrogen bonds with the counteranions. The anions are varied from monoatomic to triangular to tetrahedral species, having different metal coordinating and hydrogen bond acceptor abilities. Thus both molecular as well as hydrogen-bonding assisted supramolecular structures of these species are anticipated to differ significantly. The synthesis and characterization of these complexes and their molecular and supramolecular structures, determined by X-ray crystallography, have been described below.

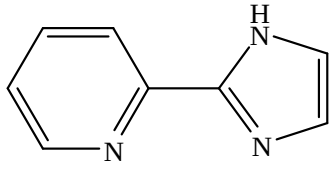

impy

4.3. Experimental:

4.3.1. Materials:

The ligand 2-(1H-imidazol-2-yl)-pyridine (impy) was prepared by following a reported procedure [17]. All other chemicals and solvents used in this work were of analytical grade available commercially and were used without further purification.

4.3.2. Physical measurements:

Elemental (C, H, N) analysis data were obtained with the help of a Thermo Finnigan Flash EA1112 series elemental analyzer. Solution electrical conductivities were measured using a Digisun DI-909 conductivity meter. A Sherwood Scientific balance was used to measure the magnetic susceptibilities with powdered samples of the complexes. Diamagnetic corrections calculated from Pascal's constants [18] were used to obtain the molar paramagnetic susceptibilities. Infrared spectra were collected by using KBr pellets on a Jasco-5300 FT-IR spectrophotometer. A Cary 100 Bio UV/vis spectrophotometer was used to record the electronic spectra. X-band EPR measurements were performed on a Jeol JES-FA200 spectrometer.

4.3.3. Synthesis of $[Cu(impy)_2Cl_2]\cdot 3H_2O$ (1):

A methanol solution (15 ml) of $CuCl_2\cdot 2H_2O$ (60 mg. 0.35 mmol) was added to a methanol solution (15 ml) of 2-(1H-imidazol-2-yl)-pyridine (impy) (100 mg, 0.70 mmol). The mixture was stirred at room temperature in air for 4 h. The resulting green solution was slowly evaporated to about 5 ml. The crystalline green complex deposited in about 3–4 days was collected by filtration. Yield was 130 mg (78%). Anal. calcd for $CuC_{16}H_{20}N_6O_3Cl_2$: C, 40.13; H, 4.21; N, 17.55%. Found: C, 39.85; H, 4.03; N, 17.32%. $\mu_{eff.}$ (μ_B) at 298 K: 1.81. Λ_M (ohm^{-1} cm^2 mol^{-1}) in CH_3CN at 298 K: 23. UV-Vis in CH_3CN: λ (nm) (ε (M^{-1} cm^{-1})) = 745 (65), 300 (19800), 264 (18900), 218 (13600). X-band EPR in C_2H_5OH-CH_3OH (1:1) at 130 K: $g_{\|}$ = 2.31, $A_{\|}$ = 133 x 10^{-4} cm^{-1} and $g_{\perp}$ = 2.11.

4.3.4. Synthesis of $[Cu(impy)_2(NO_3)]NO_3\cdot H_2O$ (2):

This complex was synthesized in 70% yield by following the same procedure as described for **1** using $Cu(NO_3)_2\cdot 3H_2O$ and 2-(1H-imidazol-2-yl)-pyridine (impy) in 1:2 mol ratio. Anal. calcd for $CuC_{16}H_{16}N_8O_7$: C, 38.75; H, 3.25; N, 22.60%. Found: C, 38.59; H, 3.10; N, 22.44%. $\mu_{eff.}$ (μ_B): 1.96. Λ_M (ohm^{-1} cm^2 mol^{-1}) in CH_3CN at 298 K:

224. UV-Vis in CH_3CN: λ (nm) (ε (M^{-1} cm^{-1})) = 715 (80), 302 (20500), 260 (17700), 222 (18700). X-band EPR in C_2H_5OH-CH_3OH (1:1) at 130 K: $g_{\|}$ = 2.29, $A_{\|}$ = 137 x 10^{-4} cm^{-1} and $g_{\perp}$ = 2.09.

4.3.5. Synthesis of $[Cu(impy)_2(ClO_4)]ClO_4 \cdot H_2O$ (3):

This complex was synthesized in 80% yield using the same procedure as described for **1** and **2** from $Cu(ClO_4)_2 \cdot 6H_2O$ and 2-(1H-imidazol-2-yl)-pyridine (impy) in 1:2 mol ratio. Anal. calcd for $CuC_{16}H_{16}N_6O_9Cl_2$ (570.79): C, 33.67; H, 2.83; N, 14.72%. Found: C, 33.41; H, 2.57; N, 14.48%. $\mu_{eff.}$ (μ_B): 1.82. Λ_M (ohm^{-1} cm^2 mol^{-1}) in CH_3CN at 298 K: 259. UV-Vis in CH_3CN: λ (nm) (ε (M^{-1} cm^{-1})) = 730 (95), 305 (21300), 259 (19200), 223 (17900). X-band EPR in C_2H_5OH-CH_3OH (1:1) at 130 K: $g_{\|}$ = 2.30, $A_{\|}$ = 135 x 10^{-4} cm^{-1} and $g_{\perp}$ = 2.09.

4.3.6. X-ray Crystallography:

Single crystals of **1**, **2** and **3** were collected directly from the products obtained during their syntheses. A Bruker-Nonius SMART APEX CCD single crystal diffractometer, equipped with a graphite monochromator and a Mo Kα fine-focus sealed tube (λ = 0.71073 Å) operated at 2.0 kW was used to determine the unit cell parameters and to collect the intensity data at 298 K for both **1** and **3**. The detector was placed at a distance of 6.0 cm from the crystal. Data were collected at 298 K with a scan width of 0.3º in ω and an exposure time of 10 s/frame. The SMART software was used for data acquisition and the SAINT-Plus software was used for data extraction [19]. The absorption corrections were performed with the help of the SADABS program [20]. On the other hand, determination of unit cell parameters and the intensity data collection for **2** were performed on an Enraf-Nonius Mach-3 single crystal diffractometer using graphite monochromated Mo Kα radiation (λ = 0.71073 Å) by the ω-scan method at 298 K. Intensities of three check reflections were measured after every 1.5 h during the data collection to monitor the crystal stability. No decay was observed in the 60 h of exposure to X-ray. An empirical absorption

correction was performed based on Ψ-scans [21] of selected reflections. The calculations for data reduction and absorption corrections were done using WinGX package [22]. The structures of all the three complexes were solved by direct method and refined on F^2 by full-matrix least-squares procedures. The non-hydrogen atoms were refined using anisotropic thermal parameters. The hydrogen atoms of the lattice water molecules were located in difference map and refined with $U_{iso}(H) = 1.5U_{iso}(O)$ and geometric restraints to place them at idealized positions [23]. All other hydrogen atoms were included in the structure factor calculations at idealized positions by using a riding model. The SHELX-97 programs [24] available in the WinGX package [22] were used for structure solution and refinement. The ORTEX6a [25] and Platon [26] packages were used for molecular graphics. Selected crystal and refinement data are summarized in Table 4.1.

Table 4.1.: Selected crystallographic data for $[Cu(impy)_2Cl_2]\cdot 3H_2O$ (**1**), $[Cu(impy)_2(NO_3)]NO_3\cdot H_2O$ (**2**) and $[Cu(impy)_2(ClO_4)]ClO_4\cdot H_2O$ (**3**)

Complex	**1**	**2**	**3**
Empirical formula	$CuC_{16}H_{20}N_6O_3Cl_2$	$CuC_{16}H_{16}N_8O_7$	$CuC_{16}H_{16}N_6O_9Cl_2$
Formula weight (g mol^{-1})	478.82	495.91	570.79
Crystal system	monoclinic	triclinic	monoclinic
Temperature (K)	298(2)	298(2)	298(2)
Crystal size (mm)	0.32 x 0.27 x 0.25	0.45 x 0.38 x 0.35	0.48 x 0.24 x 0.20
Space group	*C*c	$P\bar{1}$	$P2_1/c$
a (Å)	17.975(3)	8.098(4)	7.233(3)
b (Å)	12.166(2)	11.188(7)	26.683(7)
c (Å)	9.4124(18)	12.059(7)	11.579(4)
α (°)	90	102.53(3)	90
β (°)	102.837(3)	95.675(15)	105.214(6)
γ (°)	90	110.75(4)	90
V ($Å^3$)	2006.9(7)	978.6(9)	2156.3(1)
Z	4	2	4
Calculated density (g cm^3)	1.585	1.683	1.758
Absorption coefficient (mm^{-1})	1.385	1.177	1.325
Reflections collected	8827	5700	12909
Reflections unique	3379	5700	3448
Reflections ($I \geq 2\sigma(I)$)	2792	4350	2090
Data/restraints/Parameters	3379/16/271	5700/3/295	3448/15/313
R1, wR2 ($I \geq 2\sigma(I)$)	0.0564, 0.1409	0.0492, 0.1313	0.0757, 0.1782
R1, wR2 (all data)	0.0669, 0.1480	0.0674, 0.1439	0.1282, 0.2072
Goodness-of-fit on F^2	1.011	1.041	0.963
Largest diff. peak and hole (e $Å^{-3}$)	1.316, –0.507	0.676, –0.833	0.892, –0.363

4.4. Result and discussion:

4.4.1. Synthesis and some properties:

The hydrated complexes $[Cu(impy)_2Cl_2]\cdot 3H_2O$ (**1**), $[Cu(impy)_2(NO_3)]NO_3\cdot H_2O$ (**2**) and $[Cu(impy)_2(ClO_4)]ClO_4\cdot H_2O$ (**3**) have been synthesized in 70–80% yields from two mole equivalents of 2-(1H-imidazol-2-yl)-pyridine (impy) and one mole equivalent of the corresponding hydrated copper(II) salts in methanol medium. The elemental (C, H, N) analyses data for the three species support their molecular formulae. The effective magnetic moments of the complexes at 298 K in powder phase are within 1.81–1.96 μ_B. These moments indicate the presence of one unpaired electron at the metal centre, as expected for uncoupled copper(II) species. The electrical conductivities of the three complexes have been measured in acetonitrile. The low molar conductivity (Λ_M) value (23 ohm^{-1} cm^2 mol^{-1}) of **1** indicates that both chlorides are fairly well coordinated to the metal centre. On the other hand, the Λ_M values of **2** and **3** are comparatively much larger. These are 224 and 259 ohm^{-1} cm^2 mol^{-1} for **2** and **3**, respectively. These values are consistent with 1:2 electrolytic behaviors [27] and indicate that in solution the counteranions are not coordinated to the metal centre in either of these two complexes.

4.4.2. Spectral features:

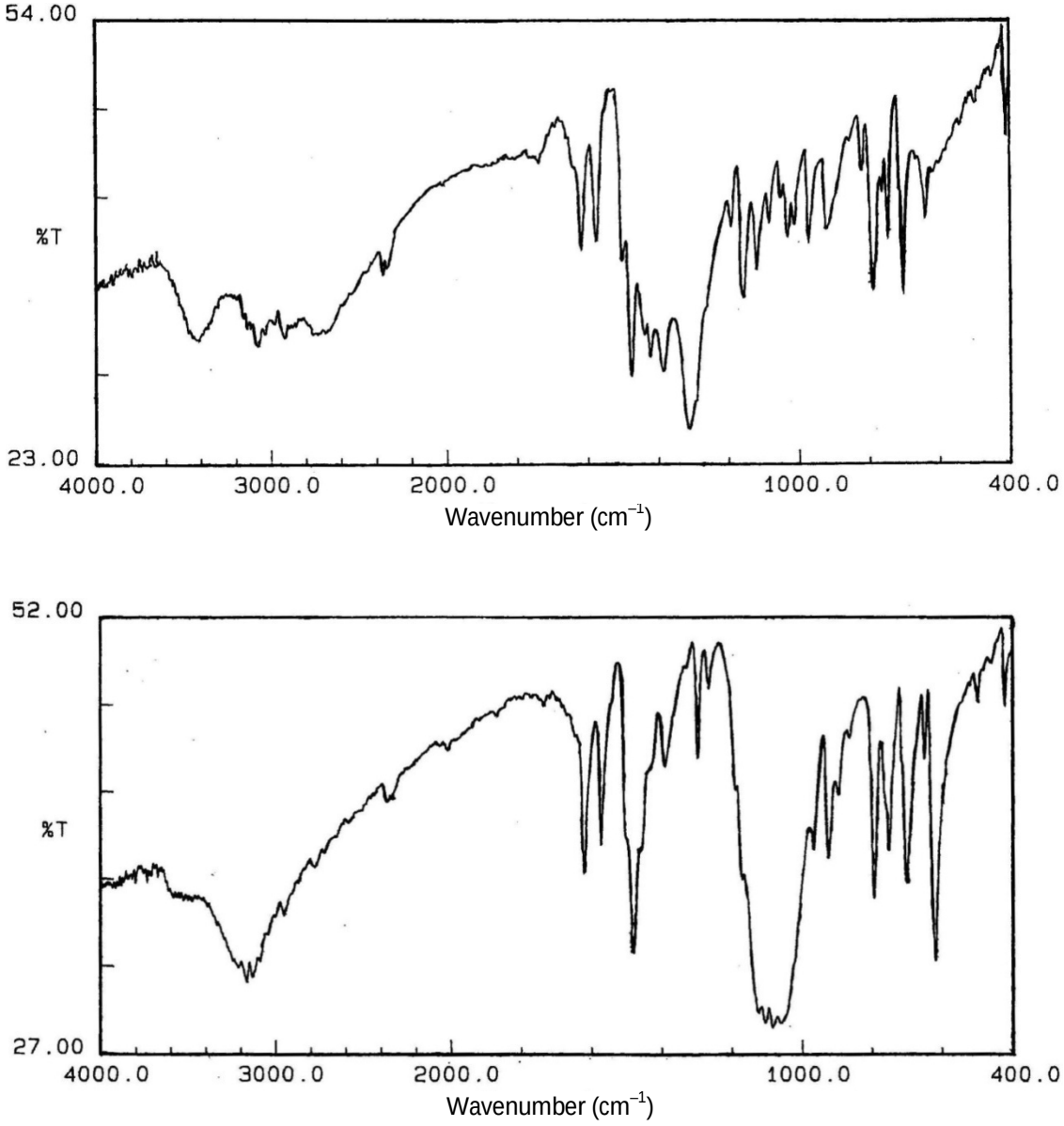

Fig. 4.1: Infrared spectra of $[Cu(impy)_2(NO_3)]NO_3 \cdot H_2O$ (**2**) (top) and $[Cu(impy)_2(ClO_4)]ClO_4 \cdot H_2O$ (**3**) (bottom).

The infrared spectra of **1**–**3** display a broad band centred in the range 3400–3500 cm^{-1} due to the water molecules. A comparatively sharper band observed within 3070–3170 cm^{-1} is attributed to the N–H stretching [8,9,28] of the imidazole fragment of the ligand impy. The strong band observed at 1312 cm^{-1} in the case of **2** is

most likely associated with the nitrate counteranion [29]. The typical perchlorate stretches for **3** are observed as a very strong broad band and a sharp band at 1080 and 620 cm^{-1}, respectively. The representative infrared spectra are given in Fig. 4.1.

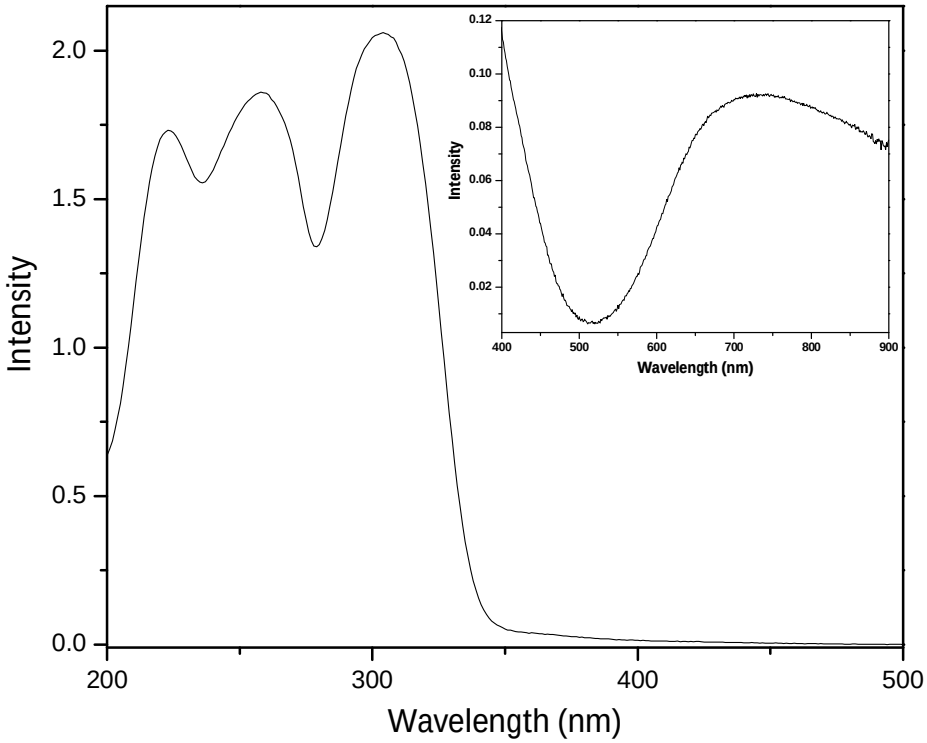

Fig. 4.2: Electronic spectra of $[Cu(impy)_2(ClO_4)]ClO_4 \cdot H_2O$ (**3**) in ~10^{-4} M acetonitrile solution (200-500 nm) and in ~10^{-3} M acetonitrile solution (400-900 nm) (inset).

The electronic spectra have been collected using acetonitrile solutions of **1**–**3**. The spectral profiles are very similar. The representative electronic spectrum is shown in Fig. 4.2. A weak broad band observed in the range 715–745 nm is followed by three very strong bands at ~300, ~260 and ~220 nm. The origin of the weak absorption is assigned to a d-d transition [30−36]. The strong absorptions in the UV region are most likely due to metal-to-ligand charge transfer and intra-ligand transitions [30,32,33].

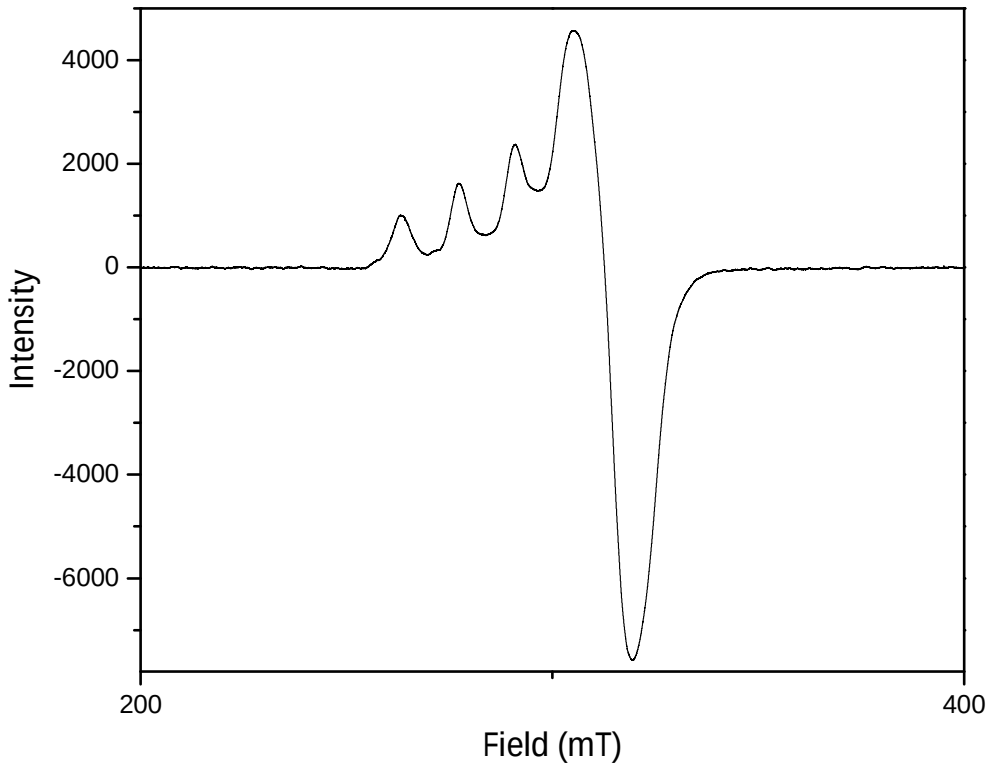

Fig. 4.3: EPR spectrum of $[Cu(impy)_2(ClO_4)]ClO_4 \cdot H_2O$ (**3**) in methanol-ethanol (1:1) solution.

The EPR spectra of **1**–**3** in frozen acetonitrile-toluene (1:1) mixture display an asymmetric signal near $g \approx 2.1$. In none of these spectra is the $g_{\|}$ signal clearly visible except for the two shoulders at the high-field half of the asymmetric signal. However, in a frozen methanol-ethanol (1:1) mixture each of the three complexes displays a well resolved axial spectrum having $g_{\|} \approx 2.3$, $A_{\|} \approx 135 \times 10^{-4}$ cm^{-1} and $g_{\perp} \approx 2.1$. The representative EPR spectrum is displayed in Fig. 4.3. Such axial spectra are typical for copper(II) species having a square-based or a tetragonally elongated octahedral coordination geometry, where the unpaired electron resides in the $d_{x^2-y^2}$ orbital [37,38].

4.4.3. Molecular structures:

The structures of the mononuclear $[Cu(impy)_2Cl_2]$ and $[Cu(impy)_2(NO_3)]^+$ and polymeric $[Cu(impy)_2(ClO_4)]^+$ are depicted in Figs. 4.4−4.6. In each complex, the ligand impy binds the metal centre through the pyridine and the imidazole imine-N atoms forming a five-membered chelate ring. It may be noted that the X-ray structures of the free ligand [39] and its iron(II) [40] and mixed-anion copper(II) [41] complexes are known. The intraligand bond parameters in **1**–**3** are unexceptional and similar to the values observed in the reported structures mentioned above. The bond parameters associated with the metal ions in $[Cu(impy)_2Cl_2]$, $[Cu(impy)_2(NO_3)]^+$ and $[Cu(impy)_2(ClO_4)]^+$ are listed in Table 4.2. The metal to coordinating atom bond lengths in these species are comparable with the bond lengths reported for copper(II) complexes having the same coordinating atoms [1–16,30–36,41,42].

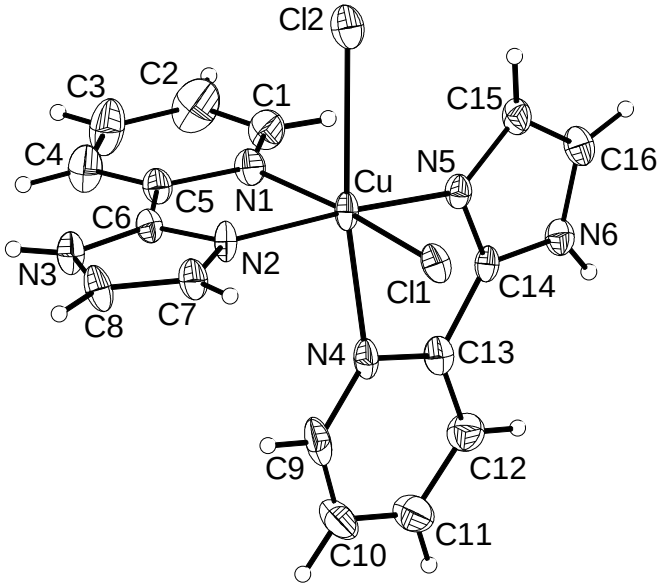

Fig. 4.4: Structures of cis-$[Cu(impy)_2Cl_2]$ with the atom labeling scheme. All non-hydrogen atoms are represented by their 30% probability thermal ellipsoids.

In the chloride containing complex (**1**), the metal centre is in a distorted octahedral N_4Cl_2 coordination sphere owing to coordination of both counteranions in a mutually *cis* orientation (Fig. 4.4). The dihedral angle ($88.9(1)^o$) between the two chelate ring planes is very close to the ideal value of 90^o. The metal to coordinating

atom bond lengths (Table 4.2) clearly indicate that there is a tetragonal elongation due to the Jahn-Teller effect commonly observed for octahedral copper(II) complexes [42,43]. One of the chlorides (Cl2) and one of the two pyridine-N atoms (N4) occupy the elongated axial sites (Fig. 4.4).

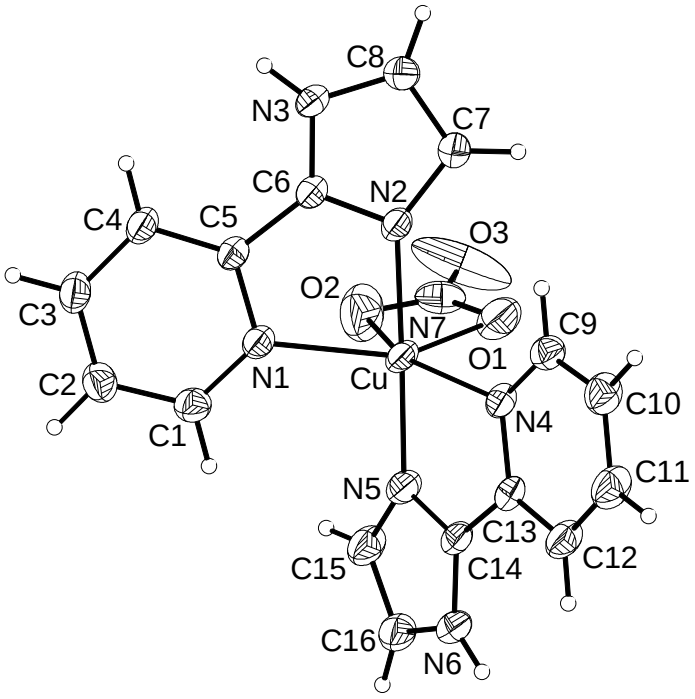

Fig. 4.5: Structures of $[Cu(impy)_2(NO_3)]^+$ (bottom) with the atom labeling scheme. All non-hydrogen atoms are represented by their 30% probability thermal ellipsoids.

For complex **2** only one nitrate is coordinated to the metal centre in an unsymmetrical (with respect to the unequal Cu–O bond lengths) bidentate fashion, forming a four membered chelate ring (Fig. 4.5). Thus the metal centre is in an irregular N_4O_2 coordination sphere. The dihedral angle ($49.3(1)^o$) between the two five membered chelate rings in $[Cu(impy)_2(NO_3)]^+$ is significantly smaller than that in $[Cu(impy)_2Cl_2]$. To have a better understanding of the coordination geometry around the metal centre in $[Cu(impy)_2(NO_3)]^+$, the N-atom (N7) of the nitrate instead of its two O-atoms (O1 and O2) has been taken into consideration. The N_5 sphere can be best described as distorted trigonal bipyramidal. The nitrate and the two pyridine N-atoms (N7, N1 and N4, respectively) form the trigonal plane and the two imidazole N-atoms (N2 and N5) occupy the axial sites (Fig. 4.5). The extent of distortion of this

trigonal bipyramidal N_5 sphere towards a square pyramidal geometry can be evaluated by the τ-value defined as $(\beta - \alpha)/60$, where α is the smallest and β is the largest trans bond angle [37]. The values of τ are zero and one for ideal square-pyramidal and trigonal-bipyramidal geometries, respectively. Considering the two impy ligands for the trans bond angles, the τ value for $[Cu(impy)_2(NO_3)]^+$ is calculated as 0.79.

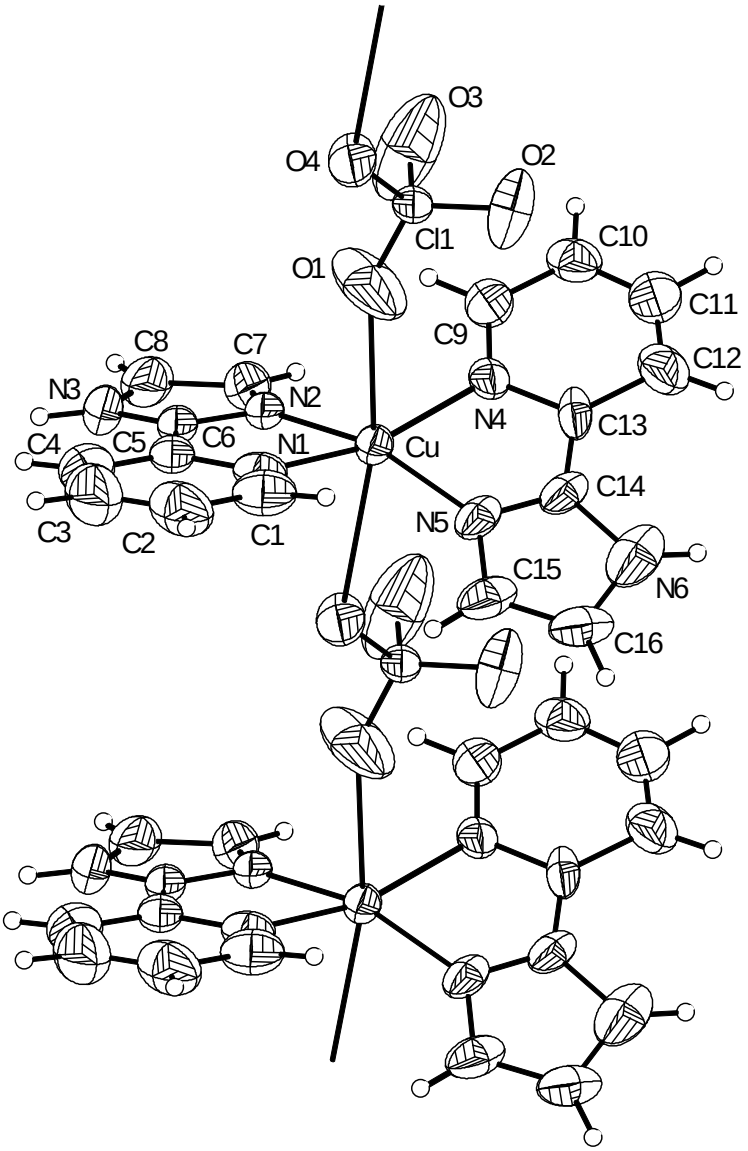

Fig. 4.6: Polymeric structure of $[Cu(impy)_2(ClO_4)]^+$ with the atom labeling scheme. All non-hydrogen atoms are represented by their 30% probability thermal ellipsoids.

As in complex **2**, only one of the two counteranions is coordinated to the metal centre in complex **3**. However, here the coordinated counteranion acts as a bridge and provides a polymeric structure for $[Cu(impy)_2(ClO_4)]^+$ (Fig. 4.6). Consequently, the metal ions are in tetragonally elongated octahedral *trans*-N_4O_2 coordination sphere (Table 4.2). The elongation occurs along the O–Cu–O bonds. In the N_4 equatorial plane, each of the pyridine-N and the imidazole-N atom pairs are mutually *trans* to each other. However, the equatorial N-atoms do not form a perfect square-plane due to the non-planarity of the two chelate rings formed by the two impy moieties. The dihedral angle ($28.3(1)^o$) between the two chelate ring planes in $[Cu(impy)_2(ClO_4)]^+$ is significantly smaller than that in $[Cu(impy)_2Cl_2]$ and $[Cu(impy)_2(NO_3)]^+$.

Table 4.2.: Selected bond lengths [Å] and angles [°] for $[Cu(impy)_2Cl_2]\cdot 3H_2O$ (**1**), $[Cu(impy)_2(NO_3)]NO_3\cdot H_2O$ (**2**) and $[Cu(impy)_2(ClO_4)]ClO_4\cdot H_2O$ (**3**)

$[Cu(impy)_2Cl_2]\cdot 3H_2O$ (**1**)			
Cu–N(1)	2.165(6)	Cu–N(2)	1.963(4)
Cu–N(4)	2.343(6)	Cu–N(5)	1.983(5)
Cu–Cl(1)	2.444(2)	Cu–Cl(2)	2.718(2)
N(1)–Cu–N(2)	79.0(2)	N(1)–Cu–N(4)	90.62(19)
N(1)–Cu–N(5)	93.0(2)	N(1)–Cu–Cl(1)	171.56(14)
N(1)–Cu–Cl(2)	86.88(15)	N(2)–Cu–N(4)	95.5(2)
N(2)–Cu–N(5)	168.9(3)	N(2)–Cu–Cl(1)	92.65(17)
N(2)–Cu–Cl(2)	94.89(16)	N(4)–Cu–N(5)	76.81(19)
N(4)–Cu–Cl(1)	91.52(14)	N(4)–Cu–Cl(2)	168.67(13)
N(5)–Cu–Cl(1)	95.47(14)	N(5)–Cu–Cl(2)	92.28(15)
Cl(1)–Cu–Cl(2)	92.56(6)		
$[Cu(impy)_2(NO_3)]NO_3\cdot H_2O$ (**2**)			
Cu–N(1)	2.103(2)	Cu–N(2)	1.965(2)
Cu–N(4)	2.076(2)	Cu–N(5)	1.945(2)
Cu–O(1)	2.359(4)	Cu–O(2)	2.474(4)
N(1)–Cu–N(2)	81.00(9)	N(1)–Cu–N(4)	131.41(9)
N(1)–Cu–N(5)	97.56(9)	N(1)–Cu–O(1)	129.26(9)
N(1)–Cu–O(2)	79.66(11)	N(2)–Cu–N(4)	100.11(9)
N(2)–Cu–N(5)	178.51(8)	N(2)–Cu–O(1)	88.58(10)
N(2)–Cu–O(2)	87.65(11)	N(4)–Cu–N(5)	81.11(9)
N(4)–Cu–O(1)	99.25(9)	N(4)–Cu–O(2)	148.64(10)
N(5)–Cu–O(1)	92.06(11)	N(5)–Cu–O(2)	91.73(11)
O(1)–Cu–O(2)	50.24(11)		
$[Cu(impy)_2(ClO_4)]ClO_4\cdot H_2O$ (**3**)			
Cu–N(1)	2.026(6)	Cu–N(2)	1.963(5)
Cu–N(4)	2.014(5)	Cu–N(5)	1.949(5)
Cu–O(1)	2.551(7)	Cu–O(4)[a]	2.610(5)
N(1)–Cu–N(2)	81.3(3)	N(1)–Cu–N(4)	162.03(19)
N(1)–Cu–N(5)	99.2(3)	N(1)–Cu–O(1)	78.7(3)
N(1)–Cu–O(4)[a]	86.86(19)	N(2)–Cu–N(4)	101.6(2)
N(2)–Cu–N(5)	162.42(19)	N(2)–Cu–O(1)	95.8(3)
N(2)–Cu–O(4)[a]	81.10(19)	N(4)–Cu–N(5)	83.4(3)
N(4)–Cu–O(1)	83.4(2)	N(4)–Cu–O(4)[a]	111.10(18)
N(5)–Cu–O(1)	101.5(3)	N(5)–Cu–O(4)[a]	81.4(2)
O(1)–Cu–O(4)[a]	165.5(2)		

[a] Symmetry transformation used to generate the equivalent atom: x+1, y, z.

4.4.4. Supramolecular structures:

Complexes **1**–**3** contain conventional hydrogen bond donors, such as water O–H and the impy N–H groups and acceptors, such as chloride (**1**) and O-atoms of the nitrate (**2**) and the perchlorate (**3**). In addition, the O-atoms of the water molecules can also act as hydrogen bond acceptors. We have therefore systematically investigated all the possible intermolecular hydrogen bonding interactions in **1**–**3** to reveal the resulting supramolecular structures and their variations. Four different types of hydrogen bonding are detected. These are N–H···Cl, N–H···O, O–H···Cl and O–H···O interactions. The structural parameters for these interactions are listed in Table 4.3 and the supramolecular structures that have been formed by these hydrogen bonds are illustrated in Figs. 4.7-4.9.

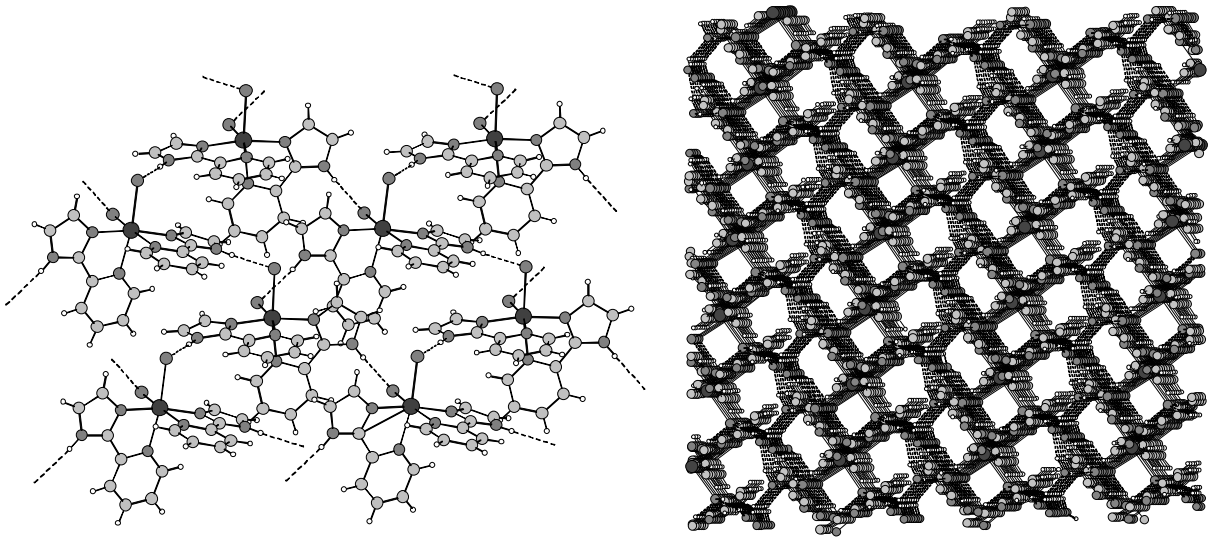

Fig. 4.7: Two-dimensional ordering of *cis*-[Cu(impy)$_2$Cl$_2$] via N–H···Cl hydrogen bonds (left) and three-dimensional honeycomb like structure of *cis*-[Cu(impy)$_2$Cl$_2$]·3H$_2$O (**1**) due to O–H···Cl and O–H···O hydrogen bonds between the two-dimensional layers (right).

The imidazole N-H groups of both impy ligands in [Cu(impy)$_2$Cl$_2$] are involved in hydrogen bonding with the metal bound chlorides of two adjacent molecules. These N–H···Cl interactions help to form a two-dimensional layered structure (Fig. 4.7). Each of the three water molecules present in the crystal lattice is

involved in two hydrogen bonds as a donor with the chlorides or with the water O-atoms (O1 and O2). Thus two of the three water molecules participate in three hydrogen bonds (Table 4.3). These O–H···Cl and O–H···O hydrogen bonds provide the links between the parallel layers of the N–H···Cl connected complex molecules and assemble a three-dimensional honeycomb like structure (Fig. 4.7).

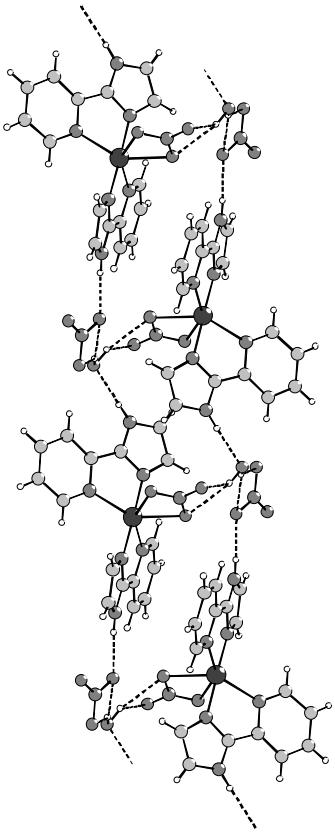

Fig. 4.8: The ladder type structure of $[Cu(impy)_2(NO_3)]NO_3 \cdot H_2O$ (**2**) assembled with the help of N–H···O and bifurcated O–H···O,O hydrogen bonds.

In the case of **2**, the water molecule plays the most crucial role to support and hold the supramolecular structure. Both H-atoms of the water molecule are involved in bifurcated hydrogen bonds (Table 4.3) with the two O-atoms of the uncoordinated nitrate (O4 and O5) and that of the coordinated nitrate (O1 and O3). In addition, the N–H groups of the two impy are also hydrogen bonded to the O-atoms of the water molecule (O7) and the metal uncoordinated nitrate (O5). These N–H···O and bifurcated O–H···O,O hydrogen bonds lead to a one-dimensional ladder like assembly

of **2** in the crystal lattice (Fig. 4.8). There is no other significant interaction between the parallel ladders.

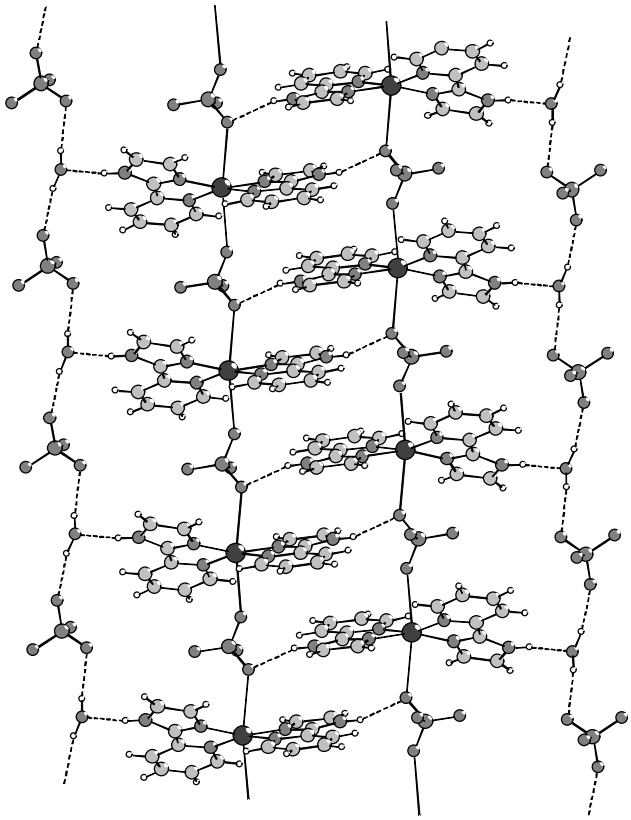

Fig. 4.9: The N–H···O and the O–H···O hydrogen bonds and the resulting ribbon like structure of $[Cu(impy)_2(ClO_4)]ClO_4 \cdot H_2O$ (**3**).

As in **2**, only two types of hydrogen bonds are observed in the case of **3**. These are N–H···O and simple O–H···O bonds. We have seen that the $[Cu(impy)_2(ClO_4)]^+$ units form parallel polymeric chains due to the bridging role of one of the two perchlorates in **3** (Fig. 4.6). Two of these neighboring polymeric chains are connected to each other by two complementary N–H···O hydrogen bonds involving one of the impy N–H groups and the metal coordinated perchlorate-O atom (O4). These N–H···O interactions lead to a ladder like structure of the $[Cu(impy)_2(ClO_4)]^+$ units (Fig. 4.9). Each of these ladders is flanked on both sides by two chains each constituted by alternate water molecule and the uncoordinated perchlorate. Here each water molecule is connected to the two adjacent perchlorates by O–H···O hydrogen

bonds. The connections between the water-perchlorate chains and the ladder of $[Cu(impy)_2(ClO_4)]^+$ are provided by the water O-atoms (O9) through N–H···O interactions involving the second N–H groups directed outwards on the two sides of the ladder like assembly of $[Cu(impy)_2(ClO_4)]^+$ units. As a result, a ribbon type structure of **3** is formed (Fig. 4.9). There is no other significant interaction between the parallel ribbons.

Table 4.3: Hydrogen bonding parameters (Å and °) for $[Cu(impy)_2Cl_2]\cdot 3H_2O$ (**1**), $[Cu(impy)_2(NO_3)]NO_3\cdot H_2O$ (**2**) and $[Cu(impy)_2(ClO_4)]ClO_4\cdot H_2O$ (**3**)

Complex	D–H···A	d (H···A)	d (D···A)	< (DHA)
$[Cu(impy)_2Cl_2]\cdot 3H_2O$ (**1**)	N3–H3A···Cl2[a]	2.26	3.116(6)	174.6
	N6–H6A···Cl1[b]	2.34	3.194(5)	176.3
	O1–H1A···Cl1	2.41(2)	3.350(6)	163(5)
	O1–H1B···O2[c]	1.80(1)	2.755(7)	165(5)
	O2–H2A···Cl2	2.29(2)	3.243(5)	165(5)
	O2–H2B···O1[d]	1.81(1)	2.758(7)	163(4)
	O3–H3B···Cl2	2.29(2)	3.199(13)	155(5)
	O3–H3C···Cl1[d]	2.68(2)	3.402(14)	131(15)
$[Cu(impy)_2(NO_3)]NO_3\cdot H_2O$ (**2**)	N3–H3A···O7	1.90	2.759(3)	172
	N6–H6A···O5	1.92	2.781(4)	174
	O7–H7A···O1[e]	2.18(2)	3.025(4)	146(3)
	O7–H7A···O3[e]	2.04(2)	2.849(5)	142(3)
	O7–H7B···O4[f]	2.18(2)	3.041(4)	150(3)
	O7–H7B···O5[f]	2.15(2)	3.001(4)	149(3)
$[Cu(impy)_2(ClO_4)]ClO_4\cdot H_2O$ (**3**)	N3–H3A···O4[g]	2.15	2.979(8)	162
	N6–H6A···O9	1.89	2.74(1)	171
	O9–H9A···O5	2.08(2)	2.98(2)	153(5)
	O9–H9B···O8[h]	1.93(2)	2.83(2)	155(6)

[a] [x, –y+1, z–1/2], [b] [x, –y+2, z–1/2], [c] [x+1/2, y–1/2, z], [d] [x–1/2, –y+3/2, z–1/2], [e] [–x, –y+1, –z+2], [f] [x, y+1, z+1], [g] [–x, –y+1, –z+1], [h] [x–1, y, z].

4.5. Conclusions:

To explore the effect of the counteranion on the molecular as well as intermolecular hydrogen bond aided supramolecular structures, three ternary complexes of copper(II) have been synthesized. In these complexes, the N,N-donor 2-(1H-imidazol-2-yl)-pyridine (impy) is the primary ligand and the counteranions, namely chloride, nitrate and perchlorate, are the ancillary ligands. The complexes $[Cu(impy)_2Cl_2]\cdot 3H_2O$ (**1**), $[Cu(impy)_2(NO_3)]NO_3\cdot H_2O$ (**2**) and $[Cu(impy)_2(ClO_4)]ClO_4\cdot H_2O$ (**3**) have been characterized by microanalytical, magnetic susceptibility and spectroscopic (IR, UV-vis and EPR) measurements. X-ray structure determinations of all the three complexes have been performed. The complex containing chloride is a neutral hexacoordinated species due to coordination of both counteranions, while the remaining two complexes are cationic species due coordination of only one of the two counteranions. $[Cu(impy)_2(ClO_4)]^+$ is polymeric while the other two complexes are monomeric. The coordination geometries are tetragonally elongated octahedral in both **1** and **3**, while it is distorted trigonal bipyramidal in **2**, when considering the N-atom instead of the two O-atoms of the bidentate chelating nitrate for the description. Complex **1** has the simplest counteranion chloride and both of them are coordinated to the metal ion, while **2** and **3** contain triangular and tetrahedral counteranion, respectively and only one counteranion is bound to the metal centre in both. Despite of that, **1** has the most complex supramolecular assembly compared to that of **2** and **3**. One of the reasons is that **1** is a trihydrate, whilst each of the other two complexes is monohydrate. In the case of **1**, a honeycomb like structure through N–H···Cl, O–H···Cl and O–H···O hydrogen bonds is observed. A much simpler one-dimensional ladder like structure is assembled in the case of **2** due to N–H···O and bifurcated O–H···O,O hydrogen bonds. Complex **3** is very similar with complex **2** with respect to the composition, but here the cationic part is a linear polymer. Here also the final supramolecular assembly via N–H···O and simple O–H···O hydrogen bonds is one-dimensional, but it is like a ribbon.

4.6. References:

[1] N. R. Sangeetha, S. N. Pal, C. E. Anson, A. K. Powell, S. Pal; *Inorg. Chem. Commun.* 3 (2000) 415.

[2] S. N. Pal, K. R. Radhika, S. Pal; *Z. Anorg. Allg. Chem.* 627 (2001) 1631.

[3] A. Mukhopadhyay, G. Padmaja, S. N. Pal, S. Pal; *Inorg. Chem. Commun.* 6 (2003) 381.

[4] S. Das, G. P. Muthukumaragopal, S. N. Pal, S. Pal; *New J. Chem.* 27 (2003) 1102.

[5] V. K. Muppidi, T. Htwe, P. S. Zacharias, S. Pal; *Inorg. Chem. Commun.* 7 (2004) 1045.

[6] V. K. Muppidi, P. S. Zacharias, S. Pal; *Chem. Commun.* (2005) 2515.

[7] V. K. Muppidi, P. S. Zacharias, S. Pal; *Inorg. Chem. Commun.* 8 (2005) 543.

[8] S. Das, S. Pal; *J. Mol. Struct.* 741 (2005) 183.

[9] S. Das, S. Pal; *J. Mol. Struct.* 753 (2005) 68.

[10] V. K. Muppidi, S. Pal; *Eur. J. Inorg. Chem.* (2006) 2871.

[11] S. Das, S. A. Maloor, S. N. Pal, S. Pal; *Cryst. Growth Des.* 6 (2006) 2103.

[12] V. K. Muppidi, P. S. Zacharias, S. Pal; *J. Solid State Chem.* 180 (2007) 132.

[13] V. K. Muppidi, S. Das, P. Raghavaiah, S. Pal; *Inorg. Chem. Commun.* 10 (2007) 234.

[14] S. Pal; *Rev. Inorg. Chem.* 29 (2009) 111.

[15] T. Ghosh, A. Mukhopadhyay, K. S. C. Dargaiah, S. Pal; *Struct. Chem.* 21 (2010) 147.

[16] S. Das, S. Pal; *Inorg. Chim. Acta* 363 (2010) 3028.

[17] K. A. Reeder, E. V. Dose, L. J. Wilson; *Inorg. Chem.* 17 (1978) 1071.

[18] W. E. Hatfield; in: E. A. Boudreaux, L. N. Mulay (Eds.), *Theory and Applications of Molecular Paramagnetism*, Wiley, New York, (1976) p. 491.

[19] SMART version 5.630, SAINT-plus version 6.45: *Pro-grams for data collection and extraction,* Bruker-Nonius Analytical X-ray Systems Inc., Madison, WI, USA, (2003).

[20] G. M. Sheldrick; SADABS: *Program for Area Detector Absorption Correction,* University of Göttingen, Göttingen, Germany, (1997).

[21] A. C. T. North, D. C. Philips, F. S. Mathews; *Acta Crystallogr. Sect. A* 24 (1968) 351.

[22] L. J. Farrugia; *J. Appl. Crystallogr.* 32 (1999) 837.

[23] T. P. Radhakrishnan, W. C. Herndon; *J. Phys. Chem.* 95 (1991) 10609.

[24] G. M. Sheldrick; XHELX-97: *Structure Determination Software,* University of Göttingen, Göttingen, Germany, (1997).

[25] P. McArdle; *J. Appl. Crystallogr.* 28 (1995) 65.

[26] A. L. Spek, Platon: *A Multipurpose Crystallographic Tool,* Utrecht University, Utrecht, The Netherlands, (2002).

[27] W. J. Geary; *Coord. Chem. Rev.* 7 (1971) 81.

[28] P. Naumov, M. Ristova, B. Šoptrajanov, M. Zugik; *J. Mol. Struct.* 598 (2001) 235.

[29] K. Nakamoto; *Infrared and Raman Spectra of Inorganic and Coordination Compunds,* Wiley, New York, (1986) p. 256.

[30] A. Paulovicova, U. El-Ayaan, K. Shibayama, T. Morita, Y. Fukuda; *Eur. J. Inorg. Chem.* (2001) 2641.

[31] A. Taha; *Spectrochim. Acta A* 59 (2003) 1611.

[32] C. P. Pradeep, P. S. Zacharias, S. K. Das; *J. Chem. Sci.* 117 (2005) 133.

[33] R. Srivastava, T. H. Bennur, D. Srinivas; *J. Mol. Catal. A* 226 (2005) 199.

[34] A. K. Patra, M. Nethaji, A. R. Chakravarty; *Dalton Trans.* (2005) 2798.

[35] P. Sarmah, R. K. Barman, P. Purkayastha, S. J. Bora, P. Phukan, B. K. Das; *Indian J. Chem. Sect. A* 48 (2009) 637.

[36] Z. Lu, T. Ladrak, O. Roubeau, J. van der Toorn, S. J. Teat, C. Massera, P. Gamez, J. Reedijk; *Dalton Trans.* (2009) 3559.

[37] A. W. Addison, T. N. Rao, J. Reedijk, J. V. Rijn, G. C. Verschoor; *J. Chem. Soc. Dalton Trans.* (1984) 1349.

[38] Z. Liu, C. Duan, Y. Tian, X. You; *Inorg. Chem.* 35 (1996) 2253.

[39] R. Kia, H.-K. Fun, H. Kargar; *Acta Crystallogr. Sect. E* 65 (2009) o780.

[40] G. S. Matouzenko, G. Molnar, N. Bréfuel, M. Perrin, A. Bousseksou, S. A. Borshch; *Chem. Mater.* 15 (2003) 550.

[41] A. Morsali, A. Ramazani, M. Babaee, F. Jamali, F. Gouranlou, H. Arjmandfar, A. Yanovsky; *J. Coord. Chem.* 56 (2003) 455.

[42] S. N. Pal, J. Pushparaju, N. R. Sangeetha, S. Pal; *Trans. Met. Chem.* 25 (2000) 529.

[43] M. Melník, M. Kabešová, Ĺ. Macášková, C. E. Holloway; *J. Coord. Chem.* 45 (1998) 31.

Chapter 5

Syntheses and structures of cerium(IV) and gadolinium(III) complexes with biacetyl bis(benzoylhydrazone)

5.1. Abstract:

[Ce(babh)$_2$] and [Gd(Hbabh)(babh)] have been synthesized by the reactions of biacetyl bis(benzoylhydrazone) (H_2babh) with $CeCl_3 \cdot 6H_2O$ and $Gd(NO_3)_3 \cdot 5H_2O$, respectively in presence of KOH in alcoholic media. Each complex has been characterized by elemental analysis, magnetic and various spectroscopic (IR, UV-Vis, NMR and EPR) measurements. In both complexes, the metal center is surrounded by a dodecahedral N_4O_4 environment provided by two tetradentate N_2O_2 donor ligands. The cerium(IV) complex crystallizes as [Ce(babh)$_2$]$\cdot CH_2Cl_2$ by diffusion of *n*-hexane in its dichloromethane solution while gadolinium(III) complex crystallizes as [Gd(babh)(Hbabh)]$\cdot H_2O$ by slow evaporation of its dichloromethane solution. The lattice water molecule in [Gd(babh)(Hbabh)]$\cdot H_2O$ is connected to the N–H group of the protonated amide functionality of $Hbabh^-$ through N–H···O hydrogen bond. Self-assembly of [Ce(babh)$_2$]$\cdot CH_2Cl_2$ via intermolecular C–H···N and C–H···Cl hydrogen bonds and π–π interactions provides one-dimensional "ladder" type structure. On the other hand, [Gd(babh)(Hbabh)]$\cdot H_2O$ forms two-dimensional "sheet" like network through intermolecular N–H···O and O–H···N hydrogen bonds.

5.2. Introduction:

In chapters 2 and 3, we have described the chemistry of copper(II) and nickel(II) with biacetyl bis(benzoylhydrazone) (H_2babh) [1,2]. In the present chapter, we report a cerium(IV) and a gadolinium(III) complex with this tetradentate N_2O_2 donor Schiff base (H_2babh). In the following sections, syntheses, characterization and physical properties of these two complexes have been described. The single crystal structures of both complex molecules have been determined and also their supramolecular networks via intermolecular non-covalent interactions have been highlighted.

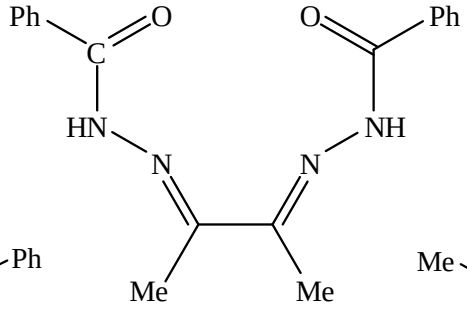

H_2babh

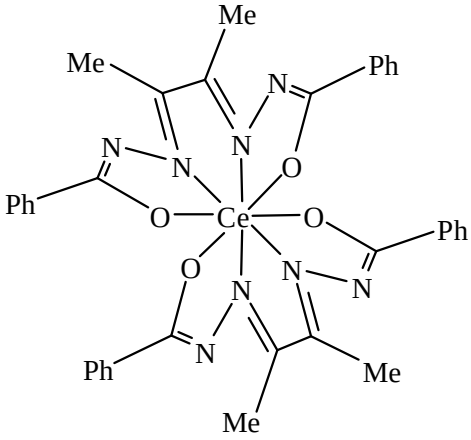

[Ce(babh)$_2$]

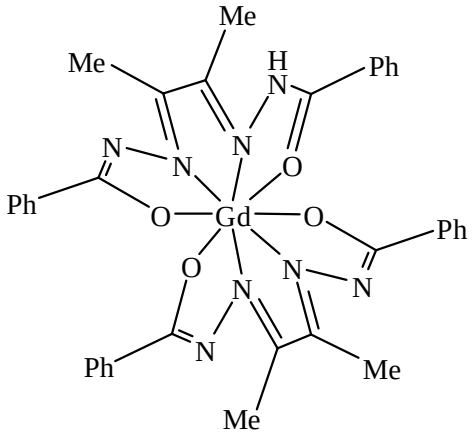

[Gd(babh)(Hbabh)]

5.3. Experimental:

5.3.1. Materials:

The tetradentate Schiff base biacetyl bis(benzoylhydrazone) (H_2babh) was synthesized by following the same procedure as described in chapter 2. All other chemicals and solvents were of analytical grade available commercially and were used as received.

5.3.2. Physical measurements:

A Thermo Finnigon Flash EA1112 series elemental analyzer was used for the microanalysis (C, H, N) data. Infrared spectra were recorded by using KBr pellets on a Jasco-5300 FT-IR spectrophotometer. A Shimadzu UV-3600 UV-VIS-NIR spectrophotometer was used to record the electronic spectra. The emission spectra were recorded by a Horiba Jobin Yvon Fluoromax-4 spectrofluorometer. The ^{1}H NMR spectrum of the cerium(IV) complex in $CDCl_3$ solution was recorded with the help of a Bruker 400 MHz NMR spectrometer. X-band EPR measurements with the gadolinium(III) complex were performed on a Jeol JES-FA200 spectrometer. Magnetic susceptibility measurements with the gadolinium(III) complex were performed in the temperature range of 2-300 K on a Quantum Design VSM-SQUID. Room temperature (300 K) magnetic susceptibilities were measured using a Sherwood Scientific balance. Diamagnetic corrections calculated from Pascal's constants [3] were used to obtain the molar paramagnetic susceptibilities. A Digisun DI-909 conductivity meter was used to measure the solution electrical conductivities.

5.3.3. Synthesis of [Ce(babh)$_2$]:

A methanol (4 ml) solution of KOH (40 mg, 0.71 mmol) was added to a methanol (25 ml) solution of H_2babh (100 mg, 0.31mmol) and the mixture was stirred at 50º C for half an hour. Then methanol (10 ml) solution of $CeCl_3 \cdot 6H_2O$ (60 mg, 0.169 mmol) was added slowly to the solution of H_2babh and KOH and refluxed for one hour. A slate black microcrystalline solid was deposited. It was collected by filtration and dried in air. The yield was 84 mg (~64%). Anal. Calcd. for $CeC_{36}H_{32}N_8O_4$ (780.81): C, 55.38; H, 4.13; N, 14.35%. Found: C, 55.62; H, 4.51; N, 10.46%. UV-Vis in CH_2Cl_2 solution: λ (nm) (10^{-3} x ε (M^{-1} cm^{-1})) = 265^{sh} (58.6), 283 (61.9), 365^{sh} (40.3), 400 (44.2), 510^{sh} (9.2).

5.3.4. Synthesis of [Gd(babh)(Hbabh)]:

At room temperature a methanol (4 ml) solution of KOH (40 mg, 0.71 mmol) was added to a methanol (25 ml) solution of H_2babh (100 mg, 0.31 mmol) and stirred for 10 min. Then methanol (10 ml) solution of $Gd(NO_3)_3 \cdot 5H_2O$ (67 mg, 0.155 mmol) was added to the mixture of H_2babh and KOH and stirred for 7 hours. The resulting yellow solution was evaporated to about 5 ml. A yellow amorphous powder precipitated within 2-3 days was collected by filtration. The yield was 93 mg (~82%). Anal. Calcd. for $GdC_{36}H_{33}N_8O_4$ (798.95): C, 54.12; H, 4.16; N, 14.03%. Found: C, 52.95; H, 4.59; N, 7.98%. UV-Vis in CH_2Cl_2 solution: λ (nm) (10^{-3} x ε (M^{-1} cm^{-1})) = 263 (42.3), 305^{sh} (29.7), 415 (49.5), 430^{sh} (47.7), 460^{sh} (26.5).

5.3.5. X-ray Crystallography:

The single crystals of the cerium(IV) complex were obtained by diffusion of *n*-hexane into dichloromethane solution of the complex, whereas the single crystals of the gadolinium(III) complex were grown by slow evaporation of its dichloromethane solution at room temperature. In each case, the unit cell parameters and the intensity data were obtained on a Bruker-Nonius SMART APEX CCD single crystal diffractometer, equipped with a graphite monochromator and a Mo Kα fine-focus sealed tube (λ = 0.71073 Å) operated at 2.0 kW. The detector was placed at a distance of 6.0 cm from the crystal. Data were collected at 100 K with a scan width of 0.3º in ω and an exposure time of 5 s/frame. The SMART software was used for data acquisition and the SAINT-Plus software was used for data extraction [4]. The absorption corrections were performed with the help of SADABS program [5]. The cerium(IV) complex crystallizes as $[Ce(babh)_2] \cdot CH_2Cl_2$ in the monoclinic $P2_1/c$ space group, whereas the gadolinium(III) complex crystallizes as $[Gd(babh)(Hbabh)] \cdot H_2O$ in monoclinic $C2/c$ space group. The structures were solved by direct methods and refined on F^2 by full-matrix least-squares procedures. In each case, the asymmetric unit contains a whole complex molecule with the corresponding solvent molecule. The non-hydrogen atoms in both structures were refined using anisotropic thermal parameters. The hydrogen atoms of the lattice water molecule of

[Gd(babh)(Hbabh)]·H_2O were located in a difference Fourier map and refined with U_{iso}(H) = 1.5U_{iso}(O). The remaining hydrogen atoms in [Gd(babh)(Hbabh)]·H2O and all the hydrogen atoms in [Ce(babh)$_2$]·CH_2Cl_2 were included in the structure factor calculations at idealized positions by using a riding model. The SHELX-97 programs [6] available in the WinGX package [7] were used for structure solution and refinement. The Diamond, Mercury 2.4 and Platon [8] packages were used for molecular graphics. Selected crystallographic data are listed in Table 5.1.

Table 5.1: Selected crystallographic data for $[Ce(babh)_2]\cdot CH_2Cl_2$ and $[Gd(babh)(Hbabh)]\cdot H_2O$

Complex	$[Ce(babh)_2]\cdot CH_2Cl_2$	$[Gd(babh)(Hbabh)]\cdot H_2O$
Empirical formula	$CeC_{37}H_{34}N_8O_4Cl_2$	$GdC_{36}H_{35}N_8O_5$
Formula weight (g mol^{-1})	865.75	816.96
Temperature (K)	100	100
Crystal size (mm)	0.48 x 0.18 x 0.14	0.28 x 0.14 x 0.08
Crystal system	monoclinic	monoclinic
Space group	$P2_1/c$	$C2/c$
a (Å)	11.5199(9)	27.003(6)
b (Å)	25.818(2)	20.395(5)
c (Å)	12.791(1)	19.854(5)
α (°)	90	90
β (°)	104.362(1)	128.806(3)
γ (°)	90	90
V ($Å^3$)	3685.6(5)	8521(3)
Z	4	8
Calculated density (g cm^3)	1.560	1.274
Absorption coefficient (mm^{-1})	1.431	1.601
Measured reflections	37702	29912
Unique reflections	7187	7474
Reflections ($I \geq 2\sigma(I)$)	7005	5228
Data/restraints/Parameters	7187/0/469	7474/23/441
$R1$, $wR2$ ($I \geq 2\sigma(I)$)	0.0237, 0.0596	0.0948, 0.2107
$R1$, $wR2$ (all data)	0.0245, 0.0601	0.1366, 0.2270
Goodness-of-fit on F^2	1.099	1.170
Largest diff. peak and hole (e $Å^{-3}$)	0.506, -0.484	2.703, -2.628

5.4. Results and discussion:

5.4.1. Synthesis and some properties:

Mononuclear eight coordinated cerium(IV) and gadolinium(III) complexes were prepared in good yields by reacting biacetyl bis(benzoylhydrazone) (H_2babh) with hydrated $CeCl_3 \cdot 6H_2O$ and $Gd(NO_3)_3 \cdot 5H_2O$, respectively in presence of KOH in alcoholic media. The products [Ce(babh)$_2$] and [Gd(babh)(Hbabh)] were isolated as slate black microcrystalline material and as amorphous yellow powder, respectively. Room temperature (300 K) magnetic moment of [Gd(babh)(Hbabh)] is 7.94 μ_B. Thus the metal centre in [Gd(babh)(Hbabh)] is highly paramagnetic with seven unpaired electrons. On the other hand, the diamagnetic nature of [Ce(babh)$_2$] confirms the +4 oxidation state of the metal ion. Each complex is highly soluble in dichloromethane, chloroform, methanol, dimethylsulfoxide and acetone. [Ce(babh)$_2$] affords a deep brown solution whereas [Gd(babh)(Hbabh)] gives a yellow solution. Both complexes behave as non-electrolyte in solution. These complexes do not show any luminescence property in solution.

5.4.2. Spectroscopic characterization:

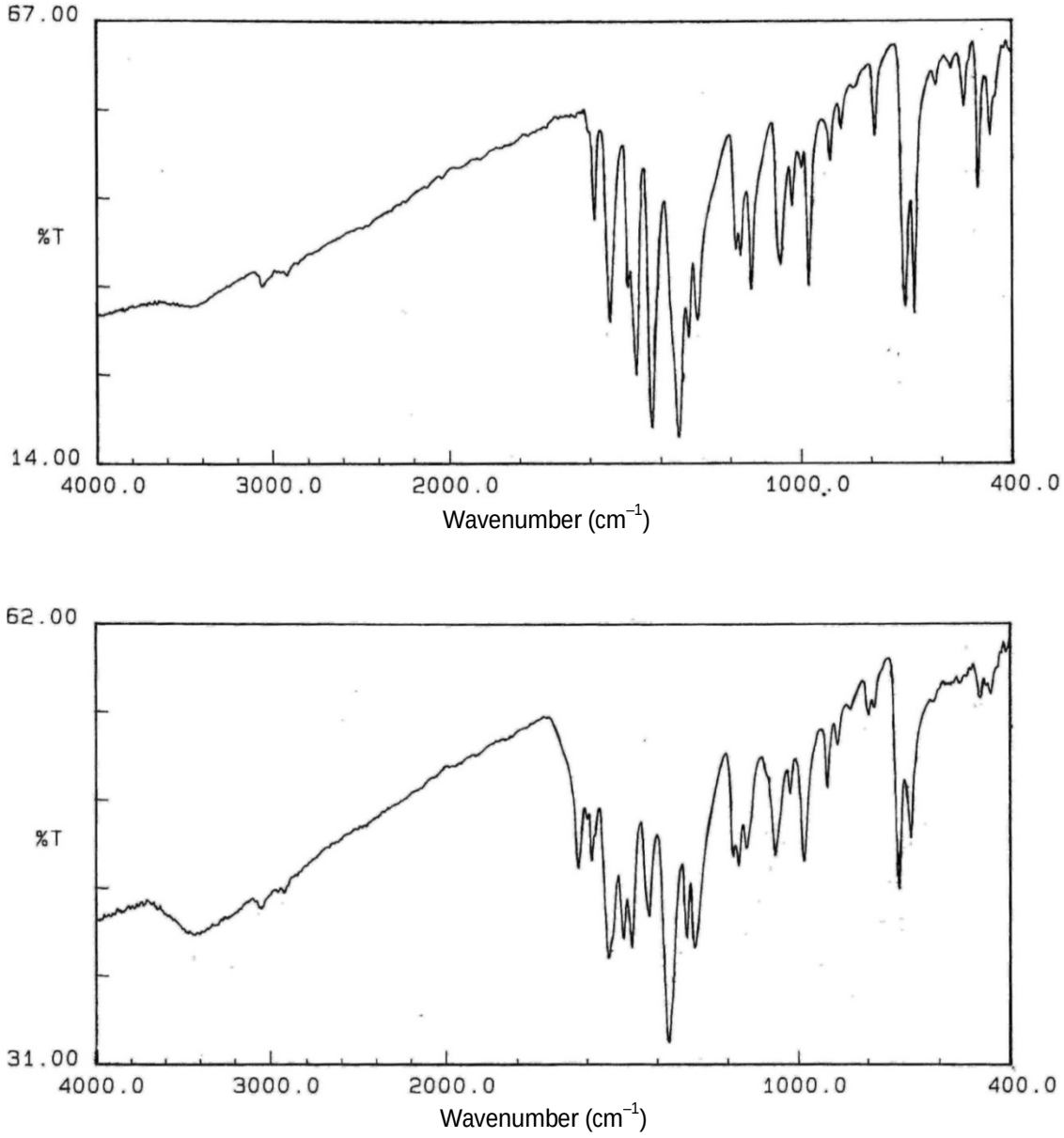

Fig.5.1: Infrared spectrum of [Ce(babh)$_2$] (top) and [Gd(babh)(Hbabh)] (bottom).

The infrared spectrum of free Schiff base H_2babh shows a medium intensity band at ~3200 cm^{-1} for the N–H stretch and a strong band at ~1655 cm^{-1} for the C=O stretch [9]. In case of [Ce(babh)$_2$], disappearance of both these bands confirms the iminolate state [10–21] of all the amide functionalities of the two coordinated ligands. In contrast, [Gd(babh)(Hbabh)] exhibits a medium intensity band at 1624 cm^{-1}. This

band is assigned to the metal coordinate C=O stretch of the protonated amide functionality in Hbabh$^-$. Absence of any such band in the spectrum of [Ce(babh)$_2$] further confirms complete deprotonation of both the ligands. Each complex displays the C=N stretch as a medium intensity band at ~1590 cm^{-1} [22–24].

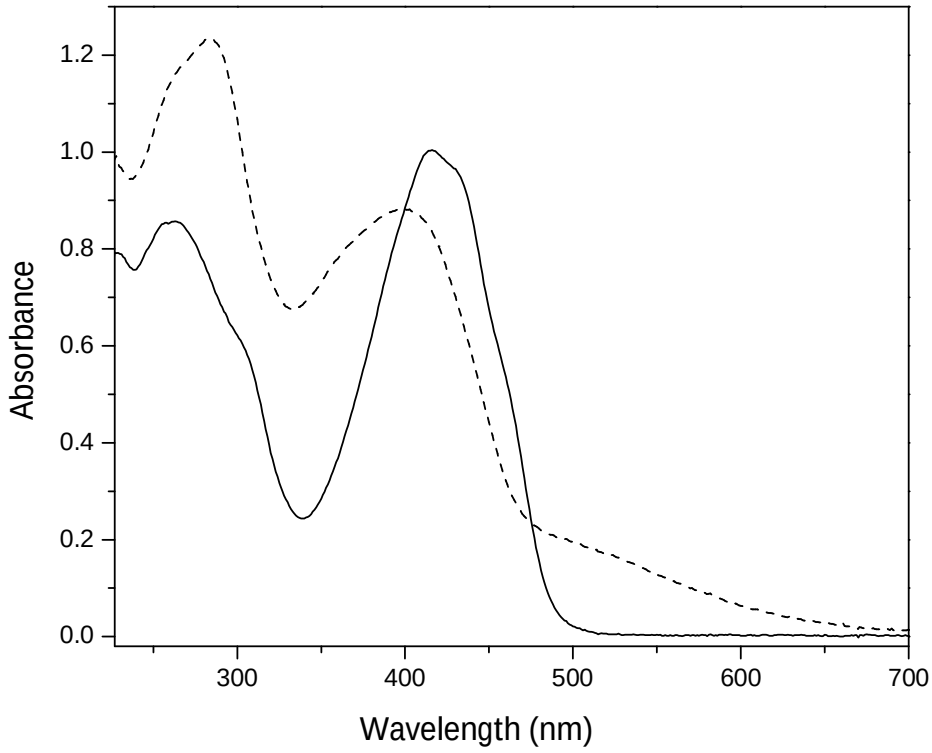

Fig. 5.2: Electronic spectra of [Ce(babh)$_2$] (----) and [Gd(babh)(Hbabh)] (—) in dichloromethane.

The electronic spectra of both complexes have been collected using their dichloromethane solutions. The spectra are shown in Fig. 5.2. The cerium(IV) complex displays a prominent shoulder at ~ 510 nm followed by two strong bands at 400 nm and 283 nm with two shoulders at 365 nm and 265 nm. The gadolinium(III) complex shows two main absorptions at 415 nm and 263 nm with several shoulders. In case of lanthanides, f orbitals are deeply seated and hence f–f electronic transitions cannot be influenced by the ligand fields. As a result, absorptions are very sharp and similar to the spectra displayed by the free ions. Such absorptions also have low extinction coefficients as f–f transitions are Laporte forbidden [25]. Sometimes,

migration of excited f electrons to the higher energy orbitals such as (n+1)s, (n+1)p and (n+2)d orbitals may cause broadening of absorption bands. Although the bands are somewhat broad in the present two complexes, but in cerium(IV) f orbitals are empty and gadolinium(III) complex has the most stable f^7 configuration due to half filled state. Therefore migration of f electrons to higher levels is not possible in both cases. Thus it is very likely that the broad low energy absorptions observed for the present complexes are due to ligand to metal orbitals ((n+1)s, (n+1)p and (n+2)d) charge transfer and the broad high energy absorptions are due to intraligand transitions [26].

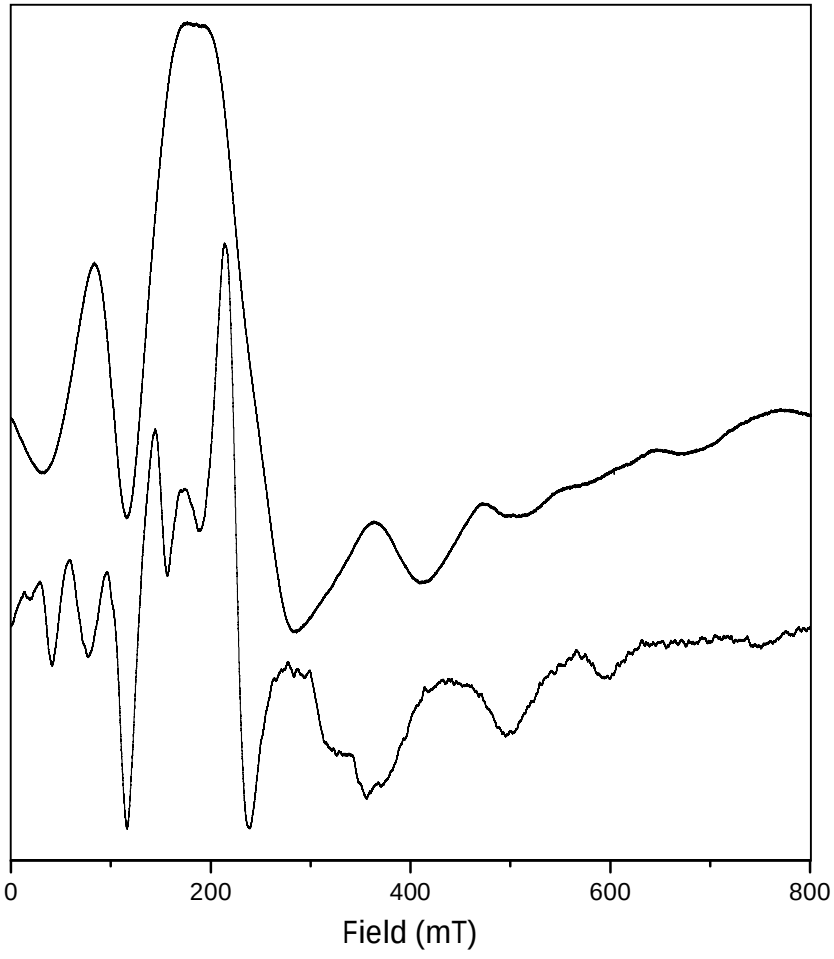

Fig. 5.3: EPR spectra of [Gd(babh)(Hbabh)] complex in powder form at room temperature (top) and in dichloromethane at –150º C (bottom).

The EPR spectra of [Gd(babh)(Hbabh)] in powder phase at 25º C and in frozen (−150º C) dichloromethane are depicted in Fig. 5.3. The spectral profiles are very typical of gadolinium(III) species [27]. Zero field effect in an f^7 odd electron system removes the degeneracy of the Kramer's doublets (S= 7/2, M_S= ±7/2, ±5/2, ±3/2 and ±1/2) and on application of magnetic field further splitting of the doublets leads to several EPR lines spreading from 0–800 mT [27].

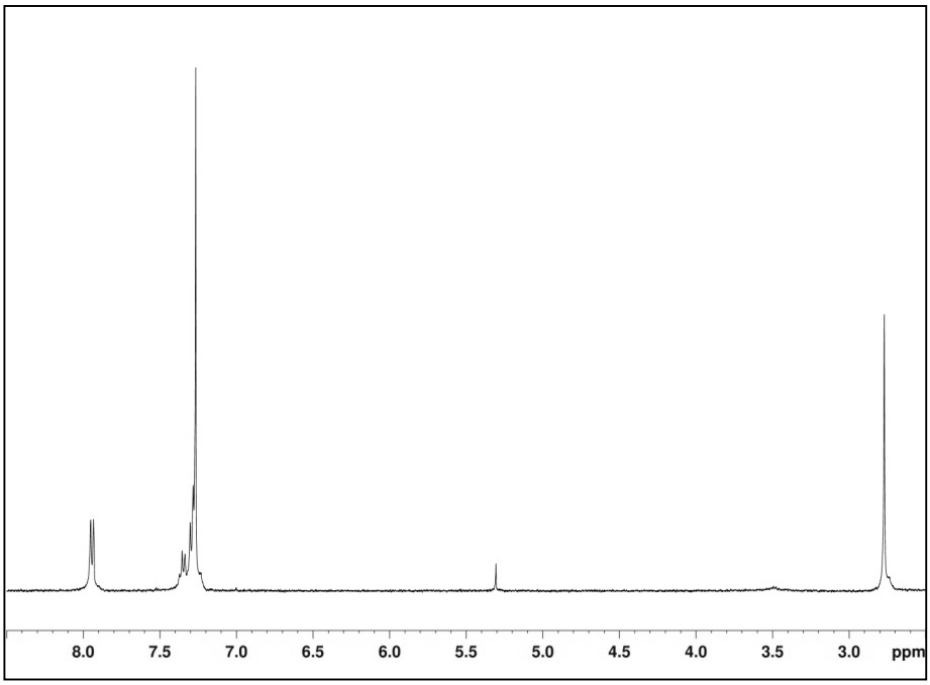

Fig. 5.4: NMR spectrum of [Ce(babh)$_2$] in $CDCl_3$.

The ^{1}H NMR spectrum (Fig. 5.4) of [Ce(babh)$_2$] has been recorded in $CDCl_3$ solution of the complex. The four methyl groups of the two babh^{2-} ligands are equivalent and generate a singlet at δ 2.77 ppm. The *ortho* and *para* protons of four phenyl groups (two from each ligand) resonate as doublet at δ 7.95 ppm (J = 7.2 Hz) and δ 7.35 ppm (J = 7.2 Hz), respectively. The *meta* protons are observed as a triplet at δ 7.30 ppm (J = 7.2 Hz).

5.4.3. Cryomagnetic behavior of [Gd(babh)(Hbabh)]:

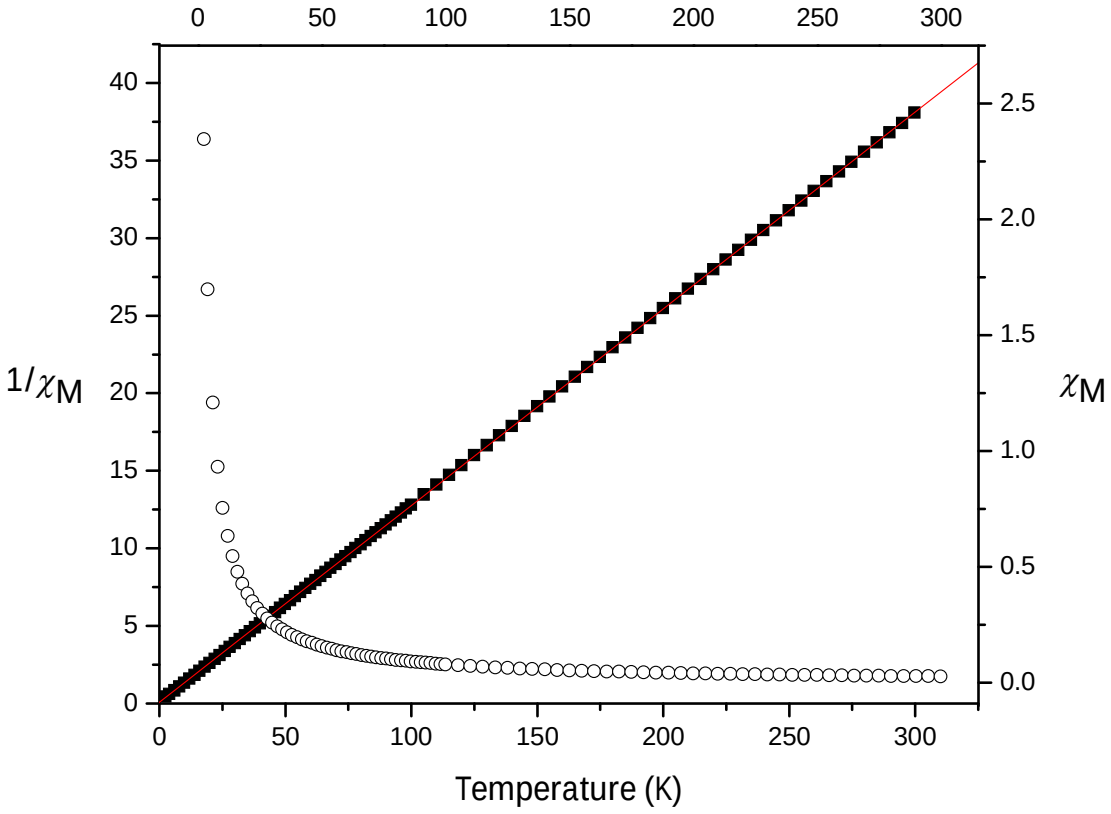

Fig. 5.5: χ_M (○) and $1/\chi_M$ (■) of [Gd(babh)(Hbabh)] as functions of temperature.

Temperature dependent magnetic susceptibility measurements of [Gd(babh)(Hbabh)] have been performed (Fig.5.5). The complex behaves as Curie-paramagnetic. The data were fit with the Curie-Weiss law, $\chi_M = C/ (T-\theta)$. The quality of the fit is very good (Fig. 5.5). The fit provides the Weiss constant θ as –0.7 K and Curie constant C as 7.9 emu/ g Oe. From Curie constant C, effective magnetic moment (μ_{eff}) of [Gd(babh)(Hbabh)] can be evaluated by using the $\mu_{eff}^2 = 3Ck/ \mu_B^2 N$ equation where k is the Boltzmann constant, μ_B is the Bohr magneton and N is the Avogadro's number. From the above equation μ_{eff} is calculated as 7.94 μ_B. The spin only magnetic moment of Gd^{3+} ion can be estimated using the equation $\mu_{eff} = \mu_S = 2[S(S+1)]^{1/2}$ since Gd^{3+}, an f^7 system, has no orbital moment ($L = 0$). The experimental μ_{eff} and the spin only μ_S values are identical.

5.4.4. Molecular structures:

In both complexes, the metal centers are in dodecahedral N_4O_4 coordination sphere (Fig. 5.6) assembled by two N_2O_2 donor tetradentate ligands. The complete structures of [Ce(babh)$_2$]·CH_2Cl_2 and [Gd(babh)(Hbabh)]·H_2O are shown in Figs. 5.7 and 5.8. In each complex, both ligands bind the metal centre through the imine-N and the protonated or deprotonated amide-O atoms forming three five membered chelate rings. The bond lengths and the bond angles related to the metal centers are given in Table. 5.2.

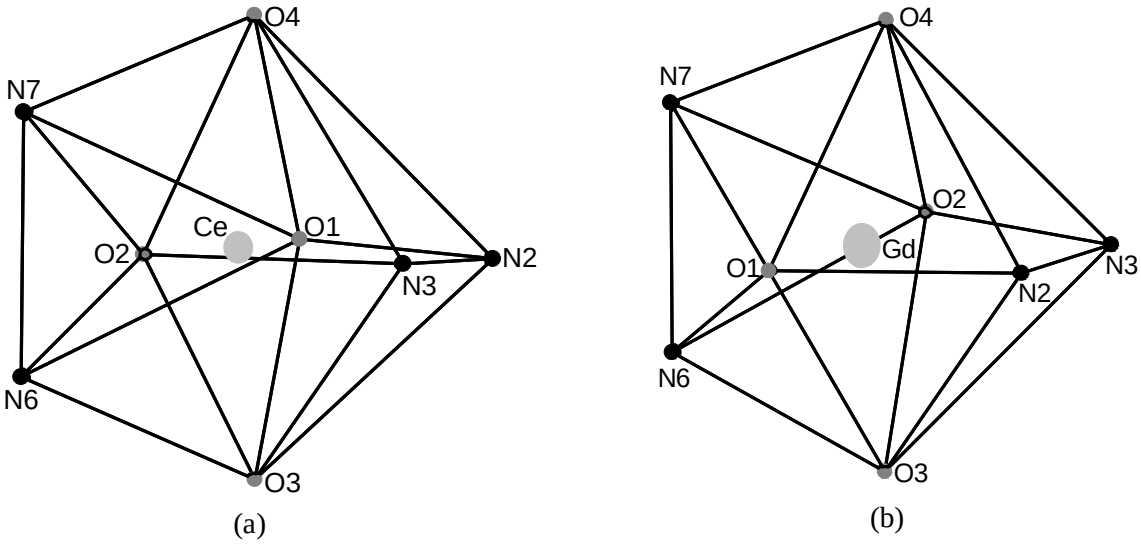

Fig. 5.6: Dodecahedral coordination sphere around metal centre in (a) [Ce(babh)$_2$]·CH_2Cl_2 and (b) [Gd(babh)(Hbabh)]·H_2O.

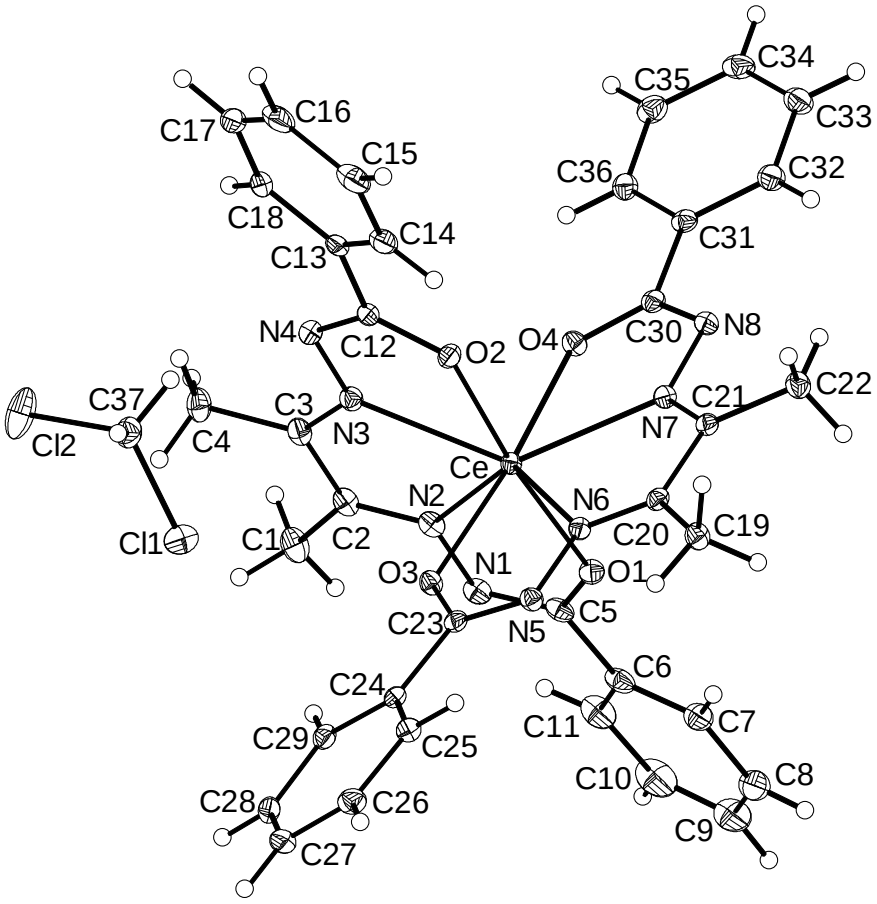

Fig. 5.7: Structure of $[Ce(babh)_2]\cdot CH_2Cl_2$ with the atom labeling scheme. All non-hydrogen atoms are represented by their 30% probability thermal ellipsoids.

In $[Ce(babh)_2]$, the amide functionalities in both $babh^{2-}$ ligands are completely deprotonated to iminolate [–C(O⁻)=N–] form. The C–O bond lengths (1.299(2)–1.304(2) Å) and the C=N bond lengths (1.308(3)–1.312(3) Å) in amide functionalities of the ligands ($babh^{2-}$) confirm the presence of O-coordinating iminolate form [10–21]. Three five-membered chelate rings formed by each N_2O_2 donor ligand excluding the phenyl rings are satisfactorily planar. For the first ligand, maximum and minimum deviations from the mean plane (mean deviation 0.034 Å) constituted by Ce, O1, O2, N1–N4, C2, C3, C5, and C12 are 0.056 and 0.008 Å, respectively. For the second ligand, maximum and minimum deviations from the mean plane (mean deviation 0.028 Å) constituted by Ce, O3, O4, N5–N8, C20, C21, C23 and C30 are 0.047 and 0.007 Å, respectively. The dihedral angle (89.8º) between these two planes indicates that they are essentially orthogonal to each other. Each

phenyl ring is twisted along the C–C bond that connects it with the terminal chelate ring. The dihedral angles formed by C(6)–C(11) phenyl ring (mean deviation 0.01 Å) and C(13)–C(18) phenyl ring (mean deviation 0.006 Å) with the mean plane containing Ce, O1, O2, N1–N4, C2, C3, C5, and C12 are 13.5 and 17.2º, respectively. The dihedral angles formed by C(24)–C(29) phenyl ring (mean deviation 0.006 Å) and C(31)–C(36) phenyl ring (mean deviation 0.003 Å) with the mean plane containing Ce, O3, O4, N5–N8, C20, C21, C23 and C30 are 14.3 and 9.4º, respectively.

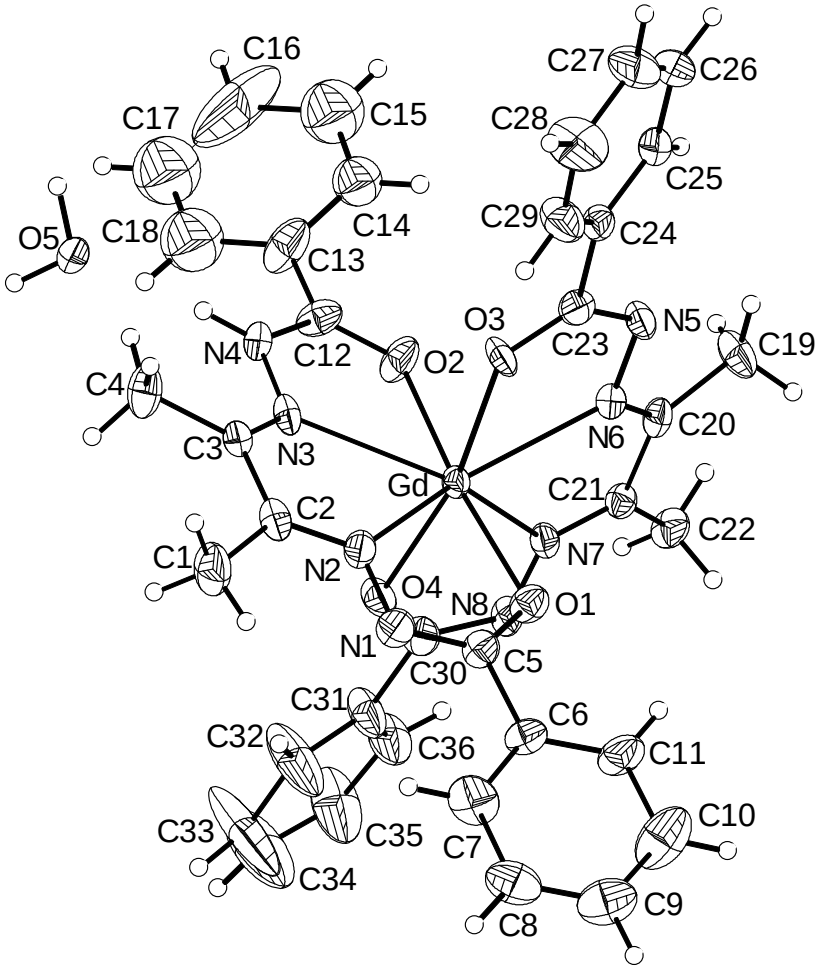

Fig. 5.8: Structure of [Gd(babh)(Hbabh)]·H_2O with the atom labeling scheme. All non-hydrogen atoms are represented by their 30% probability thermal ellipsoids.

In case of [Gd(babh)(Hbabh)]·H_2O, the amide functionalities of one ligand is completely deprotonated ($babh^{2-}$) while the other one ($Hbabh^{-}$) has one deprotonated and one protonated amide functionality. The shorter C(12)=O(2) bond length

(1.248(14) Å) and longer C(12)–N(4) bond length (1.382(15) Å) indicate the existence of the protonated O-coordinating amide [–C(O)–NH–] form in $Hbabh^{-}$. Comparatively longer C–O bond lengths (1.273(14)–1.303(14) Å) and shorter C=N bond lengths (1.287(15)–1.313(15) Å) in the remaining amide functionalities confirm their iminolate forms [10–21]. The lattice water molecule (H_2O) is connected to the protonated amide via N–H···O hydrogen bonding. The hydrogen bonding parameters are given in Table. 5.3. As in [Ce(babh)$_2$], here also the three fused chelate rings formed by each N_2O_2 donor ligand excluding the benzene rings are satisfactorily planar. The maximum and minimum deviations from the mean plane (mean deviation 0.061 Å) constituted by Gd, O1, O2, N1–N4, C2, C3, C5, and C12 are 0.107 and 0.001 Å, respectively and those deviations from the mean plane (mean deviation 0.072 Å) constituted by Gd, O3, O4, N5–N8, C20, C21, C23 and C30 are 0.119 and 0.027 Å, respectively. However, the dihedral angle (84.3º) between these two mean planes is slightly less than that (89.8º) observed for [Ce(babh)$_2$]. The twisting of the phenyl rings along the C–C bond is larger in this complex than that in the cerium(IV) complex. The dihedral angles formed by C(6)–C(11) (mean deviation 0.010 Å) and C(13)–C(18) phenyl ring planes with the mean plane built up by Gd, O1, O2, N1–N4, C2, C3, C5, and C12 are 19.9º and 38.1º, respectively. The dihedral angles generated by C(24)–C(29) (mean deviation 0.006 Å) and C(31)–C(36) phenyl ring (mean deviation 0.037 Å) planes with the mean plane constituted by Gd, O3, O4, N5–N8, C20, C21, C23 and C30 are 25.4º and 17.3º, respectively. C(13)–C(18) phenyl ring is distorted along a two-fold axis passing through C13 and C16 that are *para* to each other. The dihedral angle of the second orientation (C13, C14A, C15A, C16, C17A, C18A) of this phenyl ring with the corresponding three chelate ring plane (Gd, O1, O2, N1–N4, C2, C3, C5, and C12) is 56.6º.

Table 5.2: Selected bond lengths (Å) and angles (º) for [Ce(babh)$_2$]·CH_2Cl_2 and [Gd(babh)(Hbabh)]·H_2O

[Ce(babh)$_2$]·CH_2Cl_2 (**1**)			
Ce–O(1)	2.2671(15)	Ce–O(3)	2.2647(14)
Ce–O(2)	2.2651(14)	Ce–O(4)	2.2718(14)
Ce–N(2)	2.5100(17)	Ce–N(6)	2.5107(17)
Ce–N(3)	2.5079(17)	Ce–N(7)	2.5096(17)
O(3)–Ce–O(2)	91.83(5)	N(3)–Ce–N(7)	136.11(5)
O(3)–Ce–O(1)	88.93(5)	O(3)–Ce–N(2)	83.05(5)
O(2)–Ce–O(1)	171.35(5)	O(2)–Ce–N(2)	125.41(6)
O(3)–Ce–O(4)	171.66(5)	O(1)–Ce–N(2)	63.23(5)
O(2)–Ce–O(4)	89.40(5)	O(4)–Ce–N(2)	89.52(5)
O(1)–Ce–O(4)	91.10(5)	N(3)–Ce–N(2)	62.12(6)
O(3)–Ce–N(3)	85.34(5)	N(7)–Ce–N(2)	141.81(6)
O(2)–Ce–N(3)	63.30(5)	O(3)–Ce–N(6)	63.30(5)
O(1)–Ce–N(3)	125.35(5)	O(2)–Ce–N(6)	81.96(5)
O(4)–Ce–N(3)	87.85(5)	O(1)–Ce–N(6)	90.70(5)
O(3)–Ce–N(7)	125.06(5)	O(4)–Ce–N(6)	125.04(5)
O(2)–Ce–N(7)	82.97(5)	N(3)–Ce–N(6)	132.48(5)
O(1)–Ce–N(7)	89.55(5)	N(7)–Ce–N(6)	61.81(5)
O(4)–Ce–N(7)	63.27(5)	N(2)–Ce–N(6)	138.23(6)
[Gd(babh)(Hbabh)]·H_2O **(2)**			
Gd–O(4)	2.313(8)	Gd–O(3)	2.326(7)
Gd–O(1)	2.325(8)	Gd–O(2)	2.407(9)
Gd–N(7)	2.488(9)	Gd–N(2)	2.504(11)
Gd–N(6)	2.495(9)	Gd–N(3)	2.567(10)
O(4)–Gd–O(3)	168.0(3)	N(7)–Gd–N(6)	62.1(3)
O(4)–Gd–O(1)	90.1(3)	O(4)–Gd–N(2)	85.2(3)
O(3)–Gd–O(1)	95.7(3)	O(3)–Gd–N(2)	88.0(3)
O(4)–Gd–O(2)	89.3(3)	O(1)–Gd–N(2)	64.0(3)
O(3)–Gd–O(2)	86.4(3)	O(2)–Gd–N(2)	124.1(3)
O(1)–Gd–O(2)	171.8(3)	N(7)–Gd–N(2)	139.1(3)
O(4)–Gd−N(7)	63.8(3)	N(6)–Gd–N(2)	143.8(3)
O(3)–Gd–N(7)	126.6(3)	O(4)–Gd–N(3)	85.6(3)
O(1)–Gd–N(7)	88.8(3)	O(3)–Gd–N(3)	82.5(3)
O(2)–Gd–N(7)	83.6(3)	O(1)–Gd–N(3)	124.9(3)
O(4)–Gd–N(6)	125.6(3)	O(2)–Gd–N(3)	63.3(3)
O(3)–Gd–N(6)	64.5(3)	N(7)–Gd–N(3)	135.3(3)
O(1)–Gd–N(6)	94.3(3)	N(6)–Gd–N(3)	131.5(3)
O(2)–Gd–N(6)	79.4(3)	N(2)–Gd–N(3)	60.9(3)

5.4.5. Supramolecular structures:

In both complexes, the solvent molecules trapped in the crystal lattice play very important roles to build the corresponding supramolecular structures.

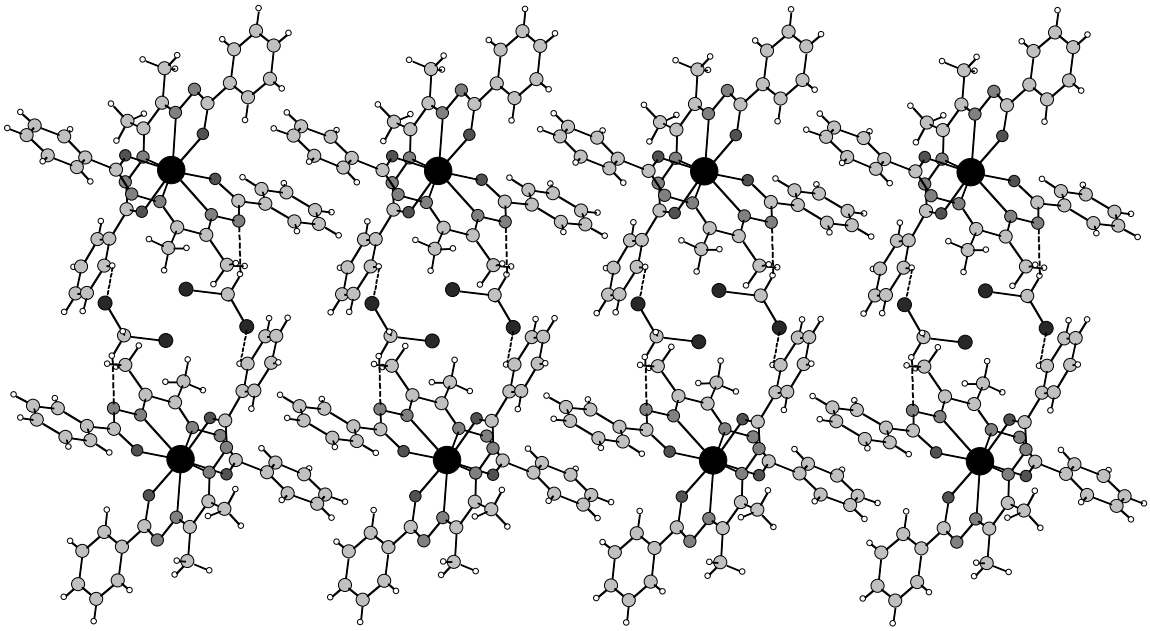

Fig. 5.9: The ladder type structure of $[Ce(babh)_2]\cdot CH_2Cl_2$ assembled via C–H···N and C–H···Cl hydrogen bonds and π–π interactions.

In the crystal lattice, $[Ce(babh)_2]\cdot CH_2Cl_2$ units exist as dimers via hydrogen bonds involving $babh^{2-}$ ligands and the CH_2Cl_2 molecules. In the dimer, one C–H and one Cl-atom of each CH_2Cl_2 participate in a C–H···N hydrogen bond with a deprotonated amide-N atom of a $babh^{2-}$ ligand of one complex molecule and a C–H···Cl hydrogen bond [28–33] with *ortho* C–H group of a phenyl ring of a $babh^{2-}$ ligand of a second complex molecule, respectively. The C–H···N and the C–H···Cl hydrogen bond parameters are listed in Table. 5.3. In the centrosymmetric $\{[Ce(babh)_2]\cdot CH_2Cl_2\}_2$, two CH_2Cl_2 molecules bridge the two $[Ce(babh)_2]$ molecules via two C–H···N and two C–H···Cl hydrogen bonds (Fig. 5.9). The phenyl rings of one $babh^{2-}$ ligand in the $[Ce(babh)_2]$ molecules of each $\{[Ce(babh)_2]\cdot CH_2Cl_2\}_2$ dimer are involved in π–π interactions with the two adjacent dimers. As a result, a one-dimensional π-stacked assembly of $\{[Ce(babh)_2]\cdot CH_2Cl_2\}_2$ dimers is formed (Fig.

5.9). The distance between the centroids (cg) of C(6)–C(11) phenyl ring of one dimer and C(13)–C(18) phenyl ring of the adjacent dimer is approximately 3.7 Å. These intermolecular C–H···N, C–H···Cl and π–π interactions assisted self-assembly pattern of [Ce(babh)$_2$]·CH_2Cl_2 can be best described as "ladder" type (Fig. 5.9) where, the steps of the ladder are made by hydrogen bonds and the two sides of the ladder are made by π–π interactions.

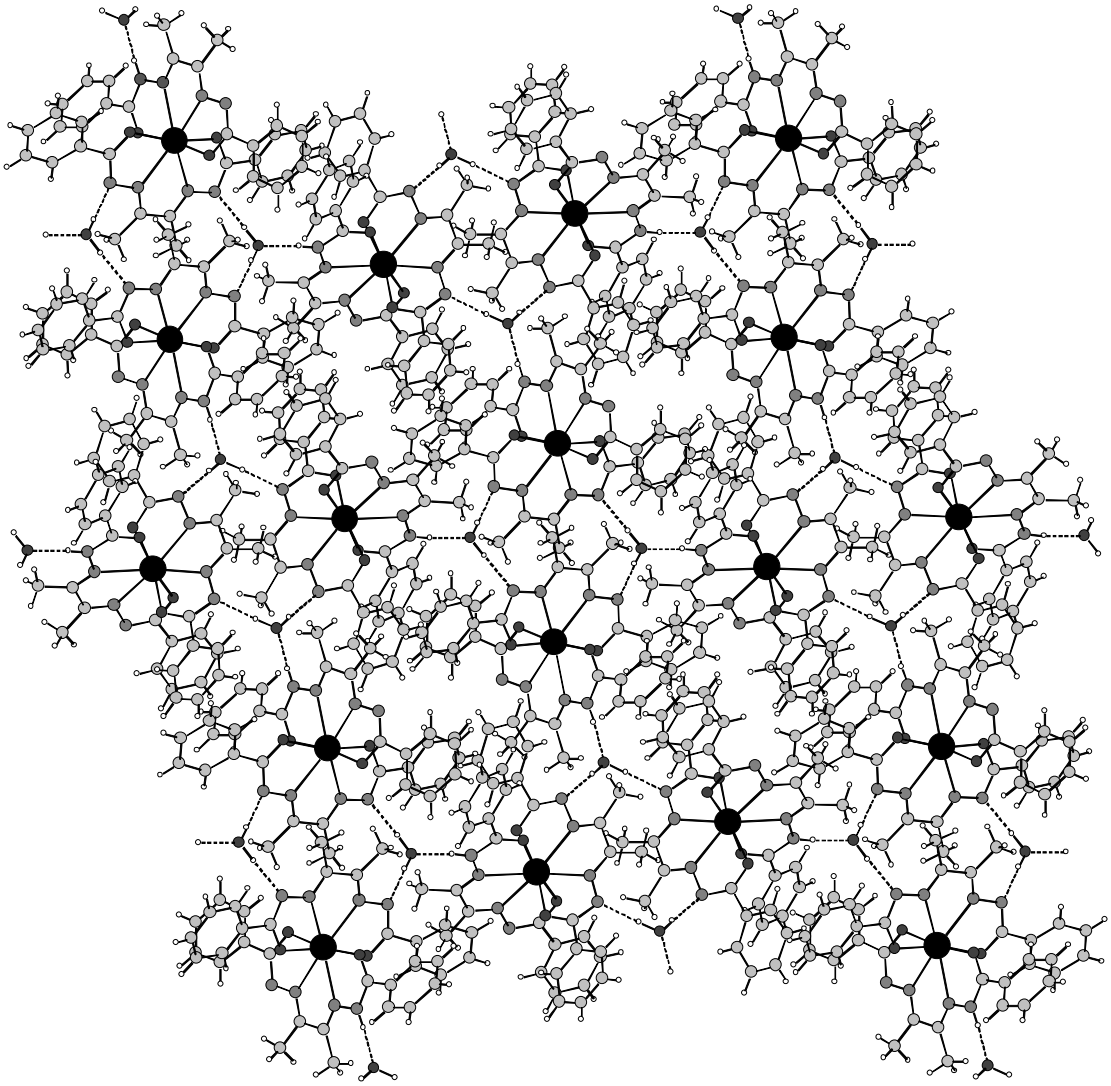

Fig. 5.10: The two-dimensional network of [Gd(babh)(Hbabh)]·H_2O via N–H···O and O–H···N hydrogen bonds.

In [Gd(babh)(Hbabh)]·H_2O complex, the water (H_2O) molecule is strongly connected to the monoanionic ligand $Hbabh^-$ through N–H···O hydrogen bond. The

N–H group of the protonated amide functionality of $Hbabh^-$ acts as the donor and O-atom of the water molecule acts as the acceptor. The water molecule also participates as donor in two O–H···N hydrogen bonds involving the deprotonated amide-N atoms of two $babh^{2-}$ ligands of two adjacent complex molecules. Thus each water molecule is connected to three complex molecules. The parameters of these three hydrogen bonds are summarized in Table. 5.3. Self-assembly of $[Gd(babh)(Hbabh)]\cdot H_2O$ via these intermolecular N–H···O and O–H···N hydrogen bonds leads to a two-dimensional "sheet" like network (Fig. 5.10).

Table 5.3.: Hydrogen-bonding parameters (Å and º) for $[Ce(babh)_2]\cdot CH_2Cl_2$ and $[Gd(babh)(Hbabh)]\cdot H_2O$

Complex	D–H···A	d (H···A) (Å)	d (D···A) (Å)	< (DHA) (º)
$[Ce(babh)_2]\cdot CH_2Cl_2$	C37–H37B···N4	2.51	3.345(3)	144
	C29–H29···Cl2	2.81	3.564(2)	138
$[Gd(babh)(Hbabh)]\cdot H_2O$	N4–H4···O5	1.97	2.818(15)	168
	O5–H5A···N5[a]	1.98(12)	2.937(18)	168(9)
	O5–H5B···N8[b]	1.93(6)	2.884(12)	167(9)

[a] [x, –y, z+1/2]

[b] [–x+1/2, y–1/2, –z+1/2]

5.5. Conclusions:

A cerium(IV) and a gadolinium(III) complex with biacetyl bis(benzoylhydrazone) (H_2babh) have been synthesized. Elemental analysis, magnetic and spectroscopic (IR, UV-Vis, EPR, and NMR spectra) measurements have been used to characterize the complexes. The molecular structures of both complexes $[Ce(babh)_2]$ and [Gd(babh)(Hbabh)] have been determined by X-ray crystallography. In each complex, two tetradentate N_2O_2 donor ligands assemble a dodecahedral N_4O_4 coordination sphere around the metal centre. Each ligand forms three five-membered fused chelate rings with the metal centre. Excluding the phenyl rings, the planar ligands are mutually orthogonal to each other. The complexes crystallize as

[Ce(babh)$_2$]·CH_2Cl_2 and [Gd(babh)(Hbabh)]·H_2O. In the crystal lattice, both species are involved in intermolecular non-covalent interactions. Self-assembly of [Ce(babh)$_2$]·CH_2Cl_2 via C–H···Cl and C–H···N hydrogen bonds and π–π interaction leads to one-dimensional "ladder" type structure. On the other hand, [Gd(babh)(Hbabh)]·H_2O forms a two-dimensional "sheet" like network through strong O–H···N and N–H···O hydrogen bonds.

5.6. References:

[1] T. Ghosh, A. Mukhopadhyay, K. S. C. Dargaiah, S. Pal; *Struct. Chem.* 21 (2010) 147.

[2] T. Ghosh, S. Pal; *Inorg. Chim. Acta.* 363 (2010) 3632.

[3] W. E. Hatfield; In: E. A. Boudreaux, L. N. Mulay (eds), *Theory and applications of molecular paramagnetism*, Wiley, New York, (1976) p 491.

[4] SMART version 5.630, SAINT-plus version 6.45: *Pro-grams for data collection and extraction,* Bruker-Nonius Analytical X-ray Systems Inc., Madison, WI, USA, (2003).

[5] G. M. Sheldrick; SADABS: *Program for empirical absorption correction,* University of Göttingen, Göttingen, Germany, (1997).

[6] G. M. Sheldrick; SHELX-97: *Programs for structure solution and refinement,* University of Göttingen, Göttingen, Germany, (1997).

[7] L. J. Farrugia; *J. Appl. Crystallogr.* 32 (1999) 837.

[8] A. L. Spek; PLATON: *A multipurpose crystallographic tool,* Utrecht University, Utrecht, The Netherlands, (2002).

[9] W. Kemp; *Organic spectroscopy,* Macmillan, Hampshire, (1987) p 62.

[10] N. R. Sangeetha, K. Baradi, R. Gupta, C. K. Pal, V. Manivannan, S. Pal; *Polyhedron* 18 (1999) 1425.

[11] N. R. Sangeetha, S. Pal; *J. Chem. Crystallogr.* 29 (1999) 287.

[12] N. R. Sangeetha, S. N. Pal, C. E. Anson, A. K. Powell, S. Pal; *Inorg. Chem. Commun.* 3 (2000) 415.

[13] N. R. Sangeetha, S. Pal; *Polyhedron* 19 (2000) 1593.

[14] N. R. Sangeetha, S. N. Pal, S. Pal; *Polyhedron* 19 (2000) 2713.

[15] S. Pal; *Proc. Indian Acad. Sci. (Chem. Sci.)* 114 (2002) 417.

[16] A. Mukhopadhyay, G. Padmaja, S. N. Pal, S. Pal; *Inorg. Chem. Commun.* 6 (2003) 381.

[17] S. Das, G. P. Muthukumaragopal, S. N. Pal, S. Pal; *New J. Chem.* 27 (2003) 1102.

[18] S. Das, S. Pal; *J. Mol. Struct.* 741(2005) 183.

[19] S. Das, S. Pal; *J. Mol. Struct.* 753 (2005) 68.

[20] A. Mukhopadhyay, S. Pal; *Eur. J. Inorg. Chem.* (2006) 4879.

[21] R. Raveendran, S. Pal; *Eur. J. Inorg. Chem.* (2008) 5540.

[22] S. G. Sreerama, S. N. Pal, S. Pal; *Inorg. Chem. Commun.* 4 (2001) 656.

[23] S. N. Pal, S. Pal; *Polyhedron* 22 (2003) 867.

[24] A. Mukhopadhyay, S. Pal; *J. Chem. Cryst.* 35 (2005) 737.

[25] K. B. Yatsimirskii, N. K. Davidenko; *Coord. Chem. Rev.* 27 (1979) 223.

[26] A. Mukhopadhyay, E. Kolehmainen, C. P. Rao; *Carbohydr. Res.* 324 (2000) 30.

[27] T. K. Prasad, M.V. Rajasekharan; *Inorg. Chem.* 48 (2009) 11543.

[28] M. Prabhakar, P. S. Zacharias, S. K. Das; *Inorg. Chem.* 44 (2005) 2585.

[29] S. Das, S. Pal; *Inorg. Chem. Acta.* 363 (2010) 3028.

[30] S. M. Mobin, A. K. Srivastava, P. Mathur, G. K. Lahiri; *Dalton Trans.* 39 (2010) 8698.

[31] V. Balamurugan, W. Jacob, J. Mukherjee, R. N. Mukherjee; *Cryst. Eng. Comm.* 66 (2004) 396.

[32] V. R. Hathwar, S. M. Roopan, R. Subashini, F. N. Khan, T. N. G. Row; *J. Chem. Sci.* 122 (2010) 677.

[33] B.-M. Ji, X.-G. Wang, C. Xu, N. Ma, S.-B. Miao; *Chin. J. Chem.* 26 (2008) 260.

List of Publications

1. Syntheses and structures of nickel(II) and copper(II) complexes with biacetyl bis(benzoylhydrazone): One-dimensional self-assembly via π–π interaction and hydrogen bonding.

   T. Ghosh, A. Mukhopadhyay, K. S. C. Dargaiah, S. Pal.

   Struct. Chem. 21 (2010) 147-152.

2. A double helical dicopper(II) complex with biacetyl bis(benzoylhydrazone).

   T. Ghosh, S. Pal.

   Inorg. Chim. Acta. 363 (2010) 3632-3636.

3. Bis(2-(1H-imidazol-2-yl)-pyridine)copper(II): Effects of counteranions on molecular and supramolecular structures.

   T. Ghosh, S. Das, S. Pal.

   Polyhedron 29 (2010) 3074-3080.

4. Syntheses and structures of cerium(IV) and gadolinium(III) complexes with biacetyl bis(benzoylhydrazone).

   T. Ghosh, S. Pal.

   (Manuscript under preparation)

Posters and Presentations

1. Mononuclear Ni(II) and Cu(II), and dinuclear double helical C(II) complexes with biacetyl bis(benzoylhydrazone).

   Poster presentation.

   Chemfest-2010, University of Hyderabad, Hyderabad.

2. Structural studies on some nickel(II) and copper(II) complexes.

   Oral and poster presentations.

   Chemfest-2011, University of Hyderabad, Hyderabad.

3. Structural studies on some nickel(II) and copper(II) complexes.

   Poster presentation.

   3rd Asian Conference on Coordination Chemistry, 2011 (ACCC-3, 2011), Indian Habitat Center, New Delhi.

4. Synthesis, characterization and structural studies on Ce(IV) and Gd(III) complexes with biacetyl bis(benzoylhydrazone).

   Poster Presentation.

   14th National Symposium in Chemistry (NSC-14) & 6th CRSI-RSC Symposium in Chemistry, 2012, Thiruvananthapuram.

5. Synthesis, characterization and structural studies on Ce(IV) and Gd(III) complexes with biacetyl bis(benzoylhydrazone).

   Poster presentation.

   Chemfest-2012, University of Hyderabad, Hyderabad.